Improved handling of lignite and lignite derived products
Final Report October 2015

Summary

This report describes the work achieved within this project, based upon the objectives set out in the original project proposal, a full comparison table for achievements versus the original objectives can be seen in the appendix, which includes scientific, training and commercial objectives. The body of this report contains general discussion, the main scientific findings of the project and suggested direction for any future work.

The project has two parts: The first part is an investigation correlating the spontaneous combustion behaviour of lignite to the coal structural properties and oxidation behaviour, Part A. The second, Part B, is a study of the granulation and drying of lignite and other lignite based products at both the laboratory and pilot scale. Therefore, this report will have two main sections of the scientific impacts: discussion and findings, followed by an overall discussion of the training and commercial impacts of the project as a whole. Details of work done and results achieved are not included in this report if they have been presented in previous milestone reports; where this is the case, a reference to the appropriate milestone report is given. Further results shall be detailed in the Theses of the PhD students and in future publications.

Contents

Scientific objectives

Part A - Spontaneous Combustion

"Part A seeks to provide new fundamental understanding into spontaneous combustion behaviour of Victorian brown coal by establishing clear correlations between observed oxidation behaviour and structural properties of raw brown coal and its dewatered products."

The aim of this part of the project was to provide fundamental understanding into the spontaneous combustion behaviour of Victorian brown coal. A series of brown coal samples and samples of brown coal dewatered products were studied in terms of their physical structure and chemical composition. Many of the brown coal products were produced in such ways as to systematically manipulate either, or both, the physical structure and the chemical composition, thus enabling correlations between observed oxidation behaviour and structural properties of brown coal and dewatered products. With a good understanding of the changes in the properties of the coals and the coal derived products established, the behaviour of these samples with respect to low temperature oxidation, reactivity and spontaneous combustion could then be investigated.

Collection of samples

A number of Victorian brown coal samples were used within the project, including: Morwell, Loy Yang Low ash (LYLA), Yallorn, Yallorn light lithotype(YLL), Yallorn Woody(YW). In addition to the raw samples, dewatering techniques were used to produce systematically adjusted samples. The dewatering methods used and the expected changes to the physical and chemical composition of the brown coal samples is summarised in the Table 1, amended from milestone report 3.

Table 1: Coal treatments and effects on physical and chemical composition

Treatment	Effect of treatment	Description
None	None	Control
Water wash/Acid wash	Chemical	Removal of some cations
Addition of cations (diffent valency*)	Chemical	Add more cations
Addition of phosphate	Chemical	Reaction with cations
Mechanical thermal expression (MTE*)varying pressure and temperature	Physical and Chemical	Some loss of cations, but mostly physical change to pore structure
Hydrothermal dewatering (HTD*)varying temperature/additives	Physical and Chemical	Greater loss of cations than with MTE, but less physical changes
Kneaded and extrusion (Kneading time*)	Physical	Change of pore sizes
Addition of alkali for Kneading then extrusion (kneading time* and alkali chemistry/ concentration*)	Physical and Chemical	Digestion of coal structure, neutralize acid groups
Oxidation treatment (gaseous or wet oxidation methods*)	Physical and Chemical	Oxygen reaction with coal surface, change in surface chemistry/ structure

*subsets for different conditions may give a range of systematic changes to properties

Preparation and evaluation of samples

Alongside the work done by the PhD student and research fellow employed for this project, this work has benefited from additional contributions from two visiting researchers from Japan, Yoshimitsu Tsukasaki (Nippon Steel Corporation, Japan) and Akimasa Yamaguchi (Central Research Institute of Electric Power Industry, Japan), support from Australia-China Joint Research Centre for Energy collaboration with a visiting Researcher from China Junjie Liao (Taiyuan University of Technology) looking at a Chinese lignite and an additional research assistant Jamileh (Shah) Taghavi Moghaddam.

Characterisation of prepared samples

Methods used for the analysis of samples are listed below in Table 2, amended from milestone report 3. Both the analysis methods and the production methods of dewatered coal products are described briefly in Appendix 2. A sample matrix which lists the associated experimental data collected can be seen in Appendix 3.

Table 2: Techniques used to evaluate brown coal and brown coal dewatered products

Pore structure/ surface area/ Physical structure	Chemical composition	Combusion behaviour	Gaseous product analysis
Gas adsorption (CO_2)	Elemental anaylsis (C,N,H, O)	CO_2/CO production	GC
Hg intrusion/extrusion	FT-IR	TGA-DTA	
He pycnometry	Ash content	Wire Basket	
Vickers' hardness	ICP-OES	DSC	
SEM	Moisture content	DTA	
	Ultimate/Proximate analysis		

Low temperature oxidation experiments

In addition to the reactivity experiments described above, the capability to carry out low temperature oxidation (LTO) reactions has been established. The reactor can hold 60-70g dry coal or coal product and can be used to expose the sample to a known throughput of oxygen in a controlled temperature environment. Evolved gases can be analysed by micro-GC. Further details of the LTO reactor and rig design, operation and results are described in the reports listed in Table 3. Samples of three different coals have been analysed before and after LTO, the oxidation process was found to affect each sample in different ways, changes were seen in the surface area, porosity, chemical structure and reactivity. The details of this work are written up for publication, listed in Appendix 4.

Table 3: LTO rig details and the corresponding reports where they can be found

Reactor design and Rig set-up	Milestone report 4
Dried raw coal , multiple temperatures	Interim report
Dried coal repetitions , for data reliability	Milestone report 7
Dried raw coal and HTD products	Milestone report 8
Comparison of different raw coals	Paper in progress

Collaboration with industry partner

In addition to the laboratory scale work carried out within this part of the project, in collaboration with industry partner ECT the opportunity to test products made at an industrial scale was provided. A pilot plant of the densification process is being run by ECT before a full scale plant is commissioned, the process is based on the laboratory scale process that was first developed in the 1980s and has been used in the lab for this project. ECT performed a run exclusively for this project using Maddingly coal and producing samples that could be analysed in the lab using the same methods as have been employed for all other lab samples. The results of the critical ignition temperature test showed that critical ignition temperature for air dried densified coal is very close to that for air dried raw coal, suggesting that the densification process does not change the spontaneous combustion propensity. Similar results were found for samples from two other coals and their densified equivalents made in the lab.

Spontaneous combustion significant findings

The heterogeneous nature of the raw material and the multi-variable outcomes from the washing and dewatering treatments used in this investigation mean that the interpretation of changes in the spontaneous combustion behaviour are also complex. However there are a few consistent trends that are worth noting:

Acid washing

Acid washing the raw coal significantly reduces inorganics such as Al, Ca, Fe, Mg and Na, whilst some inorganics are thought to increase the propensity for spontaneous combustion, others are believed to supress it, however our observations suggest that in general, acid washing, increases the critical ignition temperature (T_{crit}) and reduces the propensity for spontaneous combustion when compared to the raw coal. The measured surface area and microporosity volume are also reduced upon acid washing, a reduction in surface area, reduces the number and availability of active sites on which the oxidation reactions occur at low temperature, thus delaying T_{crit} to a higher value than that for raw coal. These combined changes result in an observed increase of T_{crit} after acid washing. This change in spontaneous combustion behaviour is seen for both Loy Yang low ash (LYLA) and Morwell coals.

Densification

Densification alone has a small or negligible effect on T_{crit}. After densification the measured surface area and microporosity decrease slightly. The addition of NaOH causes further reduction in surface area and microporosity; a significant increase in T_{crit} at higher concentration additions of NaOH is also observed. The addition of alkali causes changes in the surface chemistry reducing both the hydrophilicity of the surface and the number of active sites for low temperature oxidation. These changes in physical and chemical properties and the corresponding change in the spontaneous combustion behaviour increase with increasing NaOH addition during the densification process. The type of alkali used in the addition also affects the critical ignition temperature (sodium hydroxide shows greatest increase in T_{crit}). The addition of NaOH during the densification process also increases the Vicker's hardness of the product pellets, thus increasing the durability of the pellets for transportation. Investigations of drying method after densification have shown that the drying method can have an effect on the spontaneous combustion behaviour such that air dried products have a higher critical ignition temperature than a nitrogen dried equivalent.

Mechanical Thermal Expression (MTE)

The MTE process reduces T_{crit} and the more severe the treatment (higher applied pressure and temperature), the greater the decrease in T_{crit}. MTE increases the measured surface area and micropore volume whilst the macropore and mesopore volume are decreased. The inorganic content has minor changes (reduced Na and K) as a result of MTE, but more significant effects in changes in inorganic content are seen from acid washing. The increased propensity to undergo spontaneous combustion for MTE products is driven by the change in surface area, or microporosity which increases the availability of active sites for oxidation reactions.

Hydrothermal dewatering (HTD)

The HTD process decreases T_{crit} and a further decrease is seen with increasing severity of treatment (temperature.) The measured surface area decreases with HTD and decreases further with increased severity of treatment. The microporosity increases with HTD, but decreases with the most severe conditions tested. The HTD treatment upgrades the coal, reducing the oxygen content and removing

some organic and inorganic content. HTD coals further treated by low temperature oxidation (LTO) see an increase in T_{crit} and also an increase in measured surface area. The rate of CO_2 release during LTO is less for HTD coals than for raw coals and further reduces with the increased severity of HTD treatment. The HTD process increases the porosity of the coal and this may be the dominating factor in decreasing the critical ignition temperature when compared to raw coal.

Low temperature oxidation (LTO)

Three different source brown coals were used in LTO investigations, two became less reactive (higher T_{crit}) after LTO and one became more reactive. The change in reactivity and thus spontaneous combustion behaviour appears to be driven by the change in surface area observed after LTO: Morwell coal had an increase in surface area and a corresponding decrease in T_{crit}, whilst both Yallorn Woody and Yallorn light lithotype both had a decrease in surface area after LTO and a corresponding increase in T_{crit}. The difference observed in the behaviour of the coals after LTO may be partially explained by the different composition of the organic and inorganic matter inherent in the coal and the extent of the changes in the surface chemistry that occur as a result of LTO.

Correlating structure property relationships

- There is a structural relationship to critical ignition temperature (T_{crit}), the critical ignition temperature increases with a decreasing surface area.
- Dewatering techniques have different effects on the critical ignition temperature, related more to the surface area change or change in cation concentration resulting from the dewatering technique.
- An exothermic event observed in DSC experiments, occurring between 52-98 ^{o}C correlates with an observed structural change seen in scanning electron microscopy images taken before and after heating. The measured surface area also decreases after the heating process.

The significant finding of the spontaneous combustion behaviour of the systematically varied coal samples was that there was an inverse relationship between the surface area measured by CO_2 adsorption and the critical ignition temperature. The CO_2 surface area is really a measure of the microporosity volume of the sample (pores less than 3 nm diameter). As this value decreases then the critical ignition temperature increased, thus the propensity to undergo spontaneous combustion decreased. The critical ignition temperature is a measure of the spontaneous combustion propensity of a material, the higher the critical ignition temperature, the lower the propensity to undergo spontaneous combustion. This behaviour was observed for the densified coal treated with alkali and the MTE product, but not the HTD product.

The lack of correlation for the HTD product is, we believe, due to structural alteration that takes place in response to the thermal treatment it experiences. The surface chemistry is altered by decarboxylation and dehydration reactions. These chemical changes reduce hydrogen bonding interactions within the coal (so that the coal is less hydrophilic) but also cause more microporosity to be created, such that T_{cr} actually decreases.

Another method to calculate the microporosity is by difference between the helium density measurement and the skeletal density measured by mercury intrusion porosimetry (Bergins, Hulston et al. 2007). However, there was some confusion over the helium density measurements made as part of this work; the poor reproducibility and reliability of these measurements has prevented us

applying this secondary calculation of the microporosity. The relationship of the CO_2 surface area (microporsity) and the critical ignition temperature is still valid however.

Bergins, C., et al. (2007). "Mechanical/thermal dewatering of lignite. Part 3: Physical properties and pore structure of MTE product coals." Fuel **86**(1-2): 3-16.

Communication of findings
From this work a series of posters and presentations have been given at a variety of national and international conferences and meetings. A collection of academic papers are currently in progress. Some of this work will also be the basis of a PhD thesis. Details of all these presentations and some papers in progress are given in Appendix 4. In addition draft manuscripts can be seen in Appendix 6.

Part B - Granulation of coal and coal products

"The project will provide fundamental knowledge about the granulation behaviour of lignite and lignite-derived materials using laboratory granulation equipment followed by pilot scale trials."

Lignite granulation
The aim of this work was to produce a dried brown coal product that was cheaper and safe to transport, in combination with developing brown coal derived products for alternate uses, in particular, agricultural amendments and fertiliser products. Previous work at Monash University had demonstrated the possibility of granulating brown coal and this work continued to investigate and develop further understanding of the granulation and drying processes for brown coal. Following the regime map theory of granulation (Iveson et al, 1998) a series of experiments were conducted adjusting the moisture content and agitation (drum) speed, as well as experiments using different coals and binders were carried out. The granule growth was evaluated by measuring the particle size distribution of the granules at regular time intervals throughout the granulation experiment. The median particle size plotted against granulation time, or growth curves for each experimental run were used to determine the growth behaviour and thus plot a "regime map". From the regime map, a greater understanding of the granulation behaviour of brown coal was established. The initial regime map was presented in Milestone report 5, with additional information presented in milestone report 6 and a completed map presented in Milestone report 7.

S. M. Iveson and J. D. Litster, "*Growth Regime Map for Liquid-Bound Granules*", Particle Technology and Fluidization, July 1998 Vol. 44, NO. 7 pgs 1510-1518

Granule strength and porosity

Brown coal granules were tested for strength and a relationship between granulation conditions and strength was investigated, some of the results of which are presented in milestone report 7. A single particle strength test method was established (described in milestone report 6). A second strength testing method was also investigated where multiple granules were tested together, the compaction curve testing method, described in milestone report 7. This multi- granule strength test method, however, was felt not to be as reliable as the single granule strength test due to the difficulty in identifying the critical inflections within the compaction curve.

Granule porosity was measured initially by kerosene displacement giving a measure of the percentage porosity for the dried granules, see milestone report 7 for details. Most recently measurements of average pore diameter and pore volume were measured by mercury porosimetry

for dried granules, these results indicate that the porosity and pore size distribution of all of the granules was more or less constant, due to the significant shrinkage of the granules during drying. A full analysis of the results will be presented in Evone Tang's PhD thesis.

Alternative binders(e.g. molasses) were trialled for the brown coal granules to provide additional strength to the granules. Insufficient granule strength would cause issues for the handling of the granules and ultimately attrition during transportation could result in a loss of product and a potential safety risk from the dust produced. The results from these strength tests and the relationship to the binder used will be presented in Evone Tang's PhD thesis.

Fertiliser granulation

Initial work was also completed to investigate the granulation behaviour and strength of product granule for a fertiliser product made by one of our industry partners, LawrieCo. In order to increase the strength of the product granule alternative binders were tested and the addition of raw coal into the formulation was found to improve the granulation behaviour of the fertiliser product. The initial results of this work were presented in Milestone report 5, with a complete report in milestone report 6. Whilst this work was underway, the industry partner withdrew from the project and therefore pilot scale granulation trials at their facility were not possible. Large scale granulation experiments were, however, conducted as part of the pilot scale superheated steam drying trials at Pinches Consolidated Industries.

Granule drying

Laboratory-scale work

The granulation process produces a wet product that requires drying, therefore, additional investigations were carried out on establishing a suitable drying method for the brown coal granules. Based on previous work with superheated steam drying at Monash University the potential of superheated steam drying as a safe (no oxygen) environment for drying brown coal had been identified. Laboratory testing of granule drying in both air and steam was carried out alongside pilot trials.

Pilot-scale work

The potential for drying brown coal within a superheated steam environment and more specifically, a pilot-scale superheated steam drum drier was conducted in collaboration with industry partner Pinches Consolidated Industries. This project provided a pilot scale study of superheated steam drying in combination with granulation of brown coal within the superheated steam drum drier at Pinches Consolidated Industries. Several pilot scale runs of simultaneous granulation and drying were carried out. A description of the pilot-scale drying rig was presented in milestone report 6 along with the initial trial details. Further results from a second pilot trial of brown coal granulation and drying were given in milestone reports 7. The granules produced were of an appropriate size for agricultural use (similar to current fertiliser pellet sizes) although the granule strength is currently too weak for industrial use. Further work in collaboration with another BCIA funded project* led to pilot scale trials of the granulation and drying of Urea enriched brown coal granules, these results were discussed in milestone report 9. Lab made urea enriched brown coal granules had shown positive results when used in pot trials within the other BCIA project*. The granule strength measured for the urea-enriched granules was much lower than that of commercial fertiliser products and therefore would require further adjustments to the formulation to increase the

strength to an industrial standard. An improvement in strength could be seen with a change of binder, or use of an additive to the binder or coal. A study of the nitrogen retention within the urea enriched granules and the drying method were carried out at the lab scale and further soil tests have been carried out and are currently being written into an academic publication (see Appendix 4 and 6) in collaboration with another BCIA supported project*.

An economic assessment of the simultaneous granulation and superheated steam drying of brown coal and urea enriched brown coal has been carried out to determine the minimum breakeven price per tonne of product required for a variety of formulations. This analysis is in Appendix 5.

*"Coal-derived additives: a green option for improving soil carbon, soil fertility and agricultural productivity?"

Granulation and drying significant findings

Granulation of Lignite
- Due to its inherent moisture content, Victorian brown coal can be granulated with minimal additional water (binder).
- Regime map for lignite: The granulation behaviour for brown coal has been found to fit well with established granulation theory. Thus the granulation process for brown coal may be controlled by manipulating the granulation parameters of binder amount/type, agitation (drum) speed to ensure the granule growth follows a steady growth curve, which is the most controllable and predictable behaviour for a granulation process.
- Granule strength is insufficient for industrial use of the granules when water alone is used as a binder, thus additional binders or additives are required to enhance the granule strength.
- Brown coal granules may be enriched with inorganic fertilisers within the granulation process and have shown positive results for the retention of N within the granules and soil during leaching experiments and when used for pot trials. A reduction of nitrous oxide gases from the soil has also been observed for the urea enriched brown coal granules when compared to urea only granules.
- The addition of small amounts of brown coal to hydrophobic fertiliser formulations can improve the wetting of the fertiliser and thus improve its granulation behaviour to be that of controllable steady growth, producing a more uniform final granule size distribution.

Drying method and granule strength
- Laboratory scale drying experiments have shown that air drying produces stronger, less porous granules than those steam dried
- Granules strength is dependent on drying rate and drying method
- Final moisture content of the granule affects the granule strength, as drier granules are stronger than those with higher moisture content.
- Steam dried granules have larger average pore size, greater pore volume and have more visible surface cracks than air-dried granules at the same temperature.

Pilot-scale trial of granulation and superheated steam drying
- Simultaneous granulation and superheated steam drying has been successfully achieved at pilot scale for both brown coal and urea-enriched brown coal. The process produced

granules of a suitable size for agricultural use, although further work would be required to increase the granule strength.

- Production of a brown coal fertiliser product,(urea enriched brown coal granules) produced weak granules of a suitable size, but a suitable binder is required to improve the strength of the granules. Molasses is one possibility, but would need further work to determine whether the optimal dosage rate would provide sufficient strength and also be economic. An alternative fertiliser product would be the addition of brown coal to fertiliser granulation to improve wetting and thus improve the granulation process (making it more controllable.)

Communication of findings

The work done on this part of the project will form the basis of a PhD thesis. In addition this work has been presented at several conferences and has in progress academic publications, see Appendix 4.

Training objectives

This project has provided training for 2 PhD students, one in the School of Chemistry and one in the Department of Chemical Engineering. The students have had training in laboratory techniques, exposure to industrial scale engineering and the opportunity to present their work at conferences. Both parts of the project have supported a pilot-scale trial of processes conducted by the students at laboratory scale, for Part A, this was a pilot scale densification process and for part B, a simultaneous granulation and superheated steam drying trial of both brown coal and a urea enriched brown coal for fertiliser applications. The work from this project will form the basis for 2 PhD theses for the students involved. The postdoctoral researcher and lignite technician also took part in the granulation and drying pilot-scale trials alongside the lab based work conducted at Monash University.

Commercial objectives

A pilot scale production run of densified coal was carried out by ECT to provide samples for comparison tests within part A of the project. The samples were made from Maddingley coal and samples have been analysed for critical ignition temperature and compared with raw coal and lab produced densified coal.

Several pilot scale trials for the simultaneous granulation and superheated steam drying of brown coal and urea-enriched brown coal were conducted at Pinches Consolidated Industries over several months. Brown coal granules were successfully made and dried within the pilot-scale drum drier, thus proving the concept of the combined process and potential for further applications of the process equipment made by Pinches. Granule properties were evaluated for changes in the operating conditions for optimisation purposes, granule size and moisture content were within the desired range, but granule strength was not sufficient for the agricultural applications being investigated. Further work on the formulation of the brown coal granules, in particular, the binder type may yield stronger granules.

Future direction

Spontaneous Combustion

- Transfer knowledge of the factors that affect the spontaneous combustion behaviour of the densified product to industry partners for trial and implementation in their process.
- Develop a graphical way to present the factors affecting critical ignition temperature and determine the dominance of each property and any interrelationships.
- Further study to understand the role of moisture in the low temperature oxidation process and spontaneous combustibility.

Granulation and drying

- Improve granule strength, use data from lab trials in this study to carry out further pilot scale trials with different binders.
- Granulation studies with alternate nutrient fertilisers (Phosphorus, Potassium). Alongside further soil tests and pots trials looking at the retention, evolved gases and plant uptake of the nutrients from the brown coal granules
- Further investigation into the potential of adding small quantities (5-20 wt%) raw brown coal to hydrophobic fertiliser formulations to improve the granulation properties of the fertiliser, with possible benefits of better soil retention, lower evolution gases from soil and increased plant uptake of the fertiliser nutrients.

Acknowledgements

Appendix 1: Achievements against original objectives

Scientific objectives

Part A - Spontaneous Combustion

"Part A seeks to provide new fundamental understanding into spontaneous combustion behaviour of Victorian brown coal by establishing clear correlations between observed oxidation behaviour and structural properties of raw brown coal and its dewatered products"

Collection of samples with systematically varied (organic) chemical composition (lithotypes and macroscopically identifiable plant remains such as fossil wood, leaves, consolidated (humified) groundmass	Samples collected: Morwell run-of-mine, Loy Yang Low Ash, Yallorn, Yallorn light lithotype, Yallorn woody
Preparation and evaluation of samples with systematically varied porosity (especially microporosity), with systematically varied inorganic cation concentration and with systematically varied oxygen concentration	Densified samples with varying concentration of alkali=varied porosity. Coals with additional cations(different valency cation additions) Wet and dry oxidation techniques including HTD
Characterisation of prepared samples by a comprehensive range of analytical techniques (proximate analysis, ultimate analysis, ash characterisation, oxygen adsorption, solid state NMR, infrared spectroscopy, surface area, porosity, functional group analysis, etc).	Many techniques used to analyse samples- full list given in sample matrix, appendix 2.
Establish capability for low temperature (ca. 60°C) oxidation experiments, including the in-situ analysis of evolving gases.	Done.
Characterise the prepared variety of techniques including: oxygen adsorption capacity, low temperature reaction rates and product distributions, conventional thermogravimetric analysis (TGA) and differential scanning calorimetry (DSC), wire basket tests following our published method	TGA, DSC, wire basket tests and low temperature reactions done, no oxygen adsorption. See appendix 2 for details.
Correlate structure property relationships	Correlation between surface area and spontaneous combustion propensity found
Document and publish these results in the peer reviewed literature	Many presentations given, write-up of publications in progress

"Work with partners to identify how the results of the preceding fundamental studies can be used to reduce the spontaneous combustion propensity of their products."

Comparative studies on products from partner's pilot plant and associated research facilities.	Pilot scale run completed with samples taken for analysis
Correlate structure property relationships and consider process improvements.	In progress

Part B - Granulation of coal and coal products

"The project will provide fundamental knowledge about the granulation behaviour of lignite and lignite-derived materials using laboratory granulation equipment followed by pilot scale trials"

Review critically the formulation for both lignite and lignite-derived granules including coal (lithotypes) and additives	Literature review of granulation of coal completed. As LawrieCo pulled out of the project before formulation details were shared the review of formulation aspects was not able to be conducted..
Develop a granulation regime map[7] for lignite and lignite-derived fertilisers to determine the critical moisture content and shear required, to produce a strong granulated product. The presence or absence of drying will be included in the map(s).	Lignite regime map completed, and found to exhibit steady growth. No fertilisers due to withdrawal of Industry partner from project. Investigation relationship between drying and strength done at lab scale.
Develop a regime-separated granulation approach for lignite granulation, and determine the benefits (if any) on granule properties and control of the process	As granules were found to exhibit steady growth, the regime separated approach was not required.
Establish a mechanical testing procedure to characterise the mechanical strength and porosity of the granules produced	Mechanical testing done. Porosity measured by kerosene density and mercury porosimetry.
Determine (in conjunction with Project A) the spontaneous combustion characteristics of the granules	In progress.

"As the granulated products (lignite and lignite-derived products) must also be dried, the project will develop an integrated granulation and drying process using pilot-scale equipment"

The first strategy will be a two-step process by first granulating the material followed by drying. The energy balance for this process will be established.	Laboratory granulation and drying carried out. No energy balances.
The second strategy will be to attempt to integrate the granulation into the drying process by exploring both a co-current and counter-current drying process. The energy balance for both methods and the resulting product quality will be compared with the non-integrated approach.	Integrated granulation and drying completed successfully at pilot scale for co-current drying process. Counter-current conditions producing more extreme initial drying conditions were not carried out due to the risk of dust formation, dust in previous trials reduced the granule size observed. No energy balances.
When drying the granulated lignite products, either the laboratory instrumented steam-oven or the Keith Engineering pilot scale drier will be deployed, because of their capacity to dry lignite safely in a superheated steam environment.	Both used successfully for drying of brown coal and urea-enriched brown coal granules

Training objectives

"The project will facilitate the training of 2 PhD students, 1 postdoctoral researcher and 1 lignite technician in brown coal technologies."

One PhD student will be selected to work on the spontaneous combustion (Part A), the other on granulation and drying project (Part B).	2 PhD students enrolled,Theses details given in appendix 3.
The postdoctoral researcher and lignite technician will work across both parts of the project.	Done
Part B will involve field work, so that this individuals involved in this part of the project will be exposed to both coal science and industrial engineering, thereby providing a broad training perspective and networking opportunities. The development of skills in the important field of coal drying may be readily transferable to the power generation industry.	Both parts of the project involved pilot-scale trials: Part A- a pilot scale run of the densification process conducted with ECT. Part B-multiple superheated steam drying and simultaneous granulation and drying of coal and urea-enriched coal granules conducted with Pinches Consolidated Industries.

Commercial objectives

"ECT is developing an attrition-based approach to dewatering. It has aspirations to provide stabilized brown coal products in to new markets locally and overseas. The scientific understandings that are developed in this project can be transferred to this company to help facilitate improved process development and commercialisation prospects."

-Analysis of pilot scale produced material has been carried out for the critical ignition temperature of the densified material compared to the raw coal. The densification process has not affected the critical ignition temperature observed, but the beneficial effect of air drying has been well established.

"Keith Engineering (Pinches Consolidated Industries) is an Australian Company which has developed a superheated stream drying process which is being used commercially in New Zealand, US, Europe and Russia. In collaboration with Monash University, they have already demonstrated that the process can be used to dry lignite producing a powder product. However, they are interested in developing their technology further so that drying can be combined with the granulation of lignite and lignite-derived materials and in how this process may reduce spontaneous combustion."

-Successful granulation and drying of brown coal granules and urea-enriched brown coal granules. Granules produced are of a suitable size for agricultural use, although more work is required to produce granules of sufficient strength. A proof of concept has been achieved for the simultaneous granulation and drying process at pilot scale.

Appendix 2: Spontaneous combustion experimental methods

Dewatering procedures:

Densification process
Raw brown coal and water (and additive) are mixed for a set time within a kneading machine at a set agitation rate. The coal paste is then extruded through a circular orifice and the extruded material is cut into 5-10 mm lengths. The "pellets" are then air dried in ambient conditions for at least 72 hours.

MTE: Mechanical Thermal Expression
Raw brown coal and a small amount of additional water are placed in a pressure vessel and the vessel is heated (up to $200^{o}C$). Once at the required temperature a mechanical compressive force is applied to the sample for a set time (pressure up to 12 MPa). The compression force is then removed and the sample allowed to cool. A dewatered compressed cylindrical tablet is produced, approximately 2-3 cm thick with a diameter of 5 cm.

HTD: Hydrothermal dewatering
A coal slurry is placed in the reaction vessel and subjected to high temperature ($290^{o}C$- $350^{o}C$) whilst being stirred for a set time. After cooling the slurry is filtered and air-dried.

Wet oxidation
Raw brown coal (~50 g) was added to 500 ml of H_2O_2 solution (0.1, 0.5 and 1 M) and then stirred for 3h under UV light (wavelength 254 nm). The solution was then filtered and the oxidized coal was washed for 24 h, this washing process was done twice and then the final filtered sample was dried under nitrogen for 3h at $105^{o}C$.

Analysis techniques:

Ultimate and Proximate analysis
Proximate analysis provides percentages of volatiles, fixed carbon and ash. Ultimate analysis provides percentage carbon, hydrogen, nitrogen (sometimes Sulphur) and oxygen by difference.

Ash Content
The ash that remains after complete combustion of the coal or dewatered products, provides a measure of the inorganic content of the sample. The ash may be further analysed to determine the specific inorganic species present.

Helium Pycnometry
He-density measurements are carried out using a Micromeritics AccuPyc II 1340 Gas Pycnometer, which measures the required volume of helium required to fill the sample. The sample holder volume is accurately known and therefore the volume occupied by the sample, the skeletal density can be derived by a simple calculation.

Mercury Porosimetry
The pressure at which mercury intrude the pores of a sample is inversely proportional to the size of the pore. Measurement of the mercury intruded volume at increasing pressure points is used to calculate the pore size distribution, average pore size and total pore volume of the sample. Measurements are made by a Micromeritics Autopore IV mercury porosimeter. Samples of

approximately 0.2 g dried coal are placed within the sample holder (penetrometer) and placed within the porosimeter, which records the intrusion and extrusion volume against the applied pressure.

CO2 surface area

Carbon dioxide adsorption measured at 273K is used to calculate the coal surface area. The sample is degassed at 105 ^{o}C overnight and the CO_2 adsorption is measured on a Micromeritics Tristar II.

SEM

Scanning electron microscopy is carried out at the Monash Centre for Electron Microscopy (MCEM) using a field emission gun scanning electron microscope (FEG/SEM),Nova NanoSEM 450 operating at 5 KV.

TGA

Thermogravimetric analysis was carried out in a Setaram TAG16 Simultaneous Symmetrical Thermoanalyser. Samples are heated in nitrogen to 105 ^{o}C and maintained at this temperature for 30 minutes to remove any water present. The sample is then cooled to 60°C. The gas flow in the reactor is then switched 10 % oxygen and 90 % nitrogen and the sample heated to 400 ^{o}C at a rate of 3 ^{o}C/min and further heated to 600 ^{o}C at a rate of 10 ^{o}C/min. The heat flow and mass change are recorded throughout. After cooling, the residue in the crucible is weighed.

DSC

Differential scanning calorimetry is carried out using a Setaram micro DSC III. Tests are conducted in a closed batch cell and in a gas flow cell under nitrogen, air and oxygen (30 cm^3/min flow rate). Alpha-alumina is used as reference material.

DTA TGA

Differential thermal analysis and thermogravimetric analysis are carried out on a TGA/DSC1 STAR System. The sample is heated up from 30°C to 600°C at a rate of 2 ^{o}C/min in air and held at 600°C for 20 minutes in air and 20 minutes in nitrogen before being cooled to room temperature. The change in sample energy and mass is measured throughout.

FT-IR

FTIR spectra are acquired by a BRUKER IFS 55 FTIR spectrometer at room temperature, with a mercury cadmium telluride (MCT) detector.. A KBr pellet containing coal (mass ratio 1:300 dry basis) was made by pressing the mixture of finely ground powders at the pressure of 10 MPa for 10 min. Spectra are collected with a nominal spectral resolution of 8 cm^{-1} and range from 4000-600 cm^{-1} . The number of scans for both background and sample was 50 and the aperture was set at 1.4 nm.

Critical ignition temperature

T_{crit} is measured by the wire basket method using a custom made cubic wire basket with 25mm sides with a lid. Three thermocouples penetrate the coal sample, at the centre of the sample and 3 mm either side of the centre. The wire basket is positioned within an oven which is heated to a set temperature and a burn, or no-burn result is achieved. The oven temperature and three thermocouple temperatures are logged. The experiment is repeated with varying the oven set temperature until a burn and no-burn result are achieved within 2 ^{o}C. The temperature at which all three sample thermocouples are equal is the crossing point temperature ($T_{crossing\ point}$) and T_{crit} is

defined as the average for the crossing point temperature for the burn result and the crossing point temperature for the no-burn result :

$$T_{crit} = \frac{T_{crossing\ point\ burn} + T_{crossing\ point\ no-burn}}{2}$$

Low temperature oxidation rig with micro GC:

Approximately 70 g milled dry coal (or coal product) is placed in the reaction vessel and sealed. The reaction vessel is heated within an oven to the desired reaction temperature, during heating, the coal is subjected to a flow of dry nitrogen (50 mln/min), Once the reaction temperature has been achieved within the vessel, the gas flow is switched to 50mln/min oxygen. At regular time intervals the exit gas from the reaction vessel is analysed by a micro-GC (Gas Chromatograph) and the fraction of Carbon dioxide and carbon monoxide is within the exit stream is measured. A calculation of the volumetric flowrate per g of dry coal can then be calculated.

Appendix3: Spontaneous combustion sample matrix

Coal	Treatment	CO2 Surface area	He density	Hg porosimetry	Vickers Hardness	Ash content	Inorganic (ICP_OES)	SEM	FTIR	Ultimate & Proximate analyses	Wire basket (T$_{crit}$)	DSC	TGA/DTA	Low Temp Oxidation	Results reported
Morwell	None	Yes	Yes	Yes		Yes		Yes	Yes	Yes	Yes	Yes	Yes	Yes	In progress publication
	Oxidised 4 hours	Yes	Yes	Yes		Yes		Yes	Yes	Yes	Yes		Yes	Yes	In progress publication
	Wet oxidised UV/H2O2 Different concentrations	Yes							yes		Yes				Milestone report 8
	Acid washed	Yes								Yes					Milestone report 8
	Densified (& NaOH, different concentrations)	Yes		Yes				Some	Some		Yes	Some	Yes		Milestone report 8
	Densified (& 1M NaOH, NH4OH, Ca(OH)2 KOH)			Yes							Yes				Milestone report 8
	Acid washed & densified (& NaOH)		Yes	Yes							Yes		Yes		Milestone report 8
	MTE(mild, moderate & severe conditions)		Yes	Yes			Some				Yes	NO	Yes		Milestone report 8
	Acid washed &MTE(mild, moderate & severe conditions)		Yes	Yes							Yes				Milestone report 8
	HTD	Yes	Yes	Yes		Yes				Ultimate	Yes		Yes	Yes	Milestone report 8
	HTD and oxidised 4+hours	Yes	Yes	Yes		Yes					Yes		Yes	N/A	Milestone report 8
	Ion additions- different cations (Phosphate salts-different concentrations)	Yes		Yes		Yes					Yes		Yes	Some	Milestone report 8
Loy Yang	None	Yes		Yes		Yes	Yes	Yes	Yes	Yes	Yes	Yes	Yes		Milestone reports 5 & 8
	Acid washed	Yes								Yes					Milestone report 8
	Densified (& NaOH, different concentrations)	Yes	Yes	Yes	Yes	Yes	Yes	Some	Some		Yes	Yes	Yes		Milestone reports 5 & 8
	Water washed & densified (& NaOH)	Yes	Yes	Yes	Yes	Yes	Yes						Yes		Milestone report 5
	Acid washed & densified (& NaOH)	Yes	Yes	Yes	Yes	Yes	Yes	Some			Yes	Yes	Yes		Milestone reports 5 & 8
Yallorn Light Lithotype	None	Yes	Yes	Yes	N/A	Yes		Yes	Yes	Yes	Yes		Yes	Yes	In progress publication
	Oxidised 4 hours	Yes	Yes	Yes	N/A	Yes		Yes	Yes	Yes			Yes	N/A	In progress publication
Yallorn woody	None	Yes	Yes	Yes	N/A	Yes		Yes	Yes		Yes	Yes	Yes	Yes	In progress publication
	Oxidised 4 hours	Yes	Yes	Yes	N/A	Yes		Yes	Yes		Yes	Yes	Yes	N/A	In progress publication
Maddingly	Raw coal											Yes			
	Densified -pilot scale process											Yes			
Chinese Lignite	HTD	Yes	Yes	Yes		Yes				Yes	Yes	No	Yes		Milestone report 8

Appendix 4: Communication of findings

Presentations:

International Conference on Coal Science & Technology, September 2015, Melbourne, Australia

"The Effect of Densification with NaOH on Victorian Brown Coal Thermal Behaviour and Structure" Oral Presentation

APCChE Congress incorporating the 45th Australasian Chemical Engineering Conference Chemeca, September 2015, Melbourne, Australia

"Effect of Hot Air and Superheated Steam Drying on Properties of Brown Coal Granules" Poster Presentation

The 39th International Technical Conference on Clean Coal & Fuel Systems, June 2014, Clearwater, Florida, USA

"The Spontaneous Combustion Behaviour of Victorian Brown Coal and Some Dewatered Products" Oral presentation

2014 Australia-China Symposium on Energy, May 2014, Taiyuan, China

"Physical properties and combustion behaviour of Victorian Brown coal densified pellets" Oral Presentation

"The Effect of Hydrothermal Dewatering of Morwell Brown Coal on Spontaneous Combustion" Oral Presentation

"The Effect of Phosphate Salts on Spontaneous Combustion Behaviour of Morwell Brown Coal" Oral Presentation

"Low temperature thermal behaviour of Victorian brown coal" Oral Presentation

"Hydrothermal Dewatering of Chinese Lignite and Spontaneous Combustion Behavior of the Products" Oral Presentation

International Minerals and Resources Conference

"Granulation and Superheated Steam Drying of Brown Coal" Poster Presentation
http://www.mtec.org.au/media/pdf/Evone%20IMARC%20Poster.pdf

Low Rank coal Symposium, April 2014, Melbourne Australia:

"Low temperature differential scanning calorimetry study of Victorian brown coal" Poster Presentation

"The Effect of Hydrothermal Dewatering of Morwell Coal on Spontaneous Combustion" Poster Presentation

"Hydrothermal Dewatering of Chinese Brown Coal and Properties of the Products" Poster Presentation

The 43rd Australasian Chemical Engineering Conference, Chemeca , September 2013, Brisbane, Australia

"Simultaneous granulation and superheated steam drying of Victorian brown coal in a pilot-scale rotary drum" Oral Presentation

Australia-China Workshop on Novel Carbon Capture, March 2013, Melbourne, Australia:

"Investigating the role of low temperature oxidation within self-heating and spontaneous combustion of dewatered lignite products" Oral Presentation

Australian Coal Science Conference, November 2013, Brisbane, Australia:

"Low Temperature Oxidation study of Brown coal and dried brown coal products" Oral Presentation

6th International Granulation Workshop, June 2013, Sheffield, UK

"Granulation Regime map for Victorian brown coal" Oral Presentation

The 42nd Australasian Chemical Engineering Conference Chemeca, September 2012, Sydney, Australia

"Granulation of brown coal" Oral Presentation and Peer-reviewed conference paper

Low Rank Coal Symposium, April 2012, Melbourne Australia

"Systematic study of low temperature oxidation of brown coal" Poster presentation

Papers in progress

Densified dewatering of lignite: Physical properties and reactivity study (See Appendix 6 for draft)

Comparative study of low temperature oxidation behaviour of three Victorian brown coals (See Appendix 6 for draft)

Low temperature thermal reactivity of Victoria brown coal and its effect on spontaneous combustion (See Appendix 6 for draft)

Mechanical Thermal Dewatering of low rank coal: Physical properties and reactivity study (In progress)

A slow release nitrogen fertiliser produced by simultaneous granulation and superheated steam drying of urea with brown coal (lignite) (See Appendix 6 for draft)

PhD Theses

"Investigation of Spontaneous Combustion Behaviour of Brown Coal and the Effect of Densification Process"

Mohammad (Mehrdad) Reza Parsa expected submission February 2016

"Granulation and superheated steam drying of brown coal"

Evone C.W. Tang expected submission date December 2015

Appendix 5: Economic Assessment of brown coal granular products
Economic assessment of steam dried lignite and fertiliser granules

Scope

An economic analysis has been conducted on the combined granulation and drying of lignite and urea-enriched lignite granules. From this analysis, a breakeven product price has been determined for a series of granule products listed in Table 5.4 below. The basis of this analysis is explained here, including economic parameters, assumptions and basic calculations.

Table 5.4: Product granule types evaluated for breakeven product price

Granule type	Binder	Urea to lignite ratio	Wt% molasses in binder
Lignite only granules	Water		
Urea enriched lignite	Water	1:6	
Urea enriched lignite	Water	1:10	
Lignite only granules	Molasses in water		10
Urea enriched lignite	Molasses in water	1:6	10
Urea enriched lignite	Molasses in water	1:6	25

Basis for economic analysis

A schematic flow diagram for the granulation and drying process is presented in Figure 5.1. For this analysis, it is assumed that the particle granulation is controlled by controlling the moisture content of the mixture entering the rotating drum dryer and the residence time within the dryer. Table 5.5 summarises the main economic parameters.

In addition to these parameters, it was assumed that the energy required by the steam dryer was 2.2GJ/tonne of water evaporated. This is significantly less than the 3GJ/tonne typically required for steam drying. The lower number is justified because the dryer produces atmospheric pressure steam and therefore it has been assumed that 25% of the energy in this steam can be recovered usefully. An efficiency of 85% is assumed for the heating of the steam.

Data from the pilot scale trials have been used for the amount of binder required and the final moisture content of the product (15 wt%). The additional binder for added granule strength suggested is molasses, and data gained from lab trials is used as the basis for the required quantity and concentration of the molasses binder, a 10 wt % solution and 25 wt% solution of molasses have been evaluated.

Table 5.5: Summary of economic parameters

| Parameter	Value	Justification
Project life [years]	1 + 12	1 year design & installation and 12 years operation
Internal rate of return (IRR)	10%	Assumes public rather private financing
CAPEX (rotating comp.) A$M	2 (for 2 tph evaporation rate)	Exponential scale factor 0.85
CAPEX (static comp.) A$M	2 (for 2 tph evaporation rate)	Exponential scale factor 0.6
Fixed operating costs	7% of CAPEX	1%insurance, 1% maintenance and 5% labour
Natural gas costs	$4/GJ	
Steam revenue	$5/tonne	Low pressure steam
Raw lignite cost [AUD/tonne]	9.0	Run of Mine 65wt% moisture
Water (binder cost)	Nil	Water removed from the product as steam is condensed and used as binder
Urea prill cost[USD/tonne]	250-330	(exchange rate 1USD is 1.307 AUD)
Molasses [USD/tonne]	250-350, average $300 used	(exchange rate 1USD is 1.307 AUD)
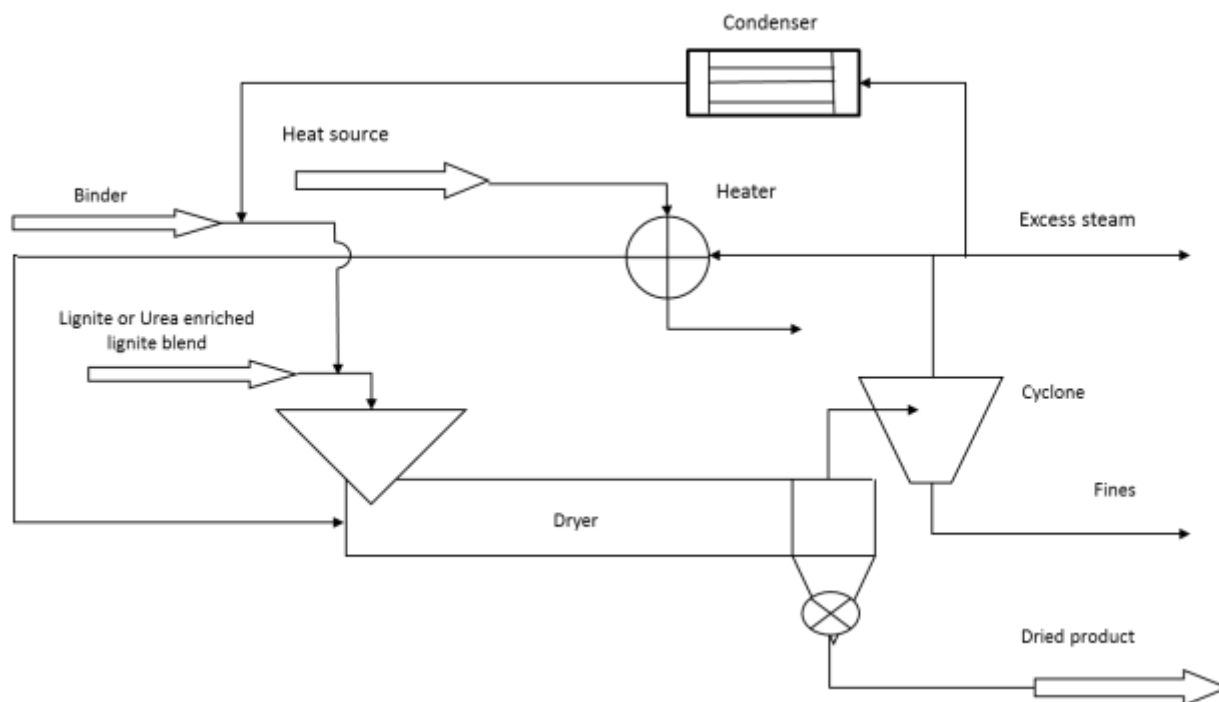
Figure 5.1: Schematic flowsheet of granulation and drying process

Basic calculations used for the analysis of lignite only granules are shown below, the addition of urea and molasses changes the mass balance calculations, but the economic analysis is modified to include the additional raw material costs and account for the change in water removal per tonne of product:

Pilot Data

Mass of lignite (kg)	1
Mass of additional water binder (kg)	0.18
Moisture content of raw lignite (%)	65
Final product moisture content (%)	15

Mass balance

Output 1 tonne product			Required input		
Solid mass (t)	=0.85*1	product solid fraction* mass of output	Wet coal	=0.85/0.35	solid fraction output/ solid fraction input
Water (t)	=0.15*1	product water fraction* mass of product	Water in wet coal	=(0.85/0.35)*0.65	wet coal mass*water content fraction
			Additional binder	=(0.85/0.35)*0.18	wet coal mass* binder requirement
Water removed	=((0.85/0.35)*(0.65+0.18))-0.15*1	Total water in- water in product			
Excess steam generated	=((0.85/0.35)*0.65)-0.15*1	Water removed-additional binder			

Costing

Costs

Cost raw coal per tonne product   =cost of lignite * lignite required for 1 tonne product

Cost of water removal   = mass of water removed *cost heat for removal of 1 tonne water* heater efficiency

CAPEX Cost of rotating and static components of plant
OPEX 7% CAPEX as defined

Operating hours/year 8000

Revenue

Steam revenue   =steam price * excess steam generated

Product revenue   =product price *production rate

Where product price is determined as the minimum price required to breakeven after 12 years of operation (ie. NPV=0)

Net Present Value (NPV)   =sum of return for each year of operation - CAPEX

Return for year x (IRR= 10%)   =(revenue -costs)/(1.1^x)

Results

The breakeven product price against the drying capacity and production rate of the dryer are shown in Figure 5.2 and Figure 5.3 respectively.
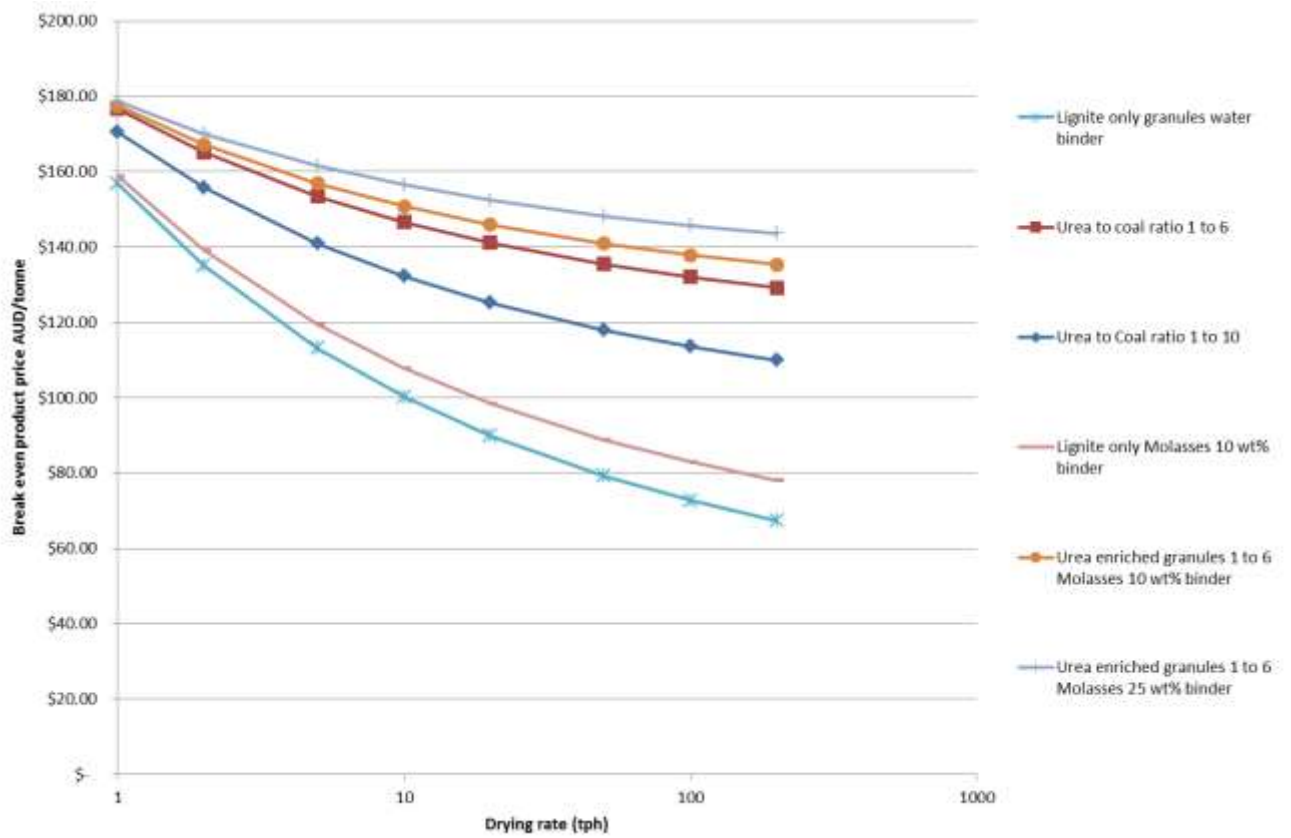

Figure 5.2: Breakeven product price for all products against drying rate
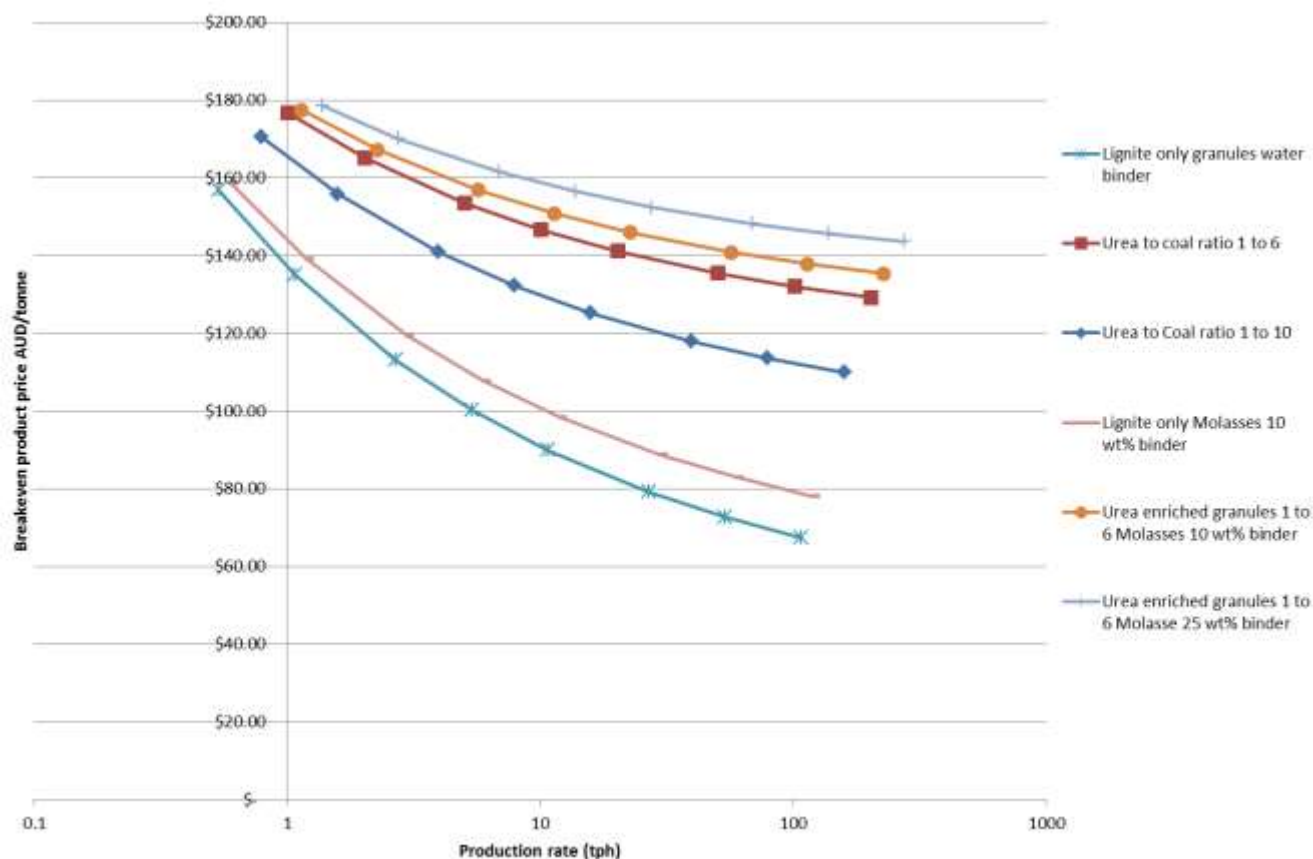
Figure 5.3: Breakeven product price against production rate

Lignite only granules

The formation and drying of the granules has increased the solid content of the product from 35% to 85%, and improved the handling properties and calorific value of the product. The lowest breakeven product price 68 AUD/tonne, just over 3 times the cost of the raw materials (one tonne of product requires 2.4 tonnes raw lignite). Further analysis would be required to determine if this price was comparable to the market value of the product, this would determine if the process for lignite alone were economically feasible. The lowest breakeven costs are seen for a drying rate of 200 tph, which equates to a production rate of 107.2 tph.

Urea enriched granules

The lowest breakeven product price for all products is seen for a drying rate of 200 tph. The introduction of urea to the brown coal increases the minimum breakeven product price to 130 AUD/tonne for 1:6 ratio and 110 AUD/tonne for 1:10 ratio. Compared to the cost of the urea prills at 250 USD/tonne, if the bioavailability of the nitrogen within the fertilizer product is sufficiently improved and loss of nitrogen by leaching and reduced emission of nitrous oxide gases is significant, this product price may be such that the market value of the product is equal to or greater than the breakeven prices calculated and therefore provides an economically favourable process.

Granules made with molasses as a binder for added strength

The addition of the molasses to bind the granules reduces the drying load by reducing the amount of water binder added and contributes to the solid component of the product, thus reducing the wet coal requirement per tonne of product, thus reducing the drying load per tonne of product. However the increased raw material costs are slightly greater than the reduced drying costs (molasses cost 300 USD/tonne compared to 9AUD/tonne for lignite and 0 AUD/tonne to use water reclaimed from drying.) The breakeven price for the Lignite only molasses bound granules (78 AUD/tonne) compared to the lignite only granules (68 AUD/tonne). The urea enriched granule breakeven product price is increased from 130 AUD/tonne for water bound granules to 135 AUD/tonne for the molasses bound granules.

Further Investigations

An evaluation of the value added to the lignite only granules must be assessed to ascertain if the product price can be achieved for the process to become economic. An important part of this further assessment may be the cost of transportation and handling of the product versus the raw lignite transportation costs. When used at the mine for power generation this cost is minimal, however, as an export product, the reduction in water content may be sufficient to make the process economic.

The benefits to soil retention and reduction in emission of greenhouse gases (nitrous oxides) for fertilizer products that are enriched into lignite granules may determine the economic success of the granulated product. Further understanding of these product properties and formulation optimization are required to fully assess this.

Appendix 6: Draft publications

The Effect of Densification on Brown Coal Physical properties and its Spontaneous Combustion Propensity

Mohammad Reza Parsa[1] ,Yoshimitsu Tsukasaki[1, 2], Emily L. Perkins[1,3], Alan L. Chaffee[1]*

[1] School of Chemistry, Monash University, Clayton, Victoria, Australia,

[2] Nippon Steel and Sumitomo Metal Corporation, 6-1 Marunouchi 2-chome, Chiyoda-ku, Tokyo, 100-8071, Japan

[3]Department of Chemical Engineering, Monash University, Clayton, Victoria, Australia

Abstract

The utilization of brown coal is strongly limited by its high moisture content which makes dewatering/drying a necessary process, particularly for export. Yet, dried brown coal is susceptible to spontaneous combustion under ambient conditions and its use therefore has been restricted to the site at which it is mined. One such product, for which, relatively little studies have been carried out is densified brown coal pellets. In this work the densification process, where brown coal is extruded after mechanical kneading and then allowed to air dry slowly to form a product known as 'densified coal', was applied to reduce the moisture content and spontaneous combustion tendency of two Victorian brown coals. NaOH at different concentrations (0.5, 1 and 1.5 M) was used as an additive in the kneading process. The spontaneous combustion of coal samples was evaluated by the wire basket method. The physical and chemical properties of densified products such as Vickers hardness, equilibrium moisture content, moisture content, CO_2 surface area and pore distribution of the densified products were measured and scanning electron microscopy (SEM) was used to examine the morphology and surface texture.

The results showed that the densification process is a very effective drying method for brown coal reducing its moisture content from 60% to around 12%. The wire basket tests showed that the critical ignition-temperature (T_{cr}) of densified products was significantly increased by increasing the NaOH concentration. Also as the concentration of NaOH increased the Vickers hardness value increased and the SEM image indicated that the coal particle surface changed from spongy and porous for raw coal to very smooth and contiguous with lines of apparent shrinkage. This correlated with a progressive decrease in CO_2 surface area, porosity and mercury surface area determined by mercury intrusion porosimetry.

Keywords: Brown coal, Densified pellet, Self-heating, Surface area, Surface morphology

1. Introduction:

The state of Victoria in Australia possesses 25% of the known world reserves of low rank coal. Victorian brown coal is a very significant source of energy because of its potential for open-cut mining (lower mining cost), high reactivity and low ash content and has the potential to remain the major energy source for the local economy in the future[1]. The main obstacle to develop Victorian brown coal usage is its high moisture content, typically around 60 %, which requires energy to remove the water in order to decrease transportation costs, ease loading and unloading, CO_2 emissions and increase power plant efficiency.

However, dried brown coal easily disintegrates into fine dust which results in an increase of spontaneous combustion propensity [2, 3]. Spontaneous combustion of coal is one of the most serious issues in the world's coal industry causing many problems such as the difficulty of transportation of coal over large distances, fires safety concerns, storage issue and long-term environmental problems [4]. Spontaneous combustion takes place when the accumulation of heat within carboniferous materials resulting from some low temperature chemical and/or physical processes is faster than the release of heat into the environment [5, 6].

Many techniques have been proposed for removing the water from brown coal by evaporative and non-evaporative techniques. Non-evaporative techniques such as hydrothermal dewatering [7], mechanical thermal dewatering [8] and the densification process [9] have advantages that include a reduced energy requirement and less severe conditions to remove the water from the coal [7, 10]. The optimum drying process would require minimal energy, produce a product of sufficient strength that it can be handled without attrition and has a reduced propensity to spontaneously combust.

The densification process developed in the late 1980s [9] transforms run-of-mine brown coal into a dense, dry, hard product. The process begins by shear attrition using a batch or continuous kneading process which leads to forming coal slurry of plastic quality. Applied shearing stress releases water from the cellular structure of the coal, forming a smooth and wet plastic mass during the kneading stage. The slurry is extruded under modest pressure to produce pellets of the desired shape and size. Finally, the pellets are air-dried at room temperature forming hard and dense coal pellets with a high crushing strength [9, 11].

In this paper the effect of the densification process with NaOH as an additive on brown coal physical properties and spontaneous combustion tendency were investigated.

2. Experimental

2.1. Coal samples:

Two Victorian brown coals, Morwell and Loy Yang low ash (LYLA), have been used in this study originating from the Latrobe Valley, Victoria, Australia. Table 1 shows proximate and ultimate analysis of both coals. The Campbell Microanalytical laboratory at the University of Otago carried out the ultimate analysis. The inorganic content of the coal samples are given in Table 2. Received samples were milled to <3 mm and then homogenised for the densification process. All samples were ground and sieved to <0.018 mm before all other analytical tests.

Table 1: Ultimate analysis and proximate analysis of Loy Yang and Morwell run-of-mine coal

sample	Moisture (% as received)	Proximate Analysis (% dry base)			Ultimate Analysis (% dry base)				
		Ash	Volatile	Fixed carbon	C	H	N	S	Cl
Morwell		1.9	48.4	49.7	67.4	4.5	0.5	0.24	0.06
LYLA		3.5	49.4	47.2	65.7	4.7	0.6	0.66	0.11

In order to remove inorganic matter, an acid washing procedure was carried out by placing 100g (wet) coal in 1.5 l conical flasks with 1 l hydrochloric acid (1.5M concentration) and stirred for 24 hours. Samples were vacuum filtered and further washed with deionized water and vacuum filtered to remove acid. This rinsing procedure was repeated until the pH of sample became constant. Water washed samples were also rinsed in the same way, so as to mimic any effects of further washing on the coal as experienced by acid washing.

Table 2: Inorganic matter analysis of Loy Yang and Morwell run-of-mine coal

Inorganic	Morwell		LYLA	
	% of ash	g/100g db	% of ash	g/100g db
SiO_2	2.9	0.10	56.6	1.98
Al_2O_3	1.0	0.02	19.2	0.67
Fe_2O_3	14.8	0.28	2.3	0.08
TiO_2	0.1	0.002	8.0	0.28
K_2O	0.2	0.004	0.2	0.007
MgO	20.1	0.38	2.4	0.084
Na_2O	2.3	0.044	4.1	0.14
CaO	36.0	0.68	1.0	0.035
SO_3	22.2	0.42	5.4	0.19
P_2O_5	0.0	0	0.2	0.007

2.2. Densification process

The process begins by applying shear attrition to 100g of wet coal and 35g water (or NaOH solution) using a IKA HKD T0.6 laboratory kneading machine (Figure 1a). During the kneading stage, the structure of the coal collapses under the applied shearing stress and water within the coal structure is released. After 1 h of kneading with a torque of 25 Ncm and speed of 120 rpm a smooth coal dough with plastic quality and approximately 5–10 μm particle size is produced. The constant ratio of water to solid was applied to washed samples with higher initial moisture content. NaOH addition is defined in terms of the equivalent mass to give the quoted molarity in 35 g of solution.

Next, the dough is extruded through an 8mm diameter steel nozzle under modest pressure using a compressed air driven rod (Figure 1b). The extruded material was collected on a tray and cut into 5-10mm length pellets with a scalpel. Finally, the pellets were air-dried at room temperature for at least 72 hours forming hard and dense coal pellets [9, 11].
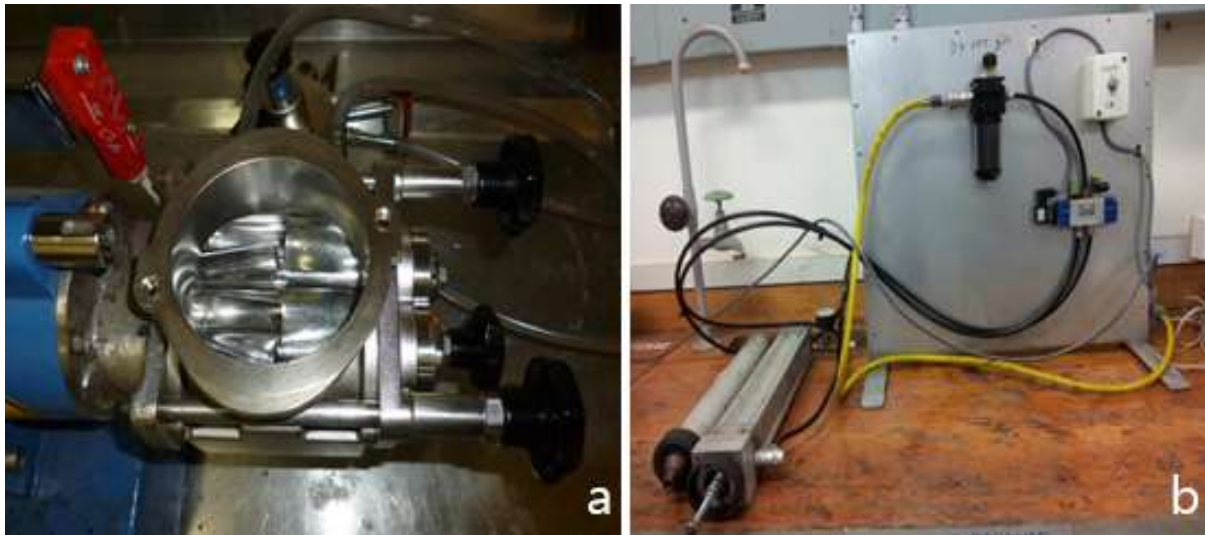

Figure 4: A) Laboratory kneader B) Extrusion apparatus using compressed air driven rod

2.3. The wire basket method

The procedure for the wire basket experiment is more fully described elsewhere [12], briefly, the test procedure is outlined: The temperature at which the coal temperature begins to exceed the surrounding temperature is the so-called critical temperature (T_{cr}). 10-13 g of sample, which varies according to packing density of sample, was loaded to fill 1 inch^3 stainless-steel mesh cube basket. The loaded basket was fixed to a sample holder. Three K-type thermocouples were inserted vertically in the middle of the sample, one at the centre of the basket and the other two half way between the centre and the two opposite outside edges of the cube. A fourth thermocouple was positioned to measure the actual oven temperature. The wire basket was suspended in a fan forced oven which could be heated to a pre-set

temperature to observe the combustion behaviour of the sample. At the start of the experiment, the oven was set to the desired temperature. Fan forcing maintained the air flow during the experiment. The temperature measured by the thermocouples was continuously logged. To obtain T_{cr} for a sample the wire basket experiments were repeated for different oven temperatures, at $2^{o}C$ intervals. The T_{cr} of each sample was determined by averaging the lowest temperature at which the thermal runaway occurred and the highest temperature at which the thermal runaway did not occur. The higher value of T_{cr} shows lower spontaneous combustion propensity [13].

2.4. Physical analysis methods

To measure the moisture content of the coals and products a 5 g sample of crushed and sieved to < 0.018 mm material, was dried in an oven at $105^{o}C$ under nitrogen flow for 3 h [1] and re-weighed. Tests were carried out in duplicate and moisture content was calculated according to equation 1.

$$\text{moisture content (\% wet basis)}=100\times \frac{\text{mass of coal before drying-mass of coal after drying}}{\text{mass of coal before drying}} \qquad [1]$$

Equilibrium moisture contents at relative vapour pressures (RVP) of 11.3%, –51.4% and 92.3% were determined by putting 4.5–5.5 g representative samples into glass dishes, the open dishes were placed in desiccators, each containing a different saturated salt–water mixture chosen to give a RVP values at $30^{o}C$ [14, 15]. A minimum equilibration time of two weeks was allowed for all samples. The total ash content of the samples was measured following the standard ashing procedure [16].

Coal samples were analysed for inorganic content by ICP-OES, according to the method developed by Low and Zhang [17] using the equipment and experimental parameters

described in [18]. Samples of coal or pellets were dissolved by microwave digestion at 1200W without the use of hydrofluoric acid.

The Vickers hardness test method was carried out by using a Wolpert Wilson Vickers hardness tester (model: 432SVA) under ambient laboratory conditions. A pyramid shape diamond with a square base and an angle of 136 degrees between opposite faces applied a load of 1 to 10 kgf on densified pellets of brown coals. The full load was kept for 15 seconds [19].

The surface area was calculated from CO_2 adsorption measurements at 0 ^oC analysed using the Dubinin–Radushkevich equation [20]. The molecular area of CO_2 was taken 0. 254 nm^2. The 100 mg of powder sample <0.018mm was placed into the analysis tube and moisture removed from the pre-dried sample by degassing at 105 ^oC overnight before the analysis. The analysis was carried out on the Coulter OMNISORB 360 CX or the Micromeritics Tristar II.

Mercury intrusion and extrusion curves were measured on a Micromeritics AUTOPORE IV, 1327. Pellet samples were crushed and sieved to have particle size <0.018 mm and after drying at 105° C, approximately 0.25 g of sample were added to calibrated 3 ml powder penetrometers. Measurements were performed by applying pressures between 3.6 kPa to 413 MPa, according to the Washburn equation for cylindrical pores [7], equates to a pore diameter, d ranging from 0.0030 to 341 µm at a surface tension of 0.485 N m^{-1} and a contact angle of 130°. In order to avoid any error caused by mercury compressibility and penetrometer deformation, all obtained data was modified by subtracting them from a blank test carried out on the empty penetrometer. All results are expressed on a volume per gram of dry coal basis. Pore size distributions, macro, meso and micro pore were determined from the intrusion curves, as per the method described previously by Bergins et al. [21].

Morphology of the samples was obtained by using field emission gun scanning electron microscope (FEG/SEM), Nova NanoSEM 450 operated at 5 KV.

3. Results and discussion

3.1. Wire basket results

The wire basket results of densified products from raw and acid washed LYLA coal, raw and acid washed Morwell and densified products with NaOH are given in Figure 2. Acid washing of brown coal resulted in higher critical temperature (T_{cr}) because of removing acid-extractable metals. Also the densification of all coals without NaOH resulted in slightly higher propensity to spontaneous combustion compared to their not densified coals by showing lower T_{cr} . In both series of LYLA coals (raw and acid washed), spontaneous combustion propensity first increased (lower T_{cr}) with adding of 0.5 M NaOH and after that decreased for 1 and 1.5 M NaOH. The wire basket results of raw LYLA and acid washed LYLA showed that all acid washed samples had higher T_{cr} than the raw coal equivalent samples.
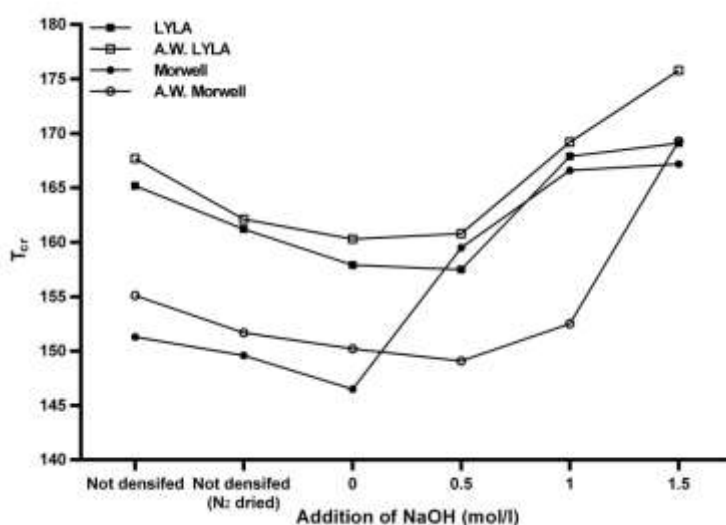
Fig. 2. Wire basket test results for densified products of raw and acid washed LYLA and Morwell coals.

37

The trend of T_{cr} was incremental for densified raw Morwell with increasing concentration of NaOH reaching 167°C for densified with 1.5 M NaOH from 147°C for densified with no NaOH addition. On the other hand, the T_{cr} values for the acid washed Morwell densified products with NaOH tended to decrease with adding of 0.5 M NaOH and after that increased for 1 and 1.5 M NaOH, similar to LYLA coals series.

3.2. Moisture content

The values of moisture content for raw, washed and acid washed coals before and after densification are given in Figure 3. The moisture content of coals after drying under nitrogen is also shown in Figure 3. The densification dewatering process of brown coals followed with air drying significantly reduces the moisture content of all products. The original moisture content for raw, water washed and acid washed LYLA were 57%, 71% and 69% respectively and after densification dropped to approximately 15%, 20% and 15%, as shown in Figure 3.

Similar decreases in moisture content were observed for raw and acid washed Morwell coal, decreasing from 60% and 66% to 15% and 14% respectively. The reduction in moisture content emphasises the important role of shear attrition on the coal particles during the kneading stage, that breaks down the coal pore structure and releases significant amounts of loosely bound water [22]. These values are comparable to those previously measured for densified coal made from brown coal from the Morwell seam, 15.9% [9] and those from the Loy Yang and Morwell seams of ~16% [22]. Acid washed and unwashed coal densified products appear to have slightly lower moisture content than that of water washed coal. It seems that the densification of brown coal with different concentrations of NaOH did not have significant effect on the moisture content of the densified products.

The results of studies reporting the effect of moisture content on the coal spontaneous combustion behaviour are complicated and sometime contradictory [23-32]. The presence of

a large quantity of water reduces the tendency of self-heating of coal by reducing the number of radical sites where oxidation can take place and obstructing the oxygen molecules access to the coal structure. In addition, the high moisture content postpones the self-heating by adsorbing the heat released by oxidation [28].

It is known that partial drying of coal decreases the T_{cr} as a result of higher exposure of the coal to oxygen until a minimum and after that increases again with further decreases of the moisture content [3, 33].

The reduction of moisture content by drying raw coal at $105^{o}C$ under nitrogen and densification without NaOH increases the oxidation at low temperature resulting in lower T_{cr} values. For densified coals with NaOH addition, any effect of moisture on T_{cr} is masked by the effect of NaOH addition. Although the moisture content of densified coals with NaOH were similar to densified coal without NaOH their T_{cr} were significantly different, inferring that NaOH addition is the dominating factor on T_{cr}..
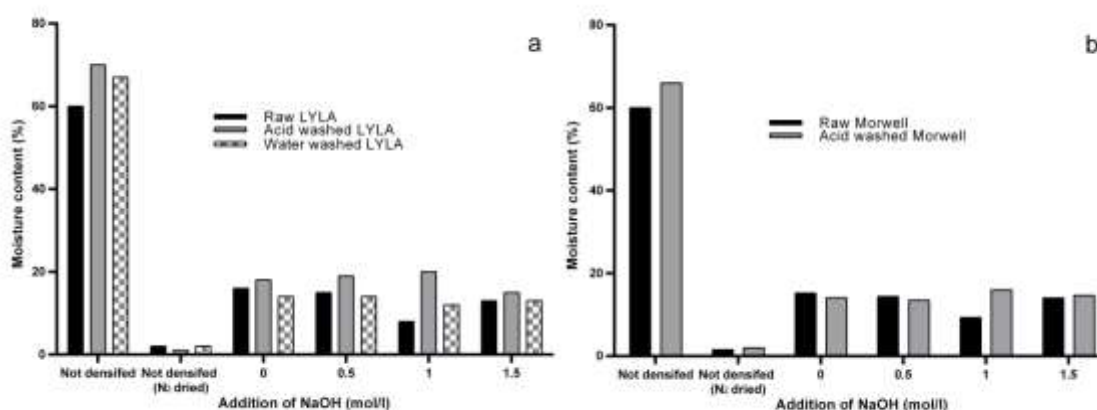
Figure 3: Moisture content of air dried densified pellets made with raw, water washed and acid washed coal with various additions of NaOH a) LYLA and b) Morwell

.

3.3. Inorganic matter and ash content

One of the important factors responsible for spontaneous combustion of brown coal is the inorganic content. Figures 4a and b show the inorganic content of raw, acid washed and water washed LYLA and raw and acid washed Morwell. It can be seen from Figure 4 and table 2, that the amount of Fe, Mg, Ca and S in Morwell coal is more than LYLA, and Na, Al and Si exist higher amounts in LYLA. It has been reported [13] that Fe and S increased the propensity of spontaneous combustion of brown coal which can explain the lower T_{cr} of Morwell coal compared to LYLA. On the other hand, Al and Si suppress the spontaneous combustion helping to postpone the LYLA T_{cr} to a higher temperature [34]. The acid washing of both coals demineralized the coal significantly. The higher T_{cr} of acid washed sample compared to raw coal can be attributed to the effect of removed inorganic material from coal.
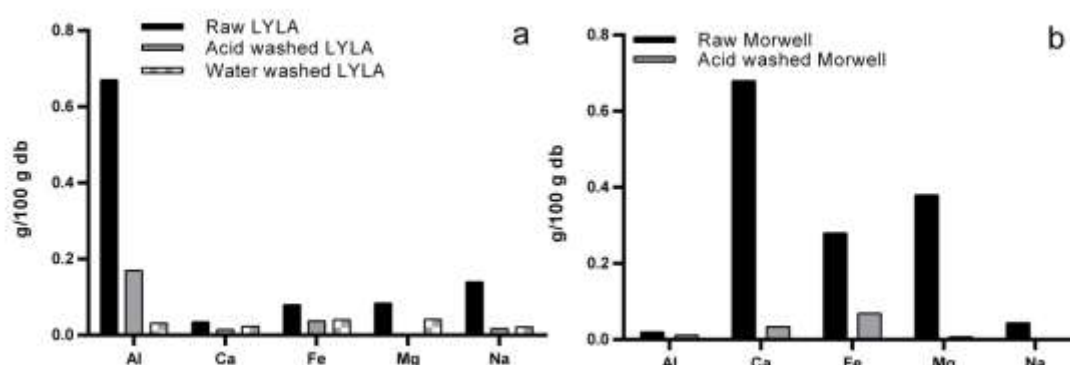
Figure 4: Inorganic content of raw, water washed and acid washed coal with LYLA-a and raw and acid washed Morwell-b.

Ash contents increase with increasing addition of NaOH, this is to be expected as the NaOH addition provides additional Na ions, thus adding to the ash content of the coal. This observation is consistent for samples made from both coals and all wash types. Both water washing and acid washing reduce the inorganic contents and therefore the ash contents of the not densified washed coals are lower than raw coals (see Figure 5).
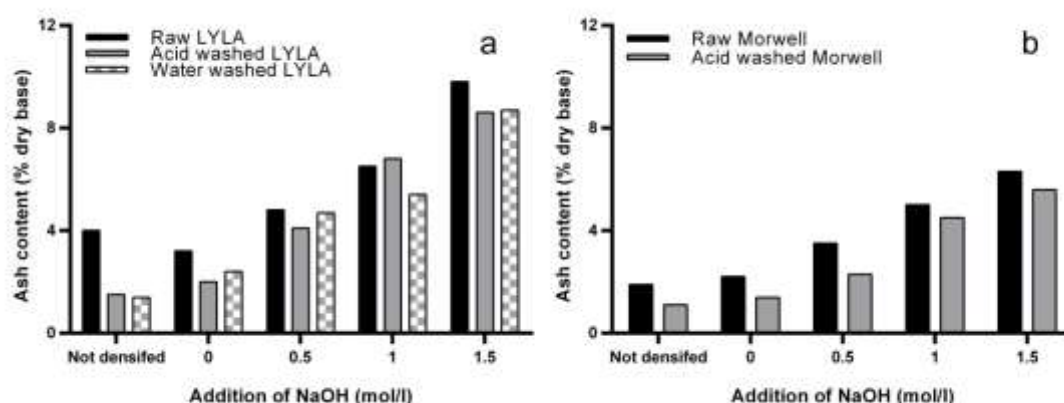
Figure 5: Ash content of air dried densified pellets made with raw, water washed and acid washed coal with various additions of NaOH a) LYLA and b) Morwell

3.4. Equilibrium Moisture Content

Table 3 shows that in all series of samples, the densification process reduced EMC at all RVP tested compared to their raw not densified coals. The effect of washing coal with water and acid was not significant on EMC for both coals, even though it has previously been reported that acid washing can decrease the EMC for some coal types [35].

Table 3: Equilibrium moisture content at relative vapour pressure 11.3 %, 51.4 % and 92.3 % for densified and not densified raw, water and acid washed LYLA coal and raw and acid washed Morwell

			LYLA EMC (mmol/g db)			Morwell EMC (mmol/g db)		
			RVP			RVP		
			11.3%	51.4%	92.3%	11.3%	51.4%	92.3%
Raw	Not densified		2.9±0.1	9.8±0.5	32.8±1.5	3.1±0.3	8.9±0.7	31.2±3.1
	Densified with NaOH	0 mol/l	1.8±0.1	5.7±0.7	5.9±0.3	2.8±0.2	5.5±0.0	14.6±0.9
		0.5 mol/l	2.1±0.7	5.4±0.5	11.2±0.6	2.3±0.4	5.0±0.3	11.6±0.9
		1.0 mol/l	2.0±0.5	5.9±0.6	11.6±0.5	1.9±0.5	5.1±0.4	9.7±0.5
		1.5 mol/l	2.7±0.1	7.0±0.0	17.7±0.2	2.0±0.4	4.2±0.0	10.4±0.4
Water wash	Not densified		2.5±0.1	8.2±0.5	33.3±3.1			
	Densified with NaOH	0 mol/l	2.1±0.5	5.9±0.1	9.3±0.9			
		0.5 mol/l	1.9±0.6	5.5±0.4	11.6±0.5			
		1.0 mol/l	1.7±0.6	5.2±0.5	11.5±1.1			
		1.5 mol/l	2.6±0.1	6.5±0.0	16.1±1.0			
Acid wash	Not densified		2.7±0.1	9.0±0.2	43.5±1.3	3.5±0.4	9.9±0.6	41.5±2.5
	Densified with NaOH	0.0 mol/l	2.2±0.5	5.8±0.3	10.4±0.2	3.0±0.1	6.1±0.1	15.4±2.0
		0.5 mol/l	1.9±0.5	5.5±0.5	10.8±0.1	2.4±0.2	5.9±0.6	13.8±1.1
		1.0 mol/l	2.1±0.7	5.5±0.2	11.2±1.0	2.4±0.1	5.6±0.4	13.3±0.5
		1.5 mol/l	2.3±0.1	6.2±0.2	15.3±0.5	2.1±0.1	5.2±0.2	10.7±1.0

The uncertainties are 90% confidence limits based on duplicate or triplicate determinations.

The brown coal oxygen containing functional groups especially carbonyl, hydroxyl, and carboxyl groups play important role on its hydrophilic nature leading to the sorption of water vapour on the surface, even though the degree of importance of each of them is unknown [36, 37]. It seems that by increasing the concentration of NaOH addition to Morwell coal, its surface became a little less hydrophilic implying a slight decrease in value of EMC for raw and acid washed Morwell coal at all RVP, whiles the densification of coal with NaOH didn't have a significant effect on LYLA coal.

3.5. Vickers Hardness determination

The Vickers hardness index (Figure 5) indicates an increasing trend with an increased addition of alkali within the kneading process, this is in agreement with previous work that measured the crushing strength of densified brown coal [22]. Pandolfo and Johns [22] reported that the addition of an alkali during the kneading process affects the coal structure in two major ways, firstly it solubilizes part of the coal and redistributes these soluble humic components within the internal pore structure of the coal, secondly the surface functionalities of the coal are changed to have more $-O^-$ and $-COO^-$ groups. In other words, by increasing the concentration of NaOH, pH increases which consequently changes the form of acidic functional groups from $-OH$ to $-O-$ and $-COOH$ to $-COO-$. This causes the weak hydrogen-bonding interactions within the coal structure that exist in an acidic natural environment are replaced with stronger van der Waals bonds in high pH environments leading to the generation of a more firm network structure.

Whilst the water washed and without wash starting coals have similar values of Vicker's hardness, the acid washed coal densified pellet appear to have a lower hardness index value than the water washed and without wash equivalents. It could be due to removing some

effective inorganic matter on hardness from coal structure by acid washing. This is consistent with the results found for crushing strength [22] where acid washing created a less dense, more porous structure that had reduced crushing strength.
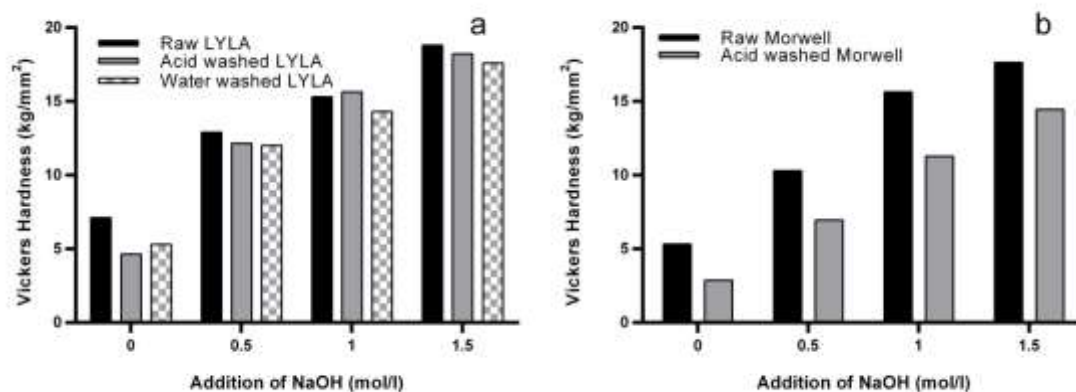

Figure 5: Vickers hardness index for raw and acid washed densified a) LYLA and b) Morwell coal pellets with varying additions of sodium hydroxide

3.6. CO_2 surface area results

The CO_2 surface areas of densified products are given in Figure 6. Water washing and acid washing the raw coal has little effect on the surface area, in agreement with earlier work [35]. The results also revealed that densification of raw and acid washed coal with NaOH decreased the CO_2 surface area significantly. The decrease of CO_2 surface areas was in direct correlation with increasing the NaOH concentration. Previous work has shown that the addition of sodium ions had a significant effect in reducing the surface area measured by CO_2 adsorption [35]. As mentioned above, it seems that the main reason of decreasing the surface are by rising the amount of NaOH is that the addition of NaOH generates strong van der Waals bonds interactions within coal structure and tightens the coal structure together more strongly.
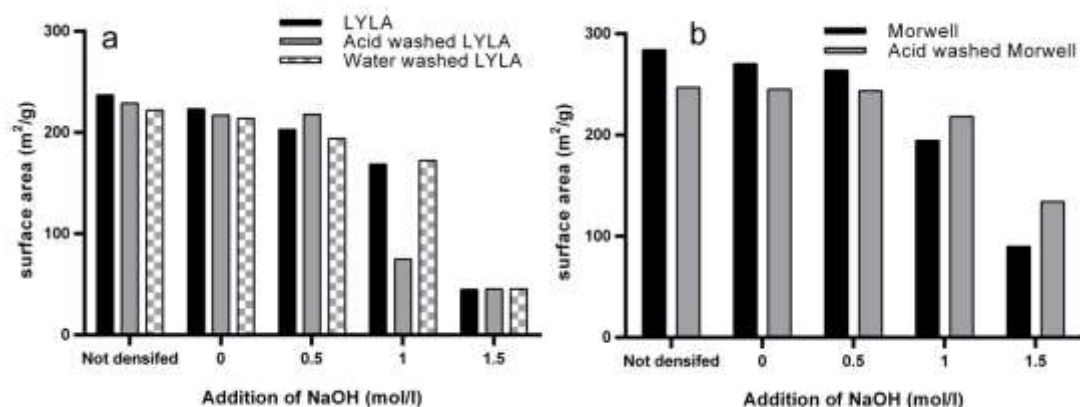
Figure 6: The CO_2 surface area of raw coal, water washed and acid washed a) LYLA and b) Morwell coal and densified pellets with additions of NaOH at 0^oC

Due to the molecular dimension of CO_2, the CO_2 surface area measurement is calculated from the adsorption of CO_2 molecules in the micropores of the coal structure, therefore a decreased surface area value is indicative of a decreased micropore volume [38]. Chemical interactions between coal particles and molecules of O_2 take place predominantly at internal surfaces of coal particle pores [6, 39]. It has been suggested that the available internal surface area has a significant effect on the self-heating phenomena of coal by controlling the rate of oxidation [40-42]. A reduction of surface area reduces the number of active sites available to interact with oxygen during the oxidation process at higher temperature leading to a lower tendency to spontaneous combustion.

It has also been reported that the decrease in surface area may cause a reduction in concentration and increased stability of hydroperoxy groups which are radicals within the coal structure that are responsible for reactions with oxygen molecules at low temperature and consequently, a reduced surface area leads to a delay in these oxidation reactions [41].

3.7. Mercury intrusion porosimetry results

Mercury intrusion porosimetry is a common means to obtain the pore size distribution of densified coal by measuring the volume of intruded mercury at a given pressure. The pore size distributions of raw, acid washed and water washed LYLA are shown in Figure 7. The intrusion volumes have been corrected for by removing compressibility effects and results have been shown as logarithmic differential intrusion curves.   The inter/ intra particle boundary (at 50 µm) and macro and meso ranges are marked on the graphs to aid the interpretation.   Figure 7 shows the major part of pore volume of all samples are in the macropore size region and by increasing the concentration of NaOH the distribution curves
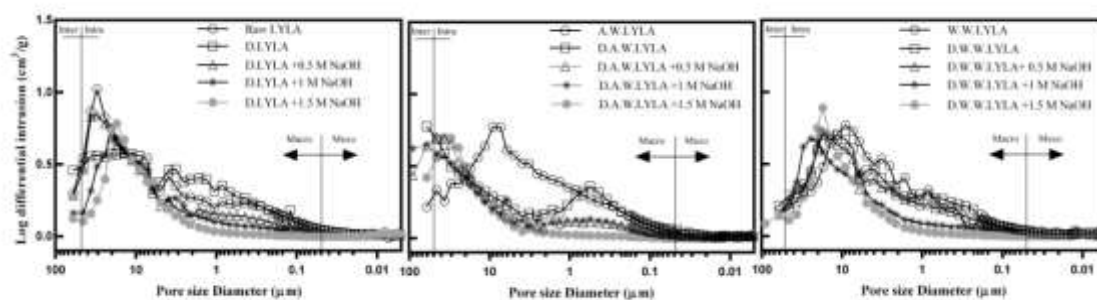
flatten significantly.

Figure 7: Effect of densification with NaOH on the logarithmic differential mercury intrusion of (a) raw, (b) acid washed and (c) water washed LYLA coal.

Figure 8 shows the raw and acid washed Morwell pore size distributions. The increase of NaOH concentration caused the same flattening effect of pore size distribution curves on Morwell coal densified products as seen with LYLA.
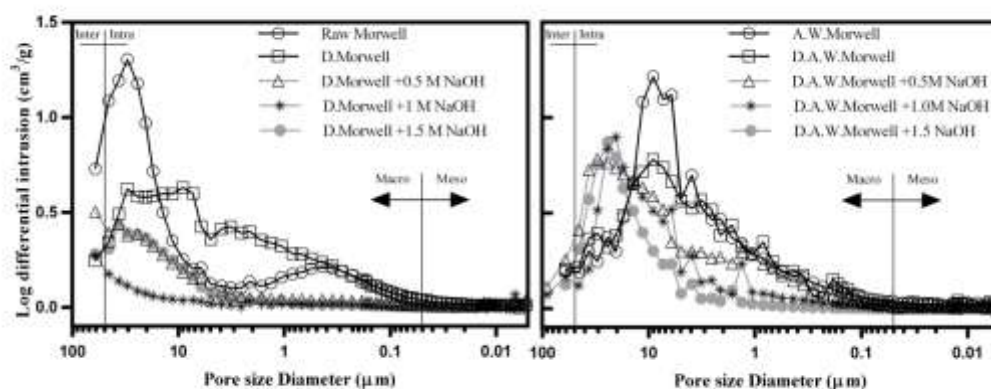
Figure 8: Effect of densification with NaOH on the logarithmic differential intrusion of (a) raw, (b) acid washed and Morwell coal.

A summary of the surface area and mean pore diameter determined from mercury intrusion porosimetry for all samples tested is given in Table 4. As seen in Table. 4, by increasing the concentration of NaOH, a shift in the corresponding mean pore diameter of samples to larger diameters occurs. The densified acid washed samples with NaOH showed higher mean pore diameters than densified water washed and raw LYLA coal samples.. Whereas the mean pore diameter of raw Morwell densified products were higher than those of the acid washed ones.

By increasing the addition of NaOH, the mercury surface area dropped in accordance with the corresponding decrease in macro, meso, micro and total pore volumes (Figure. 9a) from around 22 m^2/g for not densified coals to around 12 m^2/g for densified coals with 1.5 M NaOH. No significant difference among mercury surface area of densified products made from raw, acid washed and water washed coals was observed (Table 4).

Table 4: Mercury surface area and mean pore diameter of raw coal, water washed and acid washed a) LYLA and b) Morwell coal and densified pellets with additions of NaOH

			LYLA		Morwell	
			Mercury surface area ($m^2 g^{-1}$)	Mean pore diameter (μm)	Mercury surface area ($m^2 g^{-1}$)	Mean pore diameter (μm)
Raw	Not densified		21.7±0.5	10.4±0.2	19.3±0.7	10.2±0.3
	Densified with NaOH	0 mol/l	18.0±0.3	8.8±0.3	16.0±0.4	9.2±0.2
		0.5 mol/l	17.0±0.2	13.7±0.5	17.1±0.4	17.2±0.5
		1.0 mol/l	15.0±0.0	11.5±0.2	11.4±0.3	24.2±0.3
		1.5 mol/l	12.2±0.2	12.9±0.3	12.5±0.5	28.1±0.5
Water wash	Not densified		21.2±0.5	5.9±0.2		
	Densified with NaOH	0 mol/l	18.6±0.1	6.4±0.4		
		0.5 mol/l	15.8±0.3	7.6±0.3		
		1.0 mol/l	14.9±0.3	12.3±0.5		
		1.5 mol/l	10.8±0.4	13.5±0.5		
Acid wash	Not densified		23.4±0.3	5.3±0.4	21.8±0.6	6.2±0.1
	Densified with NaOH	0.0 mol/l	18.7±0.5	15.2±0.5	20.2±0.2	8.9±0.4
		0.5 mol/l	15.6±0.2	25.2±0.7	13.9±0.0	11.1±0.3
		1.0 mol/l	15.5±0.2	27.3±0.5	13.8±0.2	12.7±0.2
		1.5 mol/l	13.4±0.3	29.0±0.3	10.5±0.1	19.3±0.4

The water washing process produces an increase the microporosity of LYLA sample relative to raw LYLA and in contrast acid washing of LYLA coal caused a decrease in micropore volume. However, the water washed densified products with NaOH showed a more dramatic decrease of micropore volume compared to the densified raw and acid washed products with NaOH.

In general, as a function of increasing the concentration of NaOH, the macro, meso , micro and total pore volume show a decreasing trend for all three LYLA coal samples (Figure 9a) . This decrease in total pore volume was associated with a decrease in mercury surface area which was consistent with decrease in CO_2 surface area.

No significant change in micropore volume occurred for acid washed Morwell compared to raw Morwell. Even though the micro and meso pore volume of densified acid washed Morwell decreased more dramatically with increasing the NaOH concentration compared to densified raw coal samples, the lower volume of macropores for densified raw Morwell resulted in lower total pore volume for raw densified samples. This is in good agreement with

lower CO_2 surface area results for densified raw Morwell with NaOH samples when compared to the acid washed ones.
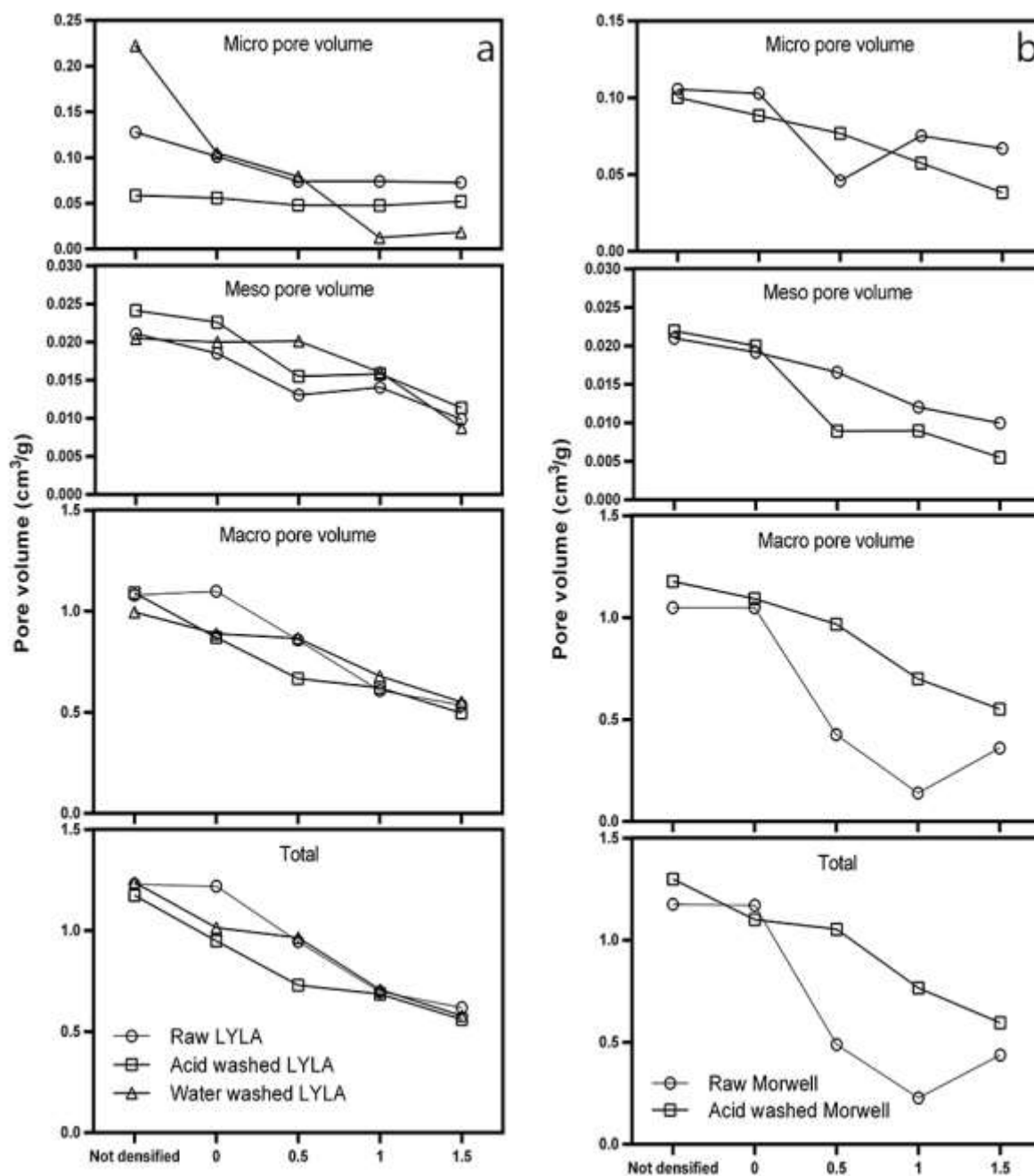

Figure 9: Macro, meso and micropore volume of raw, water washed and acid washed a) LYLA and b) Morwell coal and densified pellets with additions of NaOH.

It can be said that the reduction of micro, meso and macro pore volumes by increasing the NaOH concentration which result in lower total pore volume and mercury surface area are in

very good correlation with decreasing of T_{cr} for all series of samples in agreement with previous results [3].

3.8. SEM results

The SEM results revealed interesting features of densified coal with NaOH. As seen in Figure 10, by increasing the concentration of NaOH, the surface roughness of densified coal decreased where the surface morphology evolved from spongy and porous for raw coal to very smooth and contiguous with lines of apparent shrinkage for densified coal with 1.5 M NaOH. The layered shape of densified coals may be the result of the applied pressure on coal particles during the extrusion process. Another observation was the increase in the number of coal particles with smooth surfaces from densified coal with 0.5 M NaOH to 1M and 1.5M. SEM images of increasing smoothness compliment the results of CO_2 surface area and mercury porosimetry; which showed that the densified coal NaOH had much less accessible sites to interact with oxygen.
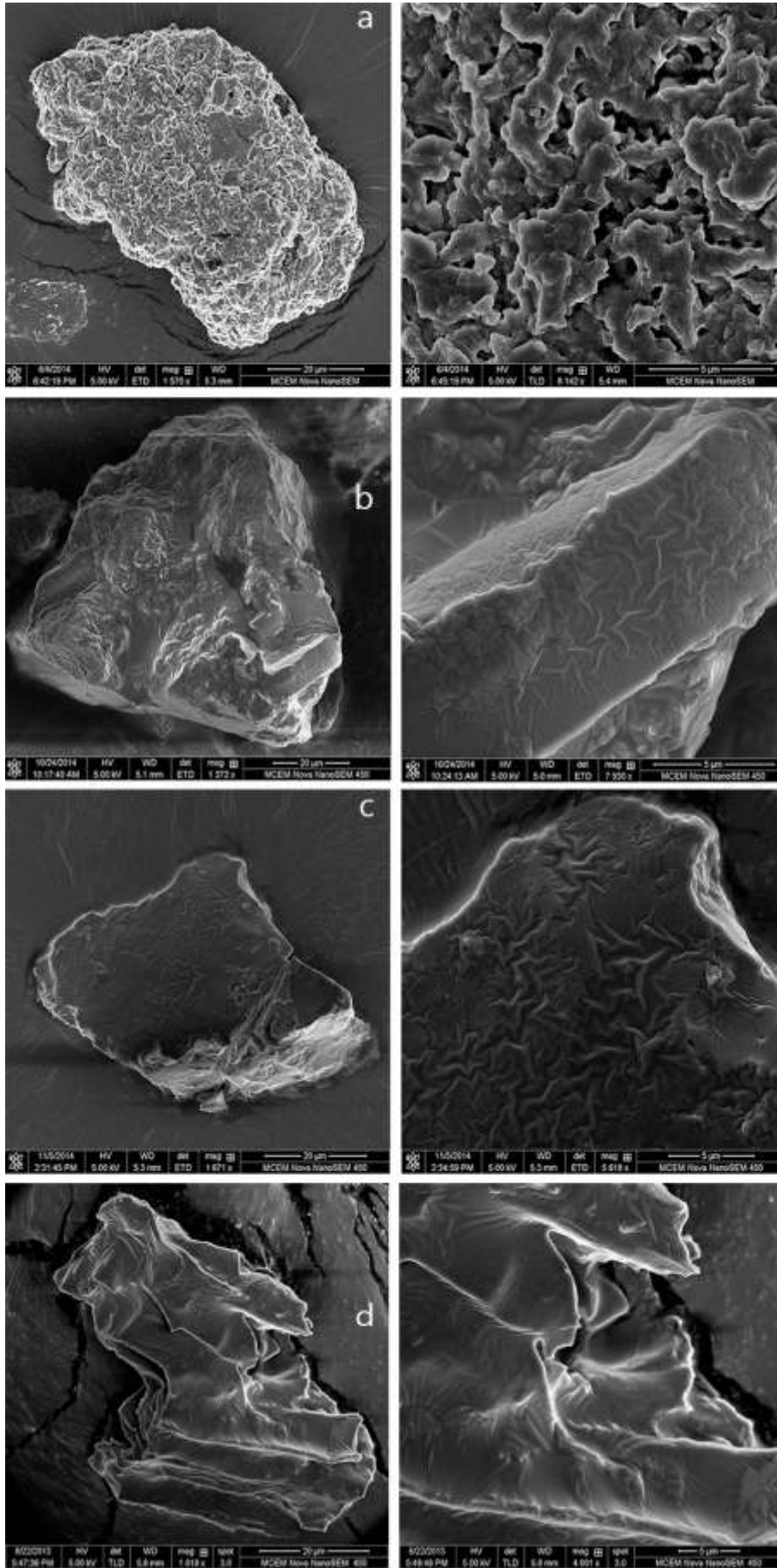
Figure 10: SEM images of a) raw LYLA, and densified LYLA with b) 0.5 M NaOH, C) 1 M NaOH and D) 1.5 M of NaOH

4. Conclusion

The densification process can be considered as a very efficient method in order to dewater brown coal by reducing the moisture content by around 80%. Using NaOH as an additive increases the hardness of the products and reduces the measured CO_2 surface areas and mercury pore size distribution of densified coals due to the replacing the major interaction within coal structure from weak hydrogen bonds to more strong ionic bonds. Also the change of surface morphology from porous for raw coal to very smooth with apparent shrinkage for densified coal with NaOH was observed by SEM imaging. These physico-chemical changes suppress the oxidation rate of coal particles by reducing the number and accessibility of active sites on the coal surface at which oxygen molecules can react. As a consequence the spontaneous combustion of densified brown coal with NaOH is postponed to significantly higher temperature up to a maximum difference of 20^oC.

5. Reference:

1. Li, C.-Z., *Chapter 1 - Introduction*, in *Advances in the Science of Victorian Brown Coal*, L. Chun-Zhu, Editor. 2004, Elsevier Science: Amsterdam. p. 1-10.
2. Durie, R.A., *The Science of Victorian brown coal: structure, properties, and consequences for utilization*. 1991: Butterworth-Heinemann.
3. Fei, Y., et al., *The spontaneous combustion behavior of some low rank coals and a range of dried products.* Fuel, 2009. **88**(9): p. 1650-1655.
4. Wang, D.-m., et al., *Test method for the propensity of coal to spontaneous combustion.* Procedia Earth and Planetary Science, 2009. **1**(1): p. 20-26.
5. Nugroho, Y.S., A.C. McIntosh, and B.M. Gibbs, *Low-temperature oxidation of single and blended coals.* Fuel, 2000. **79**(15): p. 1951-1961.
6. Carras, J.N. and B.C. Young, *Self-heating of coal and related materials: Models, application and test methods.* Progress in Energy and Combustion Science, 1994. **20**(1): p. 1-15.
7. Favas, G. and W.R. Jackson, *Hydrothermal dewatering of lower rank coals. 1. Effects of process conditions on the properties of dried product.* Fuel, 2003. **82**(1): p. 53-57.
8. Bergins, C., *Mechanical/thermal dewatering of lignite. Part 2: A rheological model for consolidation and creep process.* Fuel, 2004. **83**(3): p. 267-276.
9. Johns, R.B., et al., *The conversion of brown coal to a dense, dry, hard material.* Fuel Processing Technology, 1989. **21**(3): p. 209-221.
10. Bergins, C., *Kinetics and mechanism during mechanical/thermal dewatering of lignite ☆.* Fuel, 2003. **82**(4): p. 355-364.

11.   R.B. Johns, D.A. Cain, A.L. Chaffee, A.S. Buchanan, *Upgrading solid fuels*, U.S. Patent, Editor. 1986: U.S.

12.   Fei, Y., et al., *The spontaneous combustion behaviour of some low rank coals and a range of dried products.* Fuel, 2009. **88**: p. 1650-1655.

13.   Sujanti, W. and D.-k. Zhang, *A laboratory study of spontaneous combustion of coal: the influence of inorganic matter and reactor size.* Fuel, 1999. **78**(5): p. 549-556.

14.   Greenspan, L., *Humidity Fixed Points of Binary Saturated Aqueous Solutions.* JOURNAL OF RESEARCH of the National Bureau of Standards- A. Physics and Chemistry 1977. **81 A**(1): p. 89-96.

15.   Fei, Y., et al., *Lignite-water interactions studied by phase transition - Differential scanning calorimetry.* Fuel, 2005. **84**(12-13): p. 1557-1562.

16.   International, S.A., *Methods for the analysis and testing of lower rank coal and its chars - Lower rank coal - Determination of ash*, in *AS 2434.8-2002 (R2013)* 2002, Standards Australia International Ltd.

17.   Low, F. and L. Zhang, *Microwave digestion for the quantification of inorganic elements in coal and coal ash using ICP-OES.* Talanta, 2012. **101**: p. 346-352.

18.   Low, F. and L. Zhang, *Arsenic emissions and speciation in the oxy-fuel fly ash collected from lab-scale drop-tube furnace.* Proceedings of the Combustion Institute, 2013. **34**(2): p. 2877-2884.

19.   International, S.A., *Metallic materials - Vickers hardness test - Test methods*, in *AS 1817.1-2003*. 2003, Standards Australia International Ltd: australia.

20.   Woskoboenko, F., W.O. Stacy, and D. Raisbeck, *Physical structure and properties of brown coal.*, in *The science of Victorian brown coal: structure, properties and consequences for utilization.*

, D. RA, Editor. 1991, Butterworth-Heinemann: Oxford. p. 51.

21.   Bergins, C., et al., *Mechanical/thermal dewatering of lignite. Part 3: Physical properties and pore structure of MTE product coals.* Fuel, 2007. **86**(1-2): p. 3-16.

22.   Pandolfo, A.G. and R.B. Johns, *Physical and chemical characteristics of densified low-rank coals.* Fuel, 1993. **72**(6): p. 755-761.

23.   Beamish, B.B. and G.R. Hamilton, *Effect of moisture content on the R70 self-heating rate of Callide coal.* International Journal of Coal Geology, 2005. **64**(1–2): p. 133-138.

24.   Chen, X.D. and J.B. Stott, *The effect of moisture content on the oxidation rate of coal during near-equilibrium drying and wetting at 50 °C.* Fuel, 1993. **72**(6): p. 787-792.

25.   Arisoy, A. and F. Akgün, *Modelling of spontaneous combustion of coal with moisture content included.* Fuel, 1994. **73**(2): p. 281-286.

26.   Bhat, S. and P.K. Agarwal, *The effect of moisture condensation on the spontaneous combustibility of coal.* Fuel, 1996. **75**(13): p. 1523-1532.

27.   Bhattacharyya, K.K., *The role of desorption of moisture from coal in its spontaneous heating.* Fuel, 1972. **51**(3): p. 214-220.

28.   Clemens, A.H. and T.W. Matheson, *The role of moisture in the self-heating of low-rank coals.* Fuel, 1996. **75**(7): p. 891-895.

29.   Kadioğlu, Y. and M. Varamaz, *The effect of moisture content and air-drying on spontaneous combustion characteristics of two Turkish lignitesa.* Fuel, 2003. **82**(13): p. 1685-1693.

30.   Morris, R. and T. Atkinson, *Seam factor and the spontaneous heating of coal.* Mining Science and Technology, 1988. **7**(2): p. 149-159.

31.   Sondreal, E.A., R.C. Ellman, and U.S.B.o. Mines, *Laboratory determination of factors affecting storage of North Dakota lignite: computer simulation of spontaneous heating*. 1974: U.S. Bureau of Mines.

32.   Ll, Y.H. and J.L. Skinner, *Deactivation of dried subbituminous coal.* Chemical Engineering Communications, 1986. **49**(1-3): p. 81-98.

33.   Vance, W.E., X.D. Chen, and S.C. Scott, *The rate of temperature rise of a subbituminous coal during spontaneous combustion in an adiabatic device: The effect of moisture content and drying methods.* Combustion and Flame, 1996. **106**(3): p. 261-270.

34.   Speight, J.G., *The Chemistry and Technology of Coal, Third Edition*. 2012: Taylor & Francis.

35.   Fei, Y., et al., *The effect of cation content of some raw and ion-exchanged Victorian lignites on their equilibrium moisture content and surface area.* Fuel, 2007. **86**(17-18): p. 2890-2897.

36.   Berkowitz, N., *Atmospheric oxidation of coal*, in *Sample selection aging and reactivity of coal*, Klein R, Editor. 1989, Wiley;

: New York. p. 217–81.

37.   Kaji, R., et al., *Water absorption by coals: effects of pore structure and surface oxygen.* Fuel, 1986. **65**(2): p. 288-291.

38.   Woskoboenko, F., W.O. Stacy, and D. Raisbeck, *Chapter 4 - PHYSICAL STRUCTURE AND PROPERTIES OF BROWN COAL*, in *The Science of Victorian Brown Coal*, R.A. Durie, Editor. 1991, Butterworth-Heinemann. p. 151-246.

39.   Wang, H., B.Z. Dlugogorski, and E.M. Kennedy, *Coal oxidation at low temperatures: oxygen consumption, oxidation products, reaction mechanism and kinetic modelling.* Progress in Energy and Combustion Science, 2003. **29**(6): p. 487-513.

40.   Beamish, B.B., M.A. Barakat, and J.D. St. George, *Spontaneous-combustion propensity of New Zealand coals under adiabatic conditions.* International Journal of Coal Geology, 2001. **45**(2–3): p. 217-224.

41.   Clemens, A.H., T.W. Matheson, and D.E. Rogers, *Low temperature oxidation studies of dried New Zealand coals.* Fuel, 1991. **70**(2): p. 215-221.

42.   Bouwman, R. and I.L.C. Freriks, *Low-temperature oxidation of a bituminous coal. Infrared spectroscopic study of samples from a coal pile.* Fuel, 1980. **59**(5): p. 315-322.

Comparative study of low temperature oxidation behaviour of three Victorian brown coals

Jamileh Taghavi Moghaddam, Emily L Perkins and Alan L Chaffee

School of Chemistry, Monash University, Victoria 3800 Australia

Abstract

A comparative study was conducted on the low temperature oxidation (LTO) behaviour of three different Victorian brown coals (Morwell (MW), Yallourn light lithotype (YLL) and Yallourn-woody (Y-woody)). The coal samples were characterized before and after oxidation using FTIR, TGA, He-density, CO_2 surface area, SEM and mercury porosimetry. FTIR and TGA results indicate that the Y-woody sample underwent noticeable changes during oxidation, while these changes are not quite as pronounced for MW and YLL. Mercury porosimetry results demonstrate that pore size distribution (PSD) of Y-woody is quite different to MW and YLL and that MW and YLL after oxidation have higher inter-particles pore volume. Upon oxidation at low temperature Y-woody showed the lowest rate of CO_2 generation, this can be attributed to the greater content of lignin compared to MW and YLL. Lignin generates more methane, methanol, very light aldehyde and acids upon oxidation. The effect of particle size on low temperature oxidation was also investigated. The reactivity of MW coal with a particle size < 0.18 mm is about three times higher than that of the same coal with a particle size < 3 mm. This can be attributed to a higher surface area in the former coal sample being exposed to molecular oxygen.

1   Introduction

Oxidation of coal at low temperature has been the subject of extensive investigations over the last century [1]. Coal oxidation alters its composition and structure [2-8], which adversely affects important properties of coal such as coking and caking [9-12]. Moreover oxidation reactions at low temperature are known to be exothermic and therefore are responsible for temperature increases in the bulk of the coal which can lead to spontaneous combustion in stockpiles, coal mines and during coal transportation [1, 13-16].

Coal oxidation at low temperature is a complicated phenomenon, which involves four main steps [1]: (1) Physisorption of oxygen on the surface of the coal, including the external surface of the coal particle and the surface of pores of various sizes. (2) Chemisorption of oxygen on the surface of the coal and formation of unstable oxygenated intermediates. (3) Thermal decomposition of these unstable oxygenated intermediates into products and more stable oxygenated intermediates. (4) Desorption of gaseous products from the coal surface. Each of these main steps are composed of several phases which may occur in parallel. Chemical and physical properties of coal such as pore structure, elemental composition, particle size, moisture content (internal variables) as well as the environmental conditions including temperature and partial pressure of oxygen (external variables) can have a pronounced effect on each oxidation step in coal. These factors contribute to the different observed oxidation behaviour of two coals of the same rank [17] .

The rate and nature of LTO reactions are significantly affected by the porous structure of coal, which is mainly micropores and contributes considerably to the surface area. It is generally accepted that a higher surface area results in greater reactivity. Wang et al. reported that oxygen adsorption in LTO

(either physical or chemical) is controlled by diffusion of oxygen molecules into the micropores [18]. Therefore the accessibility of micropores and also the micropore volume play a key role in the rate and extent of coal oxidation at low temperature.

On the basis of general findings, coals of lower rank with higher oxygen content are more reactive at low temperature [19, 20] .Elemental composition of coal is also an important factor in coal oxidation. Since this phenomenon is characteristic of low rank coal, it is expected that the type and abundance of oxygen functional groups will affect the interaction of coal with oxygen molecules.

Moisture content has been reported to promote the oxidation of coal at low temperature up to a critical value beyond which the oxidation reactions can be prohibited. This is because oxygen diffusion can be slowed down or even prevented by the formation of water multilayers inside the pores of coal (pore blockage) [2].

Experimental studies on coal have demonstrated that temperature has a significant impact on coal oxidation behaviour. The amount of oxygen consumed was shown to double if the temperature of the oxidation reaction increased by 10 °C [2, 21, 22]. No gaseous products were detected when oxidation was conducted at either 30 °C or 60 °C [2]. While by increasing the temperature to 90 °C noticeable amounts of gaseous products were detected and also the amount of oxygen consumed increased substantially [2, 23]. In a separate study Wang et al. demonstrated that the amount of gaseous product (CO_2) increased noticeably by increasing the temperature from 50 °C to 70 °C. They also did not detect any CO at 50 °C while increasing the temperature to 70 °C, CO could be detected [24]. Several other studies on various low rank coals have shown that the oxidation rate of coal increases substantially as the temperature exceeds a threshold of 70 to 80 °C [24-26].

Coal particle size is also among the influential factors on coal oxidation behaviour. In the majority of studies for the particle size ranges between a few hundred microns to a few centimetres, the rate of oxidation increases as the particle size decreases. This is attributed to higher surface area of smaller particles being exposed to oxygen [14, 27, 28]. For particles smaller than 1 mm, it has been found that the rate of the oxidation reaction is independent of particle size [19, 22, 24].

This study presents the LTO results of three Victorian brown coals; MW, YLL and Y-woody. Coal samples before and after oxidation were characterised using fourier transform infrared spectroscopy (FTIR), thermogravimetric analysis (TGA), CO_2 surface area, He-density, scanning electron microscopy (SEM) and mercury intrusion porosimeter (MIP). The propensity of these coals to undergo spontaneous combustion before and after oxidation was measured using the wire basket technique. The effect of particle size on LTO behaviour of MW was also investigated.

2   Experimental

2.1   LTO process

The low temperature oxidation reaction was carried out in a custom built reactor, heated within an oven and the evolved gases were measured by gas chromatography (GC). The gas chromatograph used in this work was an Agilent Micro-GC fitted with a molsieve 5A and plot Q columns, each with their own TCD detector. A schematic of the experimental set-up can be seen in Fig. 5.

Samples (MW, YLL and Y-woody) were dried under nitrogen for at least 48 hours at 105 $^{\circ}$C. Approximately 60 - 70 g of dried sample was placed in the reactor vessel and weighed accurately. The reaction vessel was sealed and leak tested before each reaction. The sample in the reactor was heated under the flow of nitrogen (50 mln/min) to the desired reaction temperature, 80 $^{\circ}$C. The temperature of the sample was monitored and recorded by a data logger connected to a PC, the two thermocouples from which the data was collected were near the base and top of the reactor. The temperature difference between the base and the top of the reactor could therefore be monitored during the oxidation reaction. An additional thermocouple placed in the centre of the reactor was connected to a temperature controller that would cut power to the oxygen mass flow controller in the case of overheating from a runaway reaction. When the sample reached the required temperature, the flow of nitrogen was switched off and the flow of oxygen started, also at a rate of 50 ml/min, this time was defined as time zero for the reaction. During heating, two or three GC samples were taken to flush out the GC sample lines after which the first GC sample was taken at time zero. GC samples were taken every 5 minutes for the first 15 samples and then at 15 minute intervals until the end of the oxidation period (4 h). After the reaction, the gas flow was switched back to nitrogen, the oven was switched off and the sample allowed to cool. After cooling the nitrogen flow was switched off and the sample could be removed for further analysis. Samples after oxidation are referred to as ALTO.
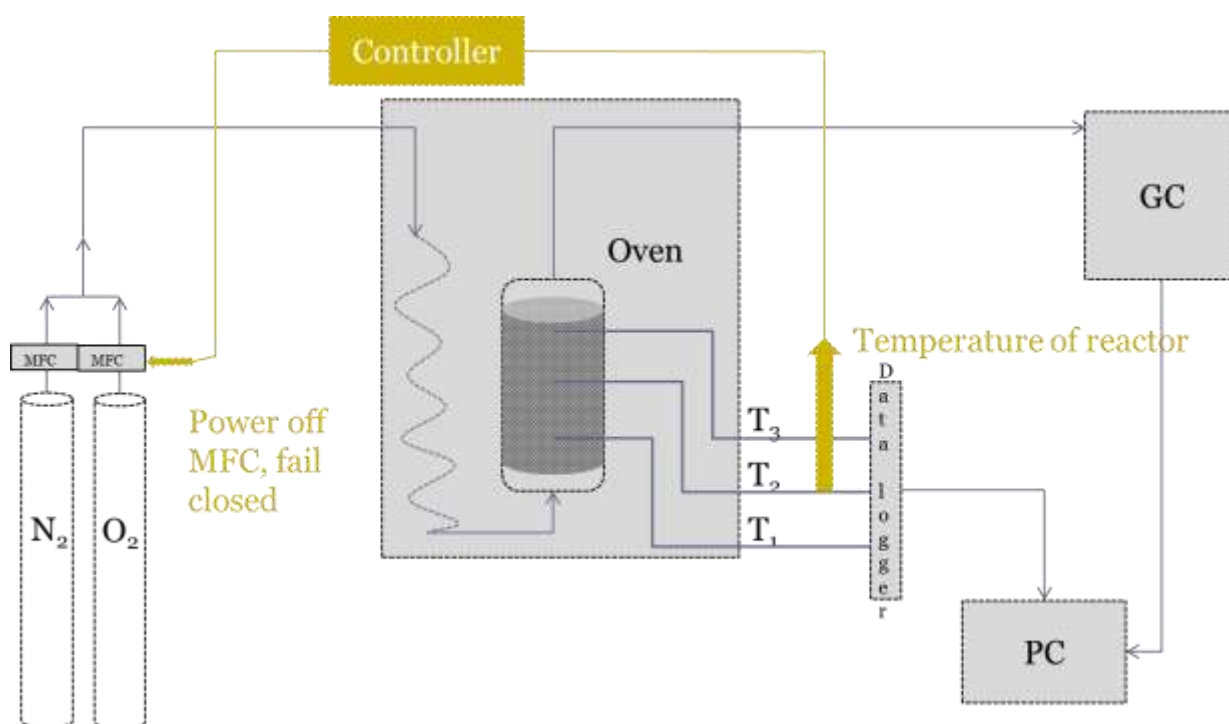
Fig. 5 **Schematic of low temperature oxidation experimental set-up**

2.2　Characterisation methods

2.2.1　FTIR spectroscopy

The FTIR spectra reported in this study were acquired using a BRUKER IFS 55 FTIR spectrometer at room temperature (RT) using the mercury cadmium telluride (MCT) detector. The dry

coal samples were diluted in KBr at a mass ratio of 1:300 and finely ground. The KBr pellet containing coal was made by compressing the mixture at a pressure of 10 MPa for 10 min. The absorbance spectra were collected with a nominal spectral resolution of 8 cm^{-1} over a range of 4000-600 cm^{-1}. The number of scans for both background and sample was 50 and the aperture was set at 1.4 nm.

2.2.2   DTA and TGA

The DTA and TGA analyses were carried out using a TGA/DSC1 STAR^e SYSTEM. In a typical experiment approximately 10 mg of coal sample was weighed into 70 μL alumina pan. The sample was heated up from 30 °C to 600 °C at a heating rate of 2 °C/min in air and remained at 600 °C for 20 min in air and 20 min in N_2 before being cooled to RT in N_2.

2.2.3 CO_2 surface area measurement

Surface area measurements were obtained from CO_2 adsorption measurements at 273 K in a Micromeritics TriStar. All samples were degassed at 105 °C overnight using a Vac Prep 061 Sample Degas System. In a typical experiment approximately 0.2 g of coal (db) was measured into a special long neck tube with a small spherical end. The tube neck was filled with a glass filler to minimise the free space. The tube was then inserted into the analytical port.. Helium gas was used to measure the remaining free space in the tube. The analysis was carried out using CO_2 flowing through the tube. Three analyses were carried out simultaneously and the tubes were immersing into an ice-water slurry to maintain the desired tube temperature. The surface area was then calculated using the Dubinin equation [29].

2.2.4   MIP

The PSD was measured using a Micromeritics AutoPore IV mercury porosimeter. In each run approximately 0.2 g of coal sample (db) was transferred into a penetrometer . The sample was first evacuated at pressures of 200 µmHg and 50 µmHg to remove gases slowly from the sample. The pressure was maintained at 50 µmHg for 5 min. Once the pressure dropped below 50 µmHg the penetrometer was filled with mercury. The pressure was increased incrementally from 5 kPa to 414 MPa to intrude pores down to 3.6 nm in diameter. After each change in pressure the system was allowed to equilibrate for 10 seconds. The empty penetrometer was calibrated in order to determine its exact volume.. All the data has been corrected for compressibility effect [30].

2.2.5   He-density measurement

All the He-density measurements were carried out using AccuPyc II 1340 Gas Pycnometer. In a typical experiment the data was collected after 20 cycles. In each cycle the coal sample (db) was purged 99 times with helium.

2.2.6   Proximate analysis

The proximate analyses were carried out using TGA/DSC1 STAR^e SYSTEM. In a typical experiment 10 mg of coal sample (db) was measured into 70 μL alumina pan. The sample was heated up from 30 °C to 120 °C at heating rate of 2 °C/min and remained at this temperature for 60 min under N_2. The sample was then heated up from 120 °C to 950 °C at heating rate of 10 °C/min under N_2 and remained at this temperature for 20 min. At this point the gas was switched to air and the

sample kept at the same temperature (950 °C) in air for 20 min for the combustion to be completed. Next the sample was cooled down to RT in air and the residue was used to calculate the ash content.

2.2.7 T_{crit} measurement using wire basket technique

The wire basket method was used to measure the critical ignition temperature (T_{crit}). Each run was carried out in a custom made cubic wire basket with 1″ height, width and depth, the basket was equipped with a lid with three holes for the thermocouples to penetrate into the bulk of the coal. In each experiment the wire basket is carefully packed with a known amount of coal. It was then transferred into the electric oven, which is equipped with four type K thermocouples. Three thermocouples, separated by a distance of 3 mm, are inserted inside the wire basket passing through the holes in the lid. Using the lid with holes assures that thermocouples are placed in the same position throughout all experiments. The middle thermocouple is always placed in the centre of the sample (T_2), with two other thermocouples on its left and right (T_3, T_4). The fourth thermocouple is placed outside the wire basket at a distance of 5 cm to measure the oven temperature (T_1). All the thermocouples are connected to the data logger to record the temperatures during the experiment.. Once the oven temperature had been set, the sample heats up and will either combust, or not.

3 Results and discussion

The ultimate, proximate analyses and ash composition results of coal samples are summarised in Table 1 and 2 respectively. Results from proximate analyses show that the volatile matter of the coal samples is increasing in the order of YLL > Y-woody > MW and that the same trend was observed after LTO. The volatile matter content did not change after LTO for MW, however it slightly decreased for YLL and increased for Y-woody. MW ash composition contained large percentages of CaO, SO3, MgO and Fe2O3, whilst YLL had large percentages of Fe2O3 and Al2O3 and Y-woody had highest percentages of SiO2, Al2O3 and Fe2O3.

Table 1
Proximate and ultimate analyses of coal samples

Sample	Proximate analysis (db)			Ultimate analysis (db) %			
	Volatile	Fixed C	Ash	C	H	N	O
	(%)	(%)	(%)				
MW	50.9	46.4	2.7	65.0	4.8	0.6	29.0
YLL	58.2	37.9	3.9	65.4	4.7	0.4	28.8
Y-woody	54.4	42.9	2.7	67.1	5.2	0.2	25.2
MW-ALTO	51.0	46.3	2.7	63.3	4.6	0.6	30.9
YLL-ALTO	57.1	39.6	3.3	61.7	4.7	0.6	32.3
Y-woody-ALTO	56.4	41.0	2.6	65.5	5.5	0.3	28.1

Table 2

Ash composition results

Sample	SiO_2	Al_2O_3	Fe_2O_3	TiO_2	K_2O	MgO	Na_2O	CaO	SO_3	P_2O_5
MW	2.9	1.0	14.8	0.1	0.2	20.1	2.3	36.0	22.2	0.0
YLL	1.9	32.8	30.4	0.5	0.5	7.9	3.2	5.8	5.8	0.1
Y-woody	33.1	22.5	16.9	1.3	0.7	5.2	3.8	3.4	7.2	2.3

Oxidation results of the coal samples are shown in Fig.2 as rates of CO_2 generation in moles per gram of dry coal per second . To investigate the effect of particle size on oxidation at low temperature, the experiment was conducted on two batches of MW coal, one with a particle size < 3 mm and the other with a particle size < 0.18 mm. As shown in Fig.2 the rate of CO_2 generation during LTO is three times greater for the MW with the smaller particle size than for the MW with the larger particle size. It is clear that particle size plays a major role in coal oxidation which results in formation of both gaseous and solid products, particles of smaller size (< 0.18 mm) have higher surface area for a given weight of coal, compared to larger particles (< 3 mm) [14, 31]. The oxidation behaviour for these two samples is also quite different. The rate of CO_2 generation for the smaller particle size sample continuously increased and reached to its maximum within 65 – 75 min after being exposed to oxygen and then decreased gradually and finally plateaued after about 5 h. This behaviour is quite different for the MW sample with larger particle size, where the maximum CO_2 is generated only after about 20 min and decreased rapidly before plateauing after about 30 min.

It is reported that the diffusion rate of oxygen into the coal particles is significant for the oxidation reactions to commence and continue at low temperature [1, 28]. Since the oxidation mainly takes place on the internal surface of the pores, more specifically micropores and mesopores, small particle size facilitates oxygen diffusion into the pores and thus the oxidation rate increases

With regards to oxidation of a variety of low rank coals several other variables including composition, pore structure as well as the nature of oxygen functional groups are known to affect the oxidation process at low temperature [1]. Y-woody sample shows the lowest rate of CO_2 generation during LTO. The FTIR study of this sample (discussed below) shows that the concentration of gualacyl groups is reasonably high which is characteristic of lignin in softwood [32]. Liu et. al. found that during the initial stage of softwood lignin pyrolysis (80 - 100 °C) the main gaseous product was water while no CO_2 was detected and that by increasing the pyrolysis temperature some alcohols, mainly methanol were also generated [33]. Yang et. al. also reported that during pyrolysis of lignin the main gaseous products were H_2 (due to cracking and deformation of aromatic C=C and C-H) and CH_4 (cracking and deformation of methoxy groups) [34]. The liquid phase oxidation of lignin in water, glacial acetic acid and hydrogen peroxide was reported to result in formation of formic and oxalic acid [35]. Based on the results collected from oxidation of Y-woody at low temperature, it is suggested that the main gaseous products of Y-woody oxidation at low temperature could be methane, methanol, formaldehyde and or formic acid.

The rate of CO_2 generation for YLL is slightly lower than that of MW. The density of this sample did not change after the oxidation (Fig.2). It can be suggested that the amount of gaseous products during LTO is the same as solid oxygenated products.
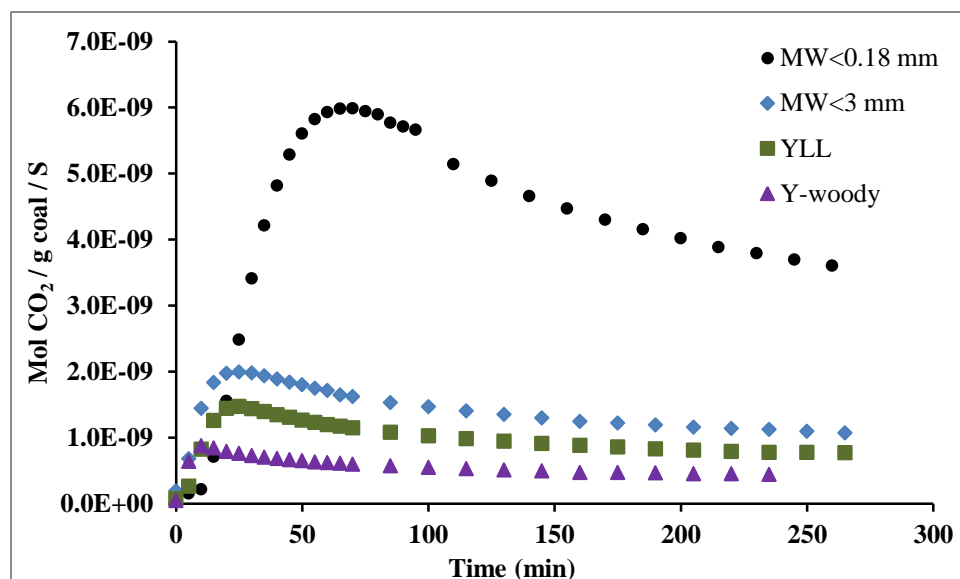
Fig.2 **Rate of CO$_2$ formation as a function of time for various coals**

Fig.3 shows the FTIR spectra for MW, YLL and Y-woody coal before and after LTO. It can be seen that the FTIR spectrum for Y-woody coal is quite different to the other coals, for instance the very low intensity of C=O band at around 1710 cm^{-1} and the presence of assorted, well-resolved bands in the range of 1500-1000 cm^{-1}. The FTIR spectrum of this sample after LTO shows that Y-woody underwent significant changes during oxidation.

Absorption bands in the range of 900-700 cm^{-1} for Y-woody coal are assigned to C-C and C-H stretching. These bands are more intense in Y-woody than other coals. A series of absorption bands in the region of 1000-1150 cm^{-1}, assigned to stretching and deformation vibration of C-O of primary alcohols and stretching vibration of C-O-C probably in pyranose rings can be seen for Y-woody coal. The appearance of the absorption bands at around 1210-1280 cm^{-1} is due to the presence of aromatic phenyl C-O in gualacyl groups (bands at around 1266 cm^{-1} and 1218 cm^{-1} for Y-woody are assigned to C-O stretching vibration of gualacyl ring) [36]. While the appearance of a band at around 1388 cm^{-1} indicates the presence of syringyl groups. Since the intensity of the bands at around 1210-1280 cm^{-1} are higher than the one at 1388 cm^{-1}, it can be suggested that the concentration of gualacyl can be higher than syringyl groups in Y-woody coal, the presence of both peaks may be used to determine the presence of hardwood lignins [33]. There are also several major absorption bands in the region of 1515-1430 cm^{-1} which are assigned to O-CH$_3$ of methoxy groups (1470-1440 cm^{-1}) and C=O groups in ketones [34]. Aromatic rings also give rise to absorption bands in this region and thus the appearance of some bands can be attributed to these aromatic groups [33, 37]. Aromatic skeletal vibration give rise to an absorption band at around 1615 cm^{-1} [37]. The appearance of carbonyl groups at 1708 cm^{-1} is assigned to stretching vibrations of C=O which are not in conjugation with an aromatic ring; including unconjugated esters and ketones. The bands at around 2950-2850 cm^{-1} (aliphatic groups CH$_3$-CH$_2$) and 3600-3000 cm^{-1} (acid and alcohol, -OH) are more intense for Y-woody than the other coals.
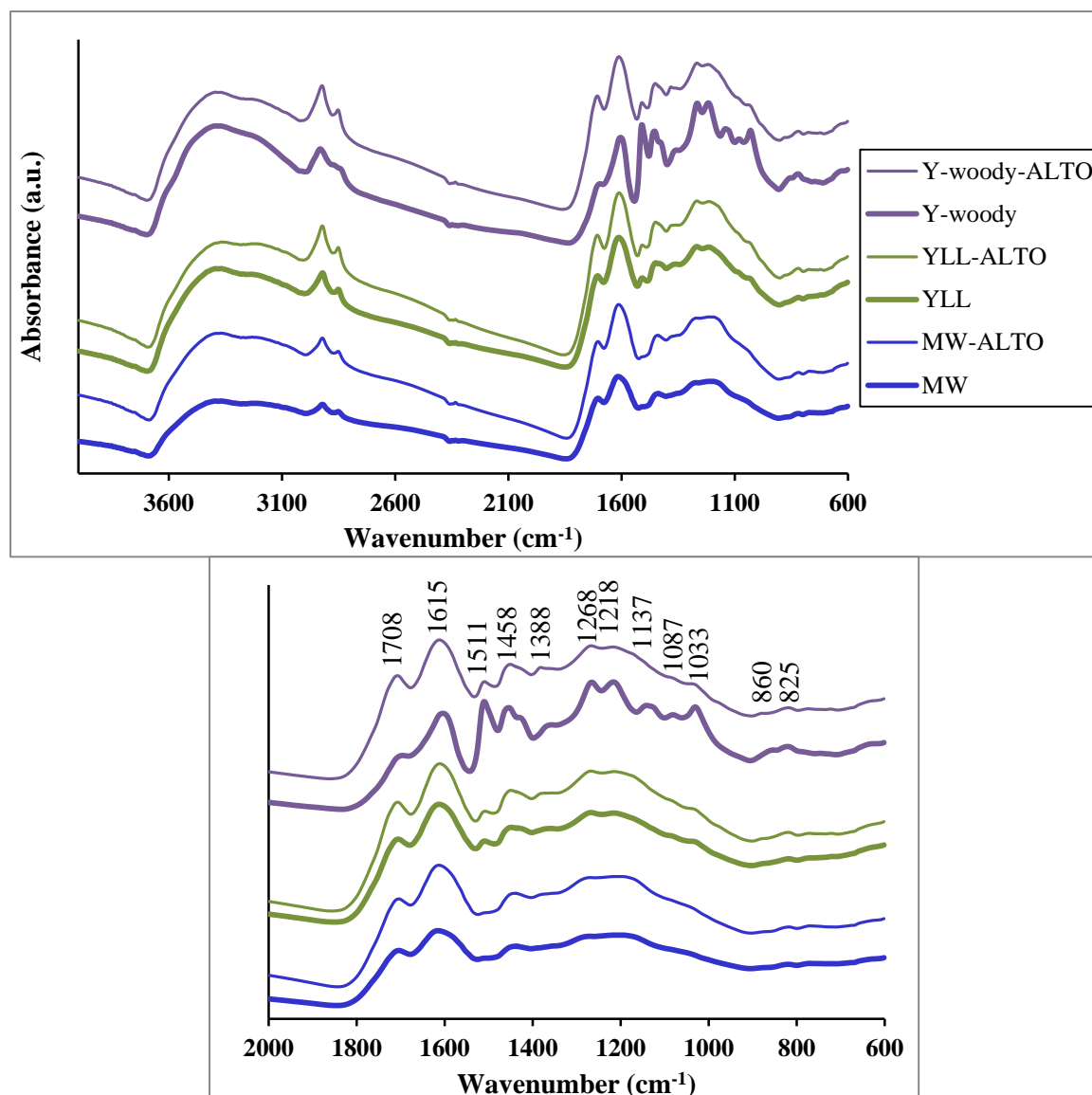
Fig.3 **FTIR spectra of MW, Y-woody and YLL before and after LTO**

The intensity of the bands in the range of 900-700 cm^{-1} decreased for Y-woody sample after LTO. In addition a drastic decrease in the intensity of all bands in the range of 1520-1000 cm^{-1} can also be observed after LTO. This can be indicative of the involvement of methoxy groups, primary alcohols and ethers in oxidation reactions at low temperature and the generation of gaseous products. On the other hand the intensity of unconjugated carbonyl groups (1708 cm^{-1}), in the Y-woody sample, increased noticeably after LTO. This suggests the formation of solid oxygenated compounds during LTO. The intensity of the band related to aromatic skeletal vibration (1615 cm^{-1}) did not change noticeably upon oxidation, which means during LTO the aromatic structure in Y-woody and other coals remained intact. The bands related to aliphatic groups became more intense in all coals especially Y-woody. This suggests that the overall concentration of aliphatic groups increased after LTO, which can be due to the generation of more gaseous products during LTO. The intensity of –OH bands decreased for Y-woody which suggests the acidic and alcoholic groups contribute to the generation of gaseous products during LTO.

FTIR spectra of MW and YLL show minor changes before and after LTO process. The intensity of the band at around 1708 cm^{-1} has increased slightly for these two samples after LTO. The intensity of

band at around 3600-3000 cm^{-1} has increased for MW but did not change noticeably for YLL after LTO.

Table 3
The calorific value, CV, (J/g) of coals before and after LTO

Sample	CV (J/g)-R1
MW	21225
MW-ALTO	20395
YLL	19826
YLL-ALTO	19876
Y-woody	20729
Y-woody-ALTO	22162

The CV for the coal samples before and after LTO was calculated using the Boie equation [38] and is summarised in Table 3. The CV for MW decreased slightly after LTO which is attributed to the higher oxygen content. This is in agreement with the FTIR results, which show that the concentration of C=O and −OH groups increased after LTO. For YLL sample no changes were observed for CV, which could suggest that the concentration of solid oxygenated compounds formed during LTO is the same as gaseous products. The CV for Y-woody increased noticeably. The chemistry of this sample also changed quite significantly during LTO as seen in the FTIR spectra . For this sample as discussed above more gaseous oxygenated compounds were generated during LTO , which were released from the sample.

The morphology of Y-woody before (a and a′) and after (b and b′) LTO are shown in Fig.4. The macrostructure of this coal comprises of fibrous as well as semi spherical (floret-like) particles with irregular contour. The average length of fibrous particles is between 700 μm – 1mm with 200 μm width. The particle surface is quite scabrous with multiple conchoidal fractures (Fig.4 a′, white arrows), fissures of various depth (Fig.4 a′, yellow arrows) and some shallow indentations. After LTO, the assessment of several particlessuggests that the overall morphology of particles did not change significantly, however it seems some craters were formed on the surface (Fig.4 b′, red arrows). The formation of craters (bubbles) on the surface of the coal particles was observed during lignin pyrolysis at higher temperature (250 °C) [39]. This was attributed to volatile matter release. In this study these craters were formed during LTO at 80 °C, which are likely due to the release of gaseous products formed from the cracking and deformation of methoxy groups.
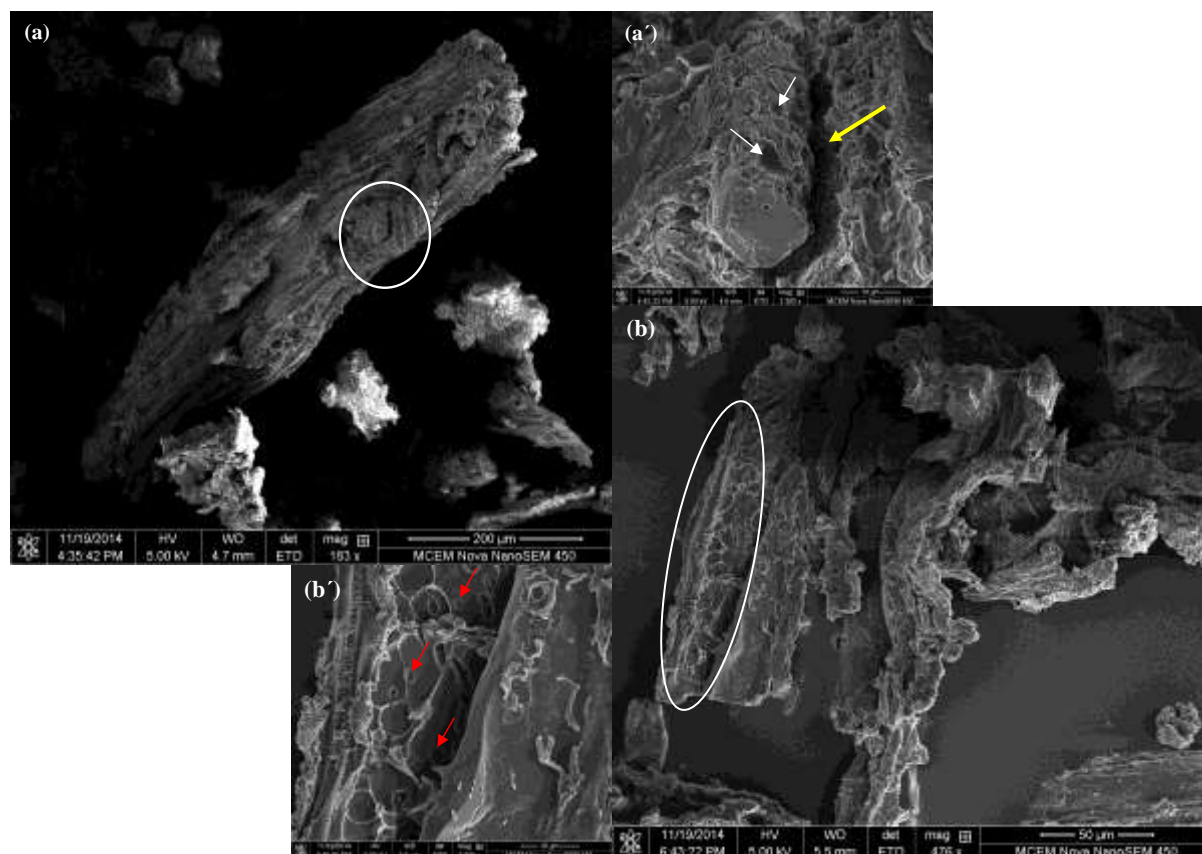
Fig.4 SEM images of Y-woody coal before and after LTO process

The thermal behaviour of MW, Y-woody and YLL before and after LTO is shown in Fig.5 (a) and (b). Three thermal events including one endothermal at low temperature and two exothermal events at higher temperature can be seen for three coal samples. The first endothermal peak, common to three coal samples, is attributed to moisture evaporation. For MW coal the second (exothermal) peak is centred at 299 °C, which is attributed to volatile matter decomposition. The third exothermal peak centred at 379 °C is due to char combustion. The total decomposition of MW coal finishes at 450 °C [40].

The DTA curve for the Y-woody sample is quite different to that of MW. The volatile matter decomposition for this sample gives rise to a shoulder rather than a peak centred at 295 °C and the char combustion peak is substantially broader than that of MW and centred at 360 °C. The total decomposition of this sample finished at a higher temperature than MW, 480 °C.. The overall DTA profile of YLL is similar to that of MW, however the volatile matter decomposition began at higher temperature (around 200 °C) compared to MW and Y-woody (around 180 °C). Here the volatile matter decomposition and the char combustion peaks are centred at 295 °C and 362°C, respectively. The total decomposition of this coal completed at 460 °C.

After LTO the DTA profile for MW and YLL coals did not show any noticeable changes, however the DTA profile for Y-woody did show noticeable changes. The peaks related to volatile matter decomposition and char combustion for Y-woody-ALTO shifted to higher temperatures, 341 °C and 430 °C, respectively. The total decomposition of this sample also shifted to a higher temperature (500 °C) compared to its corresponding sample before LTO. It can be suggested that during LTO

some of the reactive compounds interacted with oxygen to generate mostly gaseous products and left the coal with more stable species.
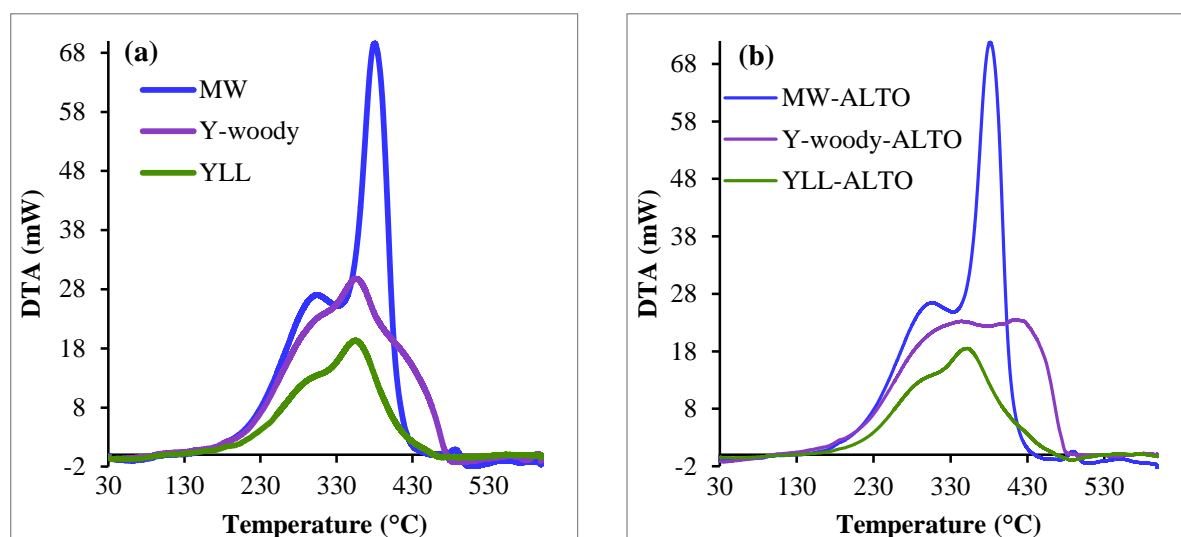

Fig.5 **DTA profiles of MW, Y-woody and YLL before and after LTO**

The CO_2 surface area of MW, YLL and Y-woody before and after LTO is summarised in Table 4. For MW coal the surface area increased slightly after LTO, however for both YLL and Y-woody coals the surface area decreased noticeably after LTO process. Several factors can account for the decreases in surface area including; (1) the presence of less oxygen functional groups on the coals surface after LTO, hence less interaction between the coal surface and CO_2 during the analysis. This is a possible explanation for less CO_2 surface area measured for Y-woody based on results collected from ultimate analysis (Table 1) and CV (Table 3) which show Y-woody-ALTO has less oxygen content. While for MW higher oxygen content results in a slightly lower CV and higher measured CO_2 surface area. (2) Formation of solid oxygenated compounds during LTO could potentially cause some pore blockage, which might account for the CO_2 surface area decrease in observed for YLL ALTO.

Table 4
Surface area of coals before and after LTO

Sample	Surface area (m^2/g)
MW	235
MW-ALTO	244
YLL	261
YLL-ALTO	232
Y-woody	245
Y-woody-ALTO	202

For all calculations the cross sectional area of CO_2 was taken as 25.4 A^2

The PSD of the coal samples before and after LTO are shown in Fig.6 It is clear that Y-woody sample has the widest PSD in the intra-particle size range, followed by YLL. This is expected since Y-woody is

composed of coarser particles, which are lighter (on weight basis) than both MW and YLL. The PSD profiles of MW and YLL before and after LTO are quite similar with minor changes in the range of intra-particle pores. After LTO the intrusion volume, in the intra-particle pore range, for both MW and YLL increased.   During LTO some gaseous products are released, the coal samples may, therefore, be left with more accessible intra-particle pores. The PSD of Y-woody sample after LTO experienced multiple changes including a shift of the dominant pore size from intra-particle region to inter-particle region. The FTIR spectra of Y-woody also confirmed many significant changes in the sample during LTO. These chemical changes which involve formation of various gaseous and solid products may alter the integrity and porous structure of the sample.
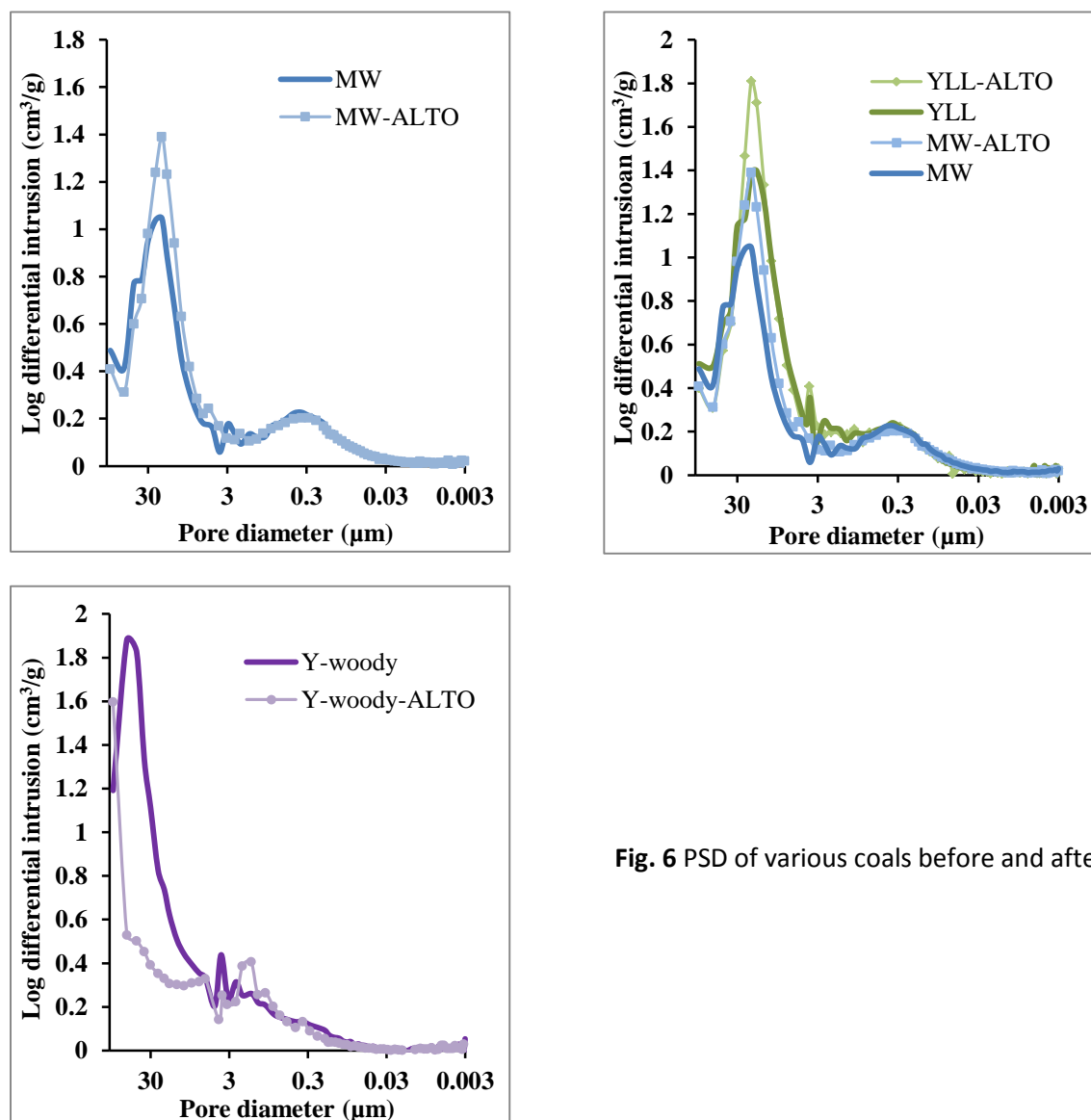
Fig. 6 PSD of various coals before and after LTO

The measured He-densities of coals before and after LTO are shown in Fig.7. As expected Y-woody coal has the lowest density due to its loose and leafy nature. The density of MW coal shows a slight decrease after LTO which can be attributed to the increase in intra-particle pore volume. The same phenomenon was also observed for the Y-woody sample, which suggests that the major products during LTO were in gaseous form. This explanation is in line with CV and CO_2 surface area results.
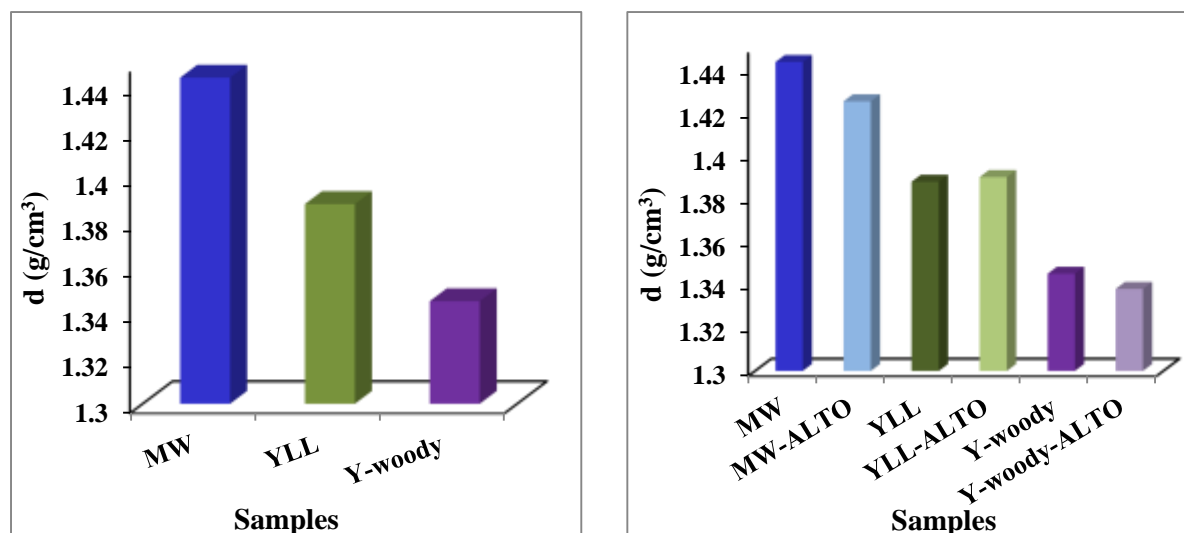
Fig.7 **He-density of MW, YLL and Y-woody before and after LTO**

The propensity to undergo spontaneous combustion of coals before and after LTO was measured by the wire basket technique and summarized in Table 5. It is reported that once MW coal undergoes oxidation at low temperature (80 °C), its propensity to undergo spontaneous combustion decreased Ref our HTD paper. However in this study T_{crit} did not change after LTO for MW. This behaviour can be attributed to the particle size (< 3 mm) and its impact on oxidation at low temperature. As we discussed above the rate of CO_2 generation from MW with different particle size is different. MW coal with smaller particle size clearly generates more CO_2 and which means more surface area was exposed to oxidation. As a result MW with smaller particles experienced more chemical changes than the one with larger particles, which in turn affects the T_{crit}.

As for YLL, the T_{crit} increased after LTO which suggests that during oxidation at low temperature some very active species in the coal were deformed to generate CO_2 and some more stable oxygenated compounds. It is noteworthy that the FTIR (shown above) did not show significant changes for the coal samples before and after LTO except for slight increase in C=O groups.

The propensity to undergo spontaneous combustion increased for Y-woody after being oxidised at low temperature. Since the chemistry of this sample also experienced many changes (previously discussed in the FTIR analysis), one explanation is by releasing some gaseous products (CH_4 or CH_3OH), the coal structure became more relaxed and accessible for molecular oxygen to interact with and thus T_{crit} decreased.

Table 5

T_{crit} of coals before and after LTO

Sample	T_{crit} (°C)	T_{crit} (°C) (ALTO)
MW	146±1	146±1
YLL	152.5±1	155.6±1
Y-woody	165.4±0.5	161.6±0.7

4   Conclusion

Oxidation at low temperature causes pronounced chemical changes for Y-woody coal compared to YLL and MW. These chemical changes cause both the measured CO_2 surface area and T_{crit} to decrease while the CV increased. The SEM images for Y-woody after LTO show the formation of craters on the surface which can be attributed to the release of gaseous products (CH_4 and CH_3OH). During the course of oxidation Y-woody generated the lowest amount of CO_2 as compared to YLL and MW. The DTA results also demonstrate that the Y-woody underwent significant changes which shifted the total decomposition to a higher temperature. The CV value and He-density of YLL did not change while its intra-particle pore volume and T_{crit} increased, which might be attributed to the formation of more stable solid oxygenate compounds. Particle size was found to play a significant role in MW coal oxidation at low temperature. MW coal with particle size < 0.18 mm generates three time more CO_2 compared to sample with particles size < 3 mm.

5   References

[1] Wang H, Dlugogorski BZ, Kennedy EM. Prog. Energy Combust. Sci. 2003;29:487-513.
[2] Clemens AH, Matheson TW, Rogers DE. Fuel 1991;70:215.
[3] Itay M, Hill CR, Glasser D. Fuel Process. Technol. 1989;21:81-97.
[4] Kaji R, Hishinuma Y, Nakamura Y. Fuel 1985;64:297.
[5] Krishnaswamy S, Bhat S, Gunn RD, Agarwal PK. Fuel 1996;75:333-43.
[6] Pisupati SV, Scaroni AW. Fuel 1993;72:531-42.
[7] Polat S, Harris IJ. Fuel 1984;63:669-72.
[8] Wang H, Dlugogorski BZ, Kennedy EM. Fuel 1999;78:1073-81.
[9] Larsen JW, Lee D, Schmidt T, Grint A. Fuel 1986;65:595-6.
[10] Maloney DJ, Jenkins RG, Walker Jr PL. Fuel 1982;61:175-81.
[11] Pis JJ, Cagigas A, Simón P, Lorenzana JJ. Fuel Process. Technol. 1988;20:307-16.
[12] Song C, Saini AK, Schobert HH. Energy & Fuels 1994;8:301-12.
[13] Van Krevelen DW. Action of Air and Molecular Oxygen on Coal. In: Van Krevelen DW (Ed.) Coal; Typology, Physics, Chemistry, Constitution, Amsterdam: Elsevier 1993, p. 627-57.
[14] Carras JN, Young BC. Prog. Energy Combust. Sci. 1994;20:1-15.
[15] Smith MA, Glasser D. Fuel 2005;84:1161-70.
[16] Jones RE, Townend DTA. Nature 1945;155:424-5.
[17] Nelson CR. Spontaneous Heating of Stored Coal. In: Chemistry of Coal Weathering, Amsterdam: Alsevier; 1989, p. 133-215.
[18] Wang H, Dlugogorski BZ, Kennedy EM. Energy & Fuels 1999;13:1173-9.
[19] Kaji R, Hishinuma Y, Nakamura Y. Fuel 1985;64:297-302.
[20] Lowry HH. In: Lowry HH (Ed.) Chemistry of Coal Utilization, New York: Wiley; 1945, p. 627.
[21] Allardice DJ. Carbon 1966;4:255-62.
[22] Wang H, Dlugogorski BZ, Kennedy EM. Fuel 2002;81:1913-23.
[23] Swann PD, Evans DG. Fuel 1979;58:276-80.
[24] Wang H, Dlugogorski BZ, Kennedy EM. Combust. Flame 2003;134:107-17.
[25] Jones RE, Townend DTA. Journal of the Society of Chemical Industry 1949;68:197-201.
[26] Kudynska J, Buckmaster HA. Fuel 1996;75:872-8.
[27] Baris K, Kizgut S, Didari V. Fuel 2012;93:423-32.
[28] Palmer AD, Cheng M, Goulet JC, Furimsky E. Fuel 1990;69:183-8.
[29] Van Krevelen DW. Coal as a Solid Colloid. In: Van Krevelen DW (Ed.) Coal: Typology, Physics, Chemistry, Constitution, Amsterdam: Elsevier; 1993, p. 193-221.
[30] Bergins C, Hulston J, Strauss K, Chaffee AL. Fuel 2007;86:3-16.
[31] Akgün F, Arisoy A. Combust. Flame 1994;99:137-46.
[32] Kudzin SF, Nord FF. J. Am. Chem. Soc. 1951;73:4619-22.

[33] Liu Q, Wang S, Zheng Y, Luo Z, Cen K. J. Anal. Appl. Pyrolysis 2008;82:170-7.

[34] Yang H, Yan R, Chen H, Lee DH, Zheng C. Fuel 2007;86:1781-8.

[35] Phillips M. Chem. Rev. 1934;14:103-70.

[36] Oikonomopoulos IK, Perraki M, Tougiannidis N, Perraki T, Frey MJ, Antoniadis P, et al. International Journal of Coal Geology 2013;115:1-12.

[37] Scholze B, Meier D. J. Anal. Appl. Pyrolysis 2001;60:41-54.

[38] Boie W. Energietechnik 1953;3:309-16.

[39] Sharma RK, Wooten JB, Baliga VL, Lin X, Geoffrey Chan W, Hajaligol MR. Fuel 2004;83:1469-82.

[40] Ma S, Hill JO, Heng S. J. Therm. Anal. 1989;35:1985-96.

Low temperature thermal reactivity of Victoria brown coal and its effect on spontaneous combustion

Mohammad Reza Parsa, Ian Mckinnon, Alan Chaffee*

School of Chemistry, Monash University, Clayton, Vic. 3800, Australia

(*Corresponding Author's E-mail:alan.chaffee@monash.edu)

ABSTRACT

The low temperature (25-110°C) thermal activity of Morwell Victorian brown coal has been studied by using differential scanning calorimetry (DSC). The DSC test, two successive non-isothermal ramps (heating and cooling) for the same sample showed an exothermal event in the first run which did not repeat in the second run for test in gas flow cell under nitrogen, air and oxygen and also in a closed (batch) cell.

Increasing the oxygen concentration increased the heat released, but the important observation was the happening of exothermal phenomenon even in the absence of oxygen. The effect of adding oxygen and water to the sample after the first run of the test in order to attempt to reproduce the exothermic event has also been investigated. The results showed that adding oxygen and water individually did not reproduce the exothermal heat flow, but purging both together reproduced the exothermal phenomenon.

The SEM image, surface area and pore size, FTIR and gas analysis results suggested that brown coal experiences an exothermal phenomenon due to physical phase change in accompany with some chemical changes at low temperature. This exothermal thermal

behaviour, similar to cold crystallization of polymer, can act as starting phenomena leading to spontaneous combustion of brown coal.

Keywords: Brown coal, differential scanning calorimetry, coal drying method

1. Introduction:

Spontaneous combustion, as a natural disaster, is one of the most serious problems in the world's coal industry. It is responsible for most fires during coal mining, transportation and storage and thus causes safety issues and property losses [1-3]. Spontaneous combustion is a consequence of self-heating of the coal where the heat released due to chemical and/or physical processes within coal particles accumulates faster than it dissipates into the environment [4, 5].

The low-temperature reactivity of brown coal is generally accepted as the initial source of self-heating leading to its spontaneous combustion.

It is believed that the low-temperature oxidation is the primary resource to generate heat which has therefor been extensively studied for decades considering the effect of various influencing factors [1, 5-8]. The generally accepted theory of coal's low-temperature oxidation divides the process into three stages: physical adsorption of oxygen molecules, chemisorption leading to generation of coal-oxygen complexes and chemical reactions releasing gaseous products, typically carbon monoxide, carbon dioxide , and water vapour [5, 9, 10].

Changes in the physical structure of coal with changing temperature may also contribute to the heat balance. Some scholar observed an endothermic process associated with enthalpy relaxation and glass transition at low temperature [11-14].

Mackinnon, et al, had carried out differential scanning calorimetriy (DSC) on lignite and reported that annealing dry sample induced a relaxation of structure in a temperature range centred at 136°C with an energy observation of 4.2 J g. Subsequent DSC run showed a reversible second-order process associated with a glass to rubbery transition at 100°C[12]. They argued that many coals are glassy solids at ambient temperature with severely restricted molecular motion.. Yun and Suuberg [14] reported that these transitions is accompanied by irreversible change to coal structure and molecular interaction; so that these transitions are not true glass-to-rubber transitions.

Nevertheless it is clear that some physical change in low rank coal structure near 100°C. It may be hypothesised that such a phase change may influence the temperature dependence of self-heating and the condition for onset of spontaneous combustion. Diffusion through glassy solids is slow and so it would be expected that the kinetics of chemical reactions would be diffusion-limited [12, 15]. . Self-heating of coal starting with slow build-up of heat can lead a transition to a rubbery like state and would consequently be accompanied by a sudden increase in diffusion rate of molecular species and modify the conditions for spontaneous combustion to occur. In this paper the effect of heating on the structure of Morwell brown coal at relatively low temperatures was studied. The main objective of this research is to investigate the effect of low temperature heating on coal structure and consequently on the spontaneous combustion behaviour of coal.

2. Materials and methods

2.1. Coal samples

Morwell brown coal was used in this study originated from the Morwell open-cut in the Latrobe Valley, Victoria, Australia. Some characteristics of this brown coal are listed in Table one. The raw coals were milled to <3 mm size and homogenised. The raw sample was dried by either vacuum drying at 30°C for 24h and oven drying at 105°C for 3 h.

Table 1: Characterization of Morwell coal sample

Properties			Ash		
				% of ash	g/ 100g db
Moisture (% as received)		60.0	SiO_2	2.9	0.10
			Al_2O_3	1.0	0.02
Proximate Analysis (% db)	Ash	1.9	Fe_2O_3	14.8	0.28
	Volatile matter	48.4	TiO_2	0.1	0.002
	Fixed carbon	49.7	K_2O	0.2	0.004
Ultimate Analysis (% db)	C	67.4	MgO	20.1	0.38
	H	4.5	Na_2O	2.3	0.044
	N	0.5	CaO	36.0	0.68
	S	0.24	SO_3	22.2	0.42
	Cl	0.06	P_2O_5	0.0	0

2.2. DSC experiments

A Setaram micro DSC III was used in this study. The DSC thermogram was obtained by temperature scanning of 200 mg coal sample (non-isothermal program) from 25 to 110°C at a heating rate of 1°C /min with the reference cell kept empty. Tests were conducted in a closed batch cell and in a gas flow cell under nitrogen, air and oxygen (30 cm^3/min flow rate). Alpha-alumina was used as reference material to measure coal sample heat capacity (C_p) by the ASTM, E 1269.

2.3. Autoclave experiment

Autoclavr experiments were carried out in order to produce enough thermally treated coal for spontaneous combustion experiments and to enable analysis of the gas produced during thermal treatment about 20 gr of coal was charged into a 70 ml autoclave fired with an outlet tube to permit sampling of the gas after the thermal treatment. The autoclave was sealed in air and treated at 110°C for 3 h, similar conditions to these used for the DSC tests. After the reaction the autoclave was co0led and gas transferred to a fur-column Agilent 3000 Micro

Gas Chromatograph. The column were: MS SA PLOT 10m×0.32mm (110°C column temperature) to analyse for H_2, N_2, CH_4 and CO, PLOT u, 8m×0.32mm (100°C column temperature) for CO, CO_2, C_2 hydrocobans, H_2S and COS, Alumina PLOT 10m×0.32mm (140°C column temperature) for C3-C5 hydrocarbons and OV-1 10m×0.15mm×20μm (90°C column temperature) for iso-C_4H_{10} and n-C_6H_{14}. The inlet and injector temperatures were 100°C. After analysis the autoclave was opened and the coal product scraped out.

2.4. Spontaneous combustion test (Wire basket)

The wire basket method is a common method of evaluating the spontaneous combustion propensity of coal. The temperature at which the coal temperature begins to exceed the surrounding temperature is the so-called critical temperature (T_{crit}). Sample (varies with density of sample) was loaded to fill 1 inch^3 stainless-steel cube basket (about 10-13 gr), and then the loaded basket was placed in the sample holder. Three thermocouples were inserted into the near two and middle of sample and the fourth was positioned to measure the oven temperature.

In next stage, the oven was set to the desired temperature. Air flowed through the oven by fixed flow rate during the experiment. The temperature logger is used to monitor the coal and oven temperatures and a data acquisition system records the temperatures.

To obtain T_{crit} for a sample the wire basket experiments were repeated for different oven temperatures, at a 2°C interval. The T_{crit} of each sample was determined by averaging the lowest temperature at which the thermal runaway occurred and the highest temperature at which the thermal runaway did not occur [16].

2.5. Sample characterisation

The morphology of the samples was exemined by field emission gun scanning electron microscope (FEG/SEM), using a Nova NanoSEM 450 operated at 5 KV. The surface area of

samples was measured by CO_2 adsorption at ^{o}C using a Micromeritics TriStar II, and the pore volume tests were carried out with Micromeritics Auto-pore IV mercury intrusion porosimeter. The produced gas after autoclave experiments was analysed by using a four column Agilent 3000 Micro Gas Chromatograph.

Coal samples for FTIR analysis were dried under vacuum and pellets prepared by mixing 3.0 mg coal sample and 300.0 mg of KBr. The spectra were recorded by running 64 scans at a resolution of 8 cm-1 using a Burker FTIR instrument (Equinox, IFS-55). Peak assignments of spectra were based on Painteret etal., [17] and Ibarra etal.,[18]. The curve-fitting analysis was based on Ibarra etal.,[18].

3. Results and discussion

3.1. DSC test of alpha- alumina as inert material:

The results of DSC tests on alpha-alumina (the reference material) in flowing air cell and in a closed cell are shown in Fig. 1. The DSC curve of alpha- alumina didn't show any peak in either test.
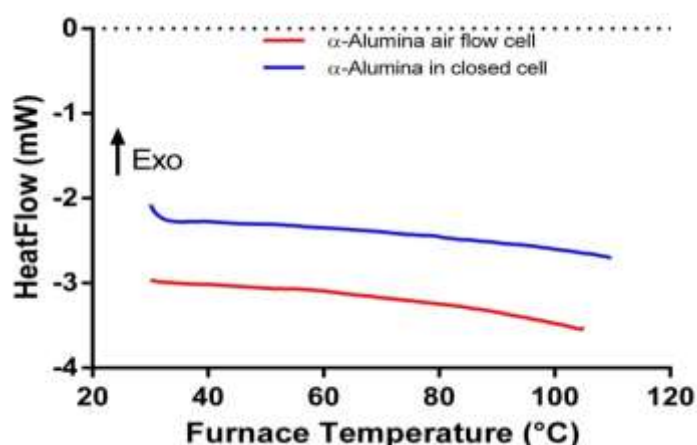

Figure 1: Non-isothermal gas flow (air) and batch cell DSC tests of Alpha-alumina

3.2.   Gas Flow DSC cell experiments:

Figure 2 showsthe results of non-isothermal DSC tests (25-110 ^{o}C) of 200 mg samples of vacuum dried Morwell coal in a flow of 30 cm^3/min nitrogen, air or oxygen. An exothermic peak was observed under all three gases in the first run. This exothermic signal cannot be the result of oxygen physisorption on the surface of coal which gives a much smaller and reversible exotherm and endotherm [19].

The first run of DSC curve starts with a large endothermic start-up hook which flow by a saturation for air and oxygen. It seems that this large starting hook is a character of brown coal on DSC test under gas flow. The attempts to remove or reducing it were not successful. This starting-up hook makes hard any interpretation about the exothermal peaks which happens around 65-70°C.
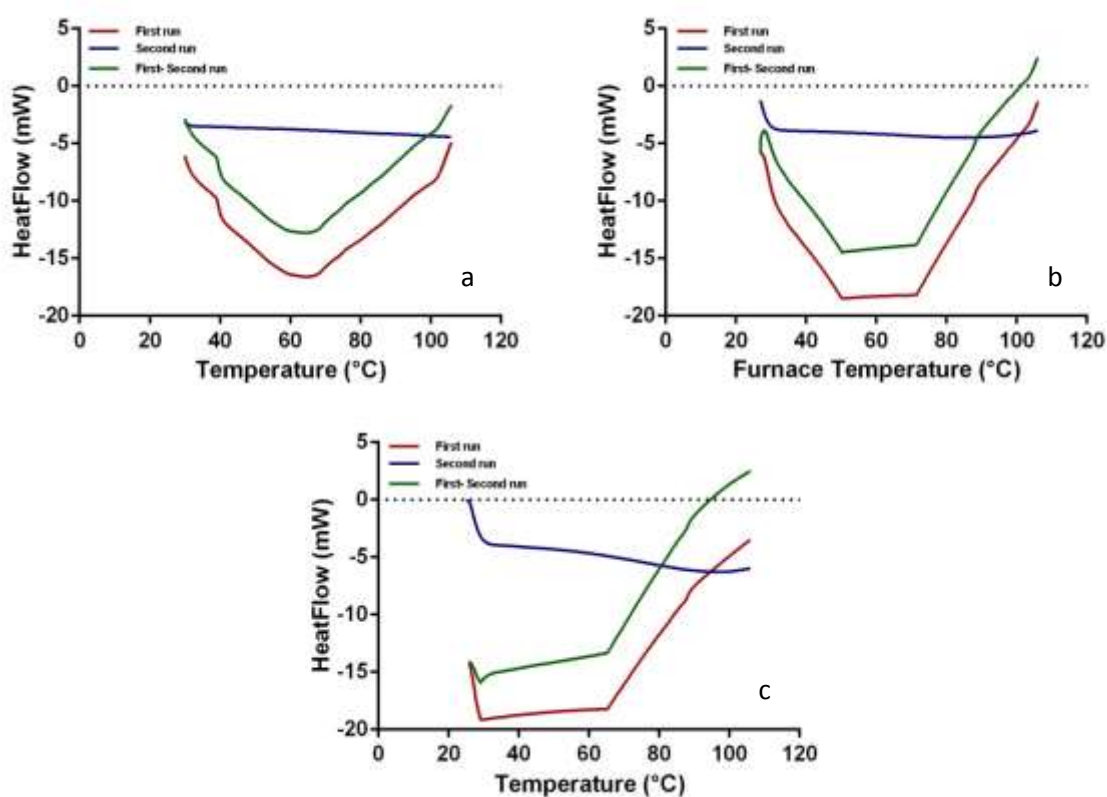

Figure 2: First and second runs from Non-isothermal DSC tests flowing nitrogen (a), air (b) and oxygen (c) of Morwell

3.3. Batch DSC cell experiments

After DSC tests of Morwell coal using the gas flow cell, DSC experiments were carried out using the batch or adiabatic cell (without gas flow). Fig. 3 shows the heat flow measured during two successive temperature ramps (heating and cooling) for the same sample within the batch cell.
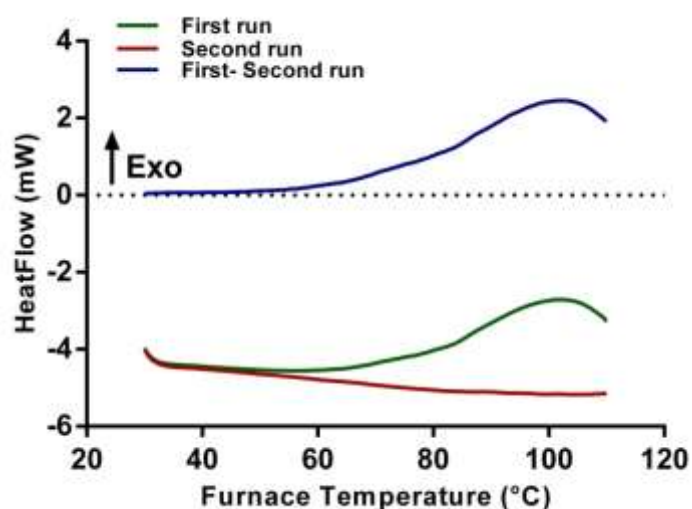

Figure 3: DSC curve of vacuum dried Morwell coal in batch cell

An exothermic peak with an enthalpy of between 13.8 to 30.8 J/g, starting temperature 53°C and maximum at 98.5°C is observed during the first temperature ramp cycle, but not during the second cycle. The DSC curve obtained in the batch cell had much better resolution than that in the gas flow cell. In the absence of gas flow the heat flow signal didn't saturate, which occurred during purging gas (Fig. 2 b and c), and the exothermic signal was much clearer. The most interesting point of DSC curve of batch system was the disappearance of the exothermic peak in the second run.

The increase in coal temperature due to the isotherm can be calculated from the equation:

$$E = Cp \times m \times \Delta T \tag{1}$$

where E is the amount of heat generated, C_p: the heat capacity and ΔT: temperature difference. The amount of heat generated increased the coal temperature by 7.6 to 17.1 ^{o}C which can be a promotion for spontaneous combustion.

3.4.   Effect of air on first run of DSC:

3.4.1.   Removing air in first run:

To determine the effect of atmospheric air existed in cell on exothermic peak, DSC was carried out in a gas flow cell. Air was removed by purging nitrogen for 1 hour, then outlet and inlet closed and the temperature increased from 25 to 110°C. The recorded DSC curve, was still showed the exothermic peak, but its intensity was reduced comparing with batch cell tests. Thus the exothermal peak in the first run was due to reactions which did not require are but the presence of air did lead to additional exothermic reactions as a results of oxidation.
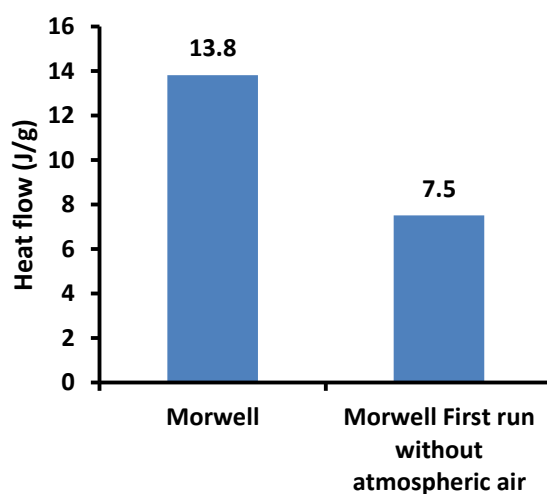

Figure 4: Effects of air on exothermic peak

3.5.   Study of effective factors on second run of DSC:

3.5.1. Effect of air on second run:

There was a possibility that existed air in cell has important role in first run of DSC which is consumed in this run, and absence of air causes no exothermic peak in second run. The effect of air on the second DSC run in a closed cell was examined by quickly opening and closing the batch cell lid to just let air goes into the cell after first run, then the putting cell back into the DSC to carry out the second run. A very small peak was observed in second run corresponding enthalpy charges of 0.1 J/g.

In a second experiment, the gas flow cell was used. After the first DSC run test, air was passed through the cell for 3 or 6 h then the inlet and outlet were closed before the second run. A very small exothermic peak was obtained in second run corresponding enthalpy charges less than 0.2 J/g in these experiments. It showed that air has a small contribution in exothermal heat release probably due to oxidation reaction.

3.5.2. Effect of moisture on second run:

The effect of moisture on the exothermic peak signal in the second run was studied by purging moisturized nitrogen with 60% relative humidity by using glycerol-water solutions [20] for 3, 6 or 12 h after first run using gas flow cell. No exothermic peak was observed in the second DSC runs. It can be concluded the disappearance of the exothermic peak in the second run was not related to absence of moisture for previously heated samples.

3.5.3. Effect of air and moisture combined on second run:

To study the effect of weathering (exposure to air and moisture combined) on a sample, the sample was taken out of the batch cell after first run and exposed to air at room temperature

for 1, 3 and 24 h and then charged back into the batch cell. During second run an exothermic peak with total area corresponding enthalpy charges of 3.2, 8.5 and 10.8 J/g was observed after 1, 3 or 24 h respectively.

The effect of weathering was also examined in gas flow cells. After the first run, moisturized air of 60% relative humidity was purged through the sample for 6 or 12 h. The results of these tests were in general agreement with those in batch cells and an exothermic peak corresponding enthalpy charges of 4.6 and 6.7 J/g was observed after 6 or 12 h.

Hence exposing the coal sample after first DSC run to atmospheric air and moisture together reproduces the exothermic signal. This suggests that water has a significant role in the adsorption on the oxygen at coal surface and consequently in generating new active sites at which the exothermic phenomena starts which have been previously stated [6, 21-23].

3.6. Autoclave experiments

3.6.1. Wire basket test:

The wire basket test showed that the T_{crit} for autoclave-heated increased by 3 ± 1 degree. Thus the changes occurring during heating up to $110^{\circ}C$ in absence of air decrease the coal's propensity for spontaneous combustion.

3.6.2. Surface area and pore distributions

A Morwell coal heated in autoclave had a lower surface area (255 m^2/g) than the same coal dried at 105 $^{\circ}C$ under nitrogen 3 h (284 m^2/g). Mercury porosimetry indicated that the micro and meso-pores volumes were lower than those for dried coal 105 $^{\circ}C$, but the macor-pore didn't change significantly. These decrease in surface area and micro and meso-pore volume may explain why the autoclave-heated coal combusted less readily (wire basket experiments)

there were less available site for oxygen to react with coal particles and it postpone the T_{crit} to higher temperature [24].
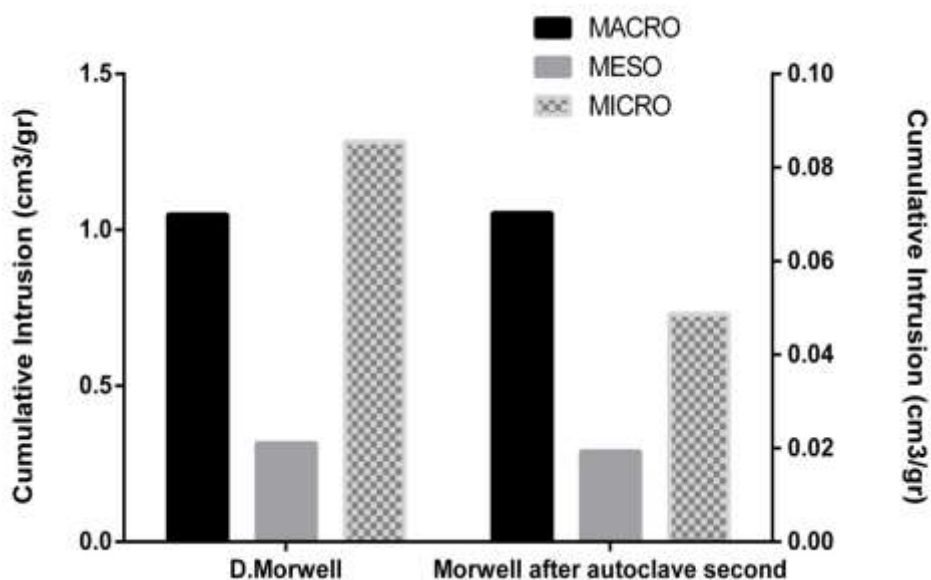

Figure 5: Pore size distribution in oven dried and sample after autoclave (micro and meso-pore on right Y axis).

3.6.3. Gas analyses:

The results of gas chromatography showed that 0.2 % of produced gas is CO_2, 0.01 CH_4 and 0.01 H_2. The generation of these gases shows that there is a possibility of chemical reaction within coal particle during the exothermal event.

3.6.4. Scanning electron microscope (SEM) results:

The coal sample before and after heating in autoclave was studied by SEM. Figure 8 shows that the morphology of coal particle clearly changed during the autoclave run as compared to of coal dried at 105 oC under N2.

Small porous particles were converted to to bigger, very smooth rounded particles implying structural change during heating associated with an exothermic phenomenon. These less

porous smooth particles can provide had fewer active sites to any available reactions which could explain why no exothermic peak was observed in second DSC run.
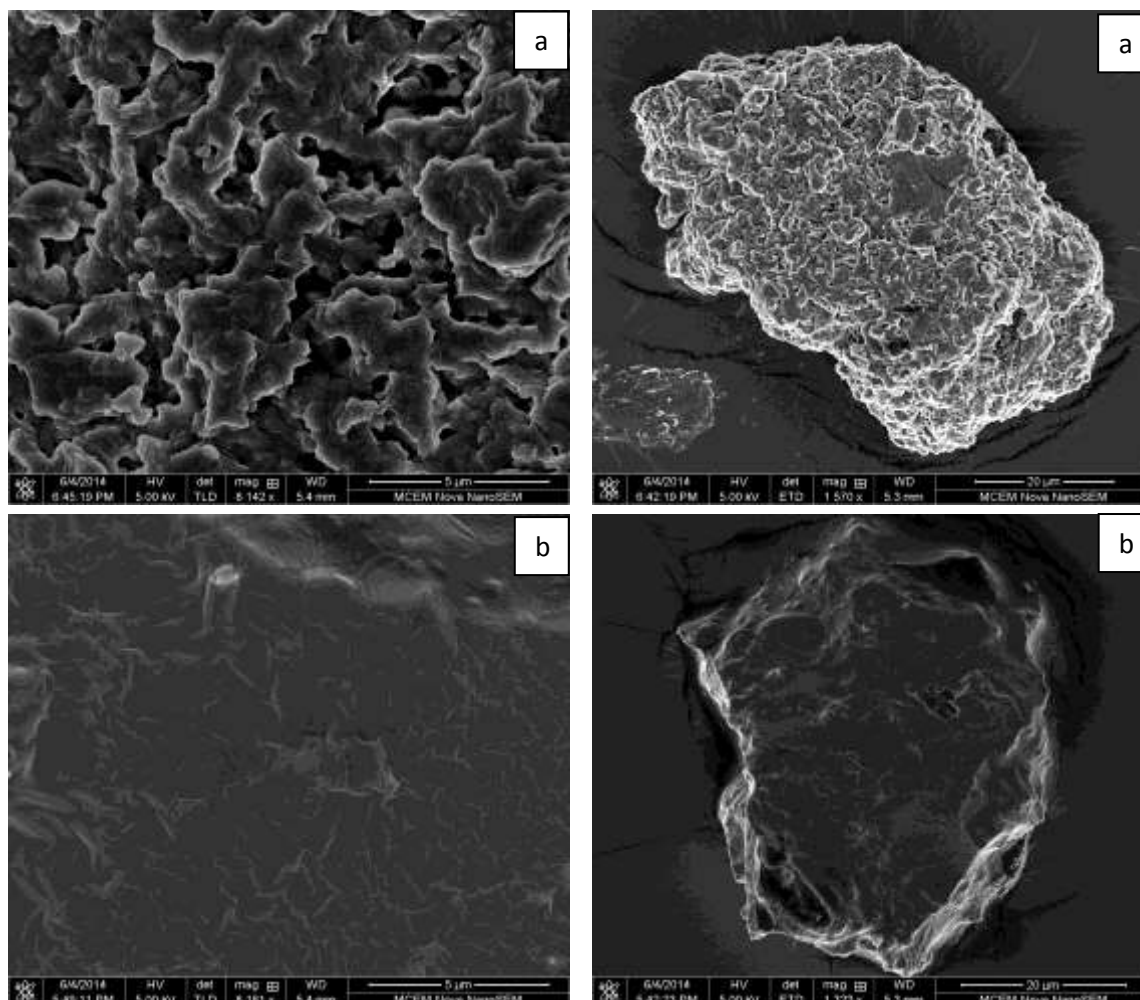

Figure 6: SEM images of oven dried Morwell coal at 105 oC under nitrogen (a) and sample after autoclave.

4. Conclusion:

The results suggest that brown coal starts a physical transition and/or molecular rearrangement similar to cold crystallization at $52^{\circ}C$ with a maximum at $98^{\circ}C$. This low temperature exothermic phenomenon changed the morphology of the coal surface from a porous to very smooth and reduced the surface area, the micro-pore and meso-pore volume. Turface probably could explain the decreasing of the T_{crit} for sample after heating and experiencing the exothermal phenomena increased by three degree Celsius which is in good

agreement with decreasing the surface area and micro-pores. However the exothermal phenomenon will increase the coal sample temperature by around 8 to 17°C which might promote and increase the tendency of the coal to combustion spontaneously.

Acknowledgment:

References

1. Baris, K., S. Kizgut, and V. Didari, *Low-temperature oxidation of some Turkish coals.* Fuel, 2012. **93**(0): p. 423-432.
2. Amel'chugov, S.P., V.I. Bykov, and S.B. Tsybenova, *Spontaneous Combustion of Brown-Coal Dust. Experiment, Determination of Kinetic Parameters, and Numerical Modeling.* Combustion, Explosion and Shock Waves, 2002. **38**(3): p. 295-300.
3. Wang, D.-m., et al., *Test method for the propensity of coal to spontaneous combustion.* Procedia Earth and Planetary Science, 2009. **1**(1): p. 20-26.
4. Nugroho, Y.S., A.C. McIntosh, and B.M. Gibbs, *Low-temperature oxidation of single and blended coals.* Fuel, 2000. **79**(15): p. 1951-1961.
5. Carras, J.N. and B.C. Young, *Self-heating of coal and related materials: Models, application and test methods.* Progress in Energy and Combustion Science, 1994. **20**(1): p. 1-15.
6. Marinov, V.N., *Self-ignition and mechanisms of interaction of coal with oxygen at low temperatures. 1. Changes in the composition of coal heated at constant rate to 250 °C in air.* Fuel, 1977. **56**(2): p. 153-157.
7. Sujanti, W., D.K. Zhang, and X.D. Chen, *Low-temperature oxidation of coal studied using wire-mesh reactors with both steady-state and transient methods.* Combustion and Flame, 1999. **117**(3): p. 646-651.
8. Clemens, A.H., T.W. Matheson, and D.E. Rogers, *Low temperature oxidation studies of dried New Zealand coals.* Fuel, 1991. **70**(2): p. 215-221.
9. Zhu, J., N. He, and D. Li, *The relationship between oxygen consumption rate and temperature during coal spontaneous combustion.* Safety Science, 2012. **50**(4): p. 842-845.
10. Wang, H., B.Z. Dlugogorski, and E.M. Kennedy, *Coal oxidation at low temperatures: oxygen consumption, oxidation products, reaction mechanism and kinetic modelling.* Progress in Energy and Combustion Science, 2003. **29**(6): p. 487-513.
11. Mackinnon, A.J., et al., *Enthalpy relaxation and glass transitions in Point of Ayr coal.* Fuel, 1995. **74**(1): p. 136.
12. Mackinnon, A.J., M.M. Antxustegi, and P.J. Hall, *Glass transitions and enthalpy relaxation in coals.* Fuel, 1994. **73**(1): p. 113-115.
13. Takanohashi, T., et al., *Irreversible Structural Changes in Coals during Heating.* Energy & Fuels, 1999. **13**(2): p. 506-512.

14.   Yun, Y. and E.M. Suuberg, *New applications of differential scanning calorimetry and solvent swelling for studies of coal structure: Prepyrolysis structural relaxation.* Fuel, 1993. **72**(8): p. 1245-1254.
15.   Mackinnon, A.J. and P.J. Hall, *Glass transitions in coal.* Fuel, 1992. **71**(8): p. 974-975.
16.   Sujanti, W. and D.-k. Zhang, *A laboratory study of spontaneous combustion of coal: the influence of inorganic matter and reactor size.* Fuel, 1999. **78**(5): p. 549-556.
17.   Painter, P., M. Starsinic, and M. Coleman, *DETERMINATION OF FUNCTIONAL GROUPS IN COAL BY FOURIER TRANSFORM INTERFEROMETRY*, in *Fourier Transform Infrared Spectra*, J.R. Ferraro and L.J. Basile, Editors. 1985, Academic Press: San Diego. p. 169-241.
18.   Ibarra, J., E. Muñoz, and R. Moliner, *FTIR study of the evolution of coal structure during the coalification process.* Organic Geochemistry, 1996. **24**(6–7): p. 725-735.
19.   Clemens, A.H., T.W. Matheson, and D.E. Rogers, *DTA studies of the low temperature oxidation of low rank coals.* Fuel, 1990. **69**(2): p. 255-256.
20.   Forney, C.F. and D.G. Brandl, *Control of Humidity in Small Controlled-environment Chambers using Glycerol-Water Solutions.* Hort Technology, 1992 **2**(1): p. 52-54.
21.   Schmal, D., *Spontaneous heating of stored coal In:Chemistry of coal weathering.*, in *Chemistry of coal weathering*, C.R. Nelson, Editor 1989: Amsterdam. p. 133–215.
22.   Berkowitz, N., *An introduction to coal technology*1979: Academic Press.
23.   Clemens, A.H. and T.W. Matheson, *The role of moisture in the self-heating of low-rank coals.* Fuel, 1996. **75**(7): p. 891-895.
24.   Hayashi, J.-i. and C.-Z. Li, *Chapter 2 - Structure and Properties of Victorian Brown Coal*, in *Advances in the Science of Victorian Brown Coal*, C.-Z. Li, Editor 2004, Elsevier Science: Amsterdam. p. 11-84.

A slow release nitrogen fertiliser produced by simultaneous granulation and superheated steam drying of urea with brown coal (lignite)

Michael T. Rose *[1a], Emily L. Perkins *[1,2], Biplob K. Saha[1], Evone C. W. Tang[2], Timothy R. Cavagnaro[3], W. Roy Jackson[1], Karen P. Hapgood[2], Andrew F. A. Hoadley[2], Antonio F. Patti[1]

* Both authors contributed equally to this work

[1] School of Chemistry, Monash University, Clayton, Victoria 3800 Australia

[2] Department of Chemical Engineering, Monash University, Clayton, Victoria 3800 Australia

[3] School of Agriculture, Food and Wine, University of Adelaide, South Australia 5005 Australia.

[a] Current address: NSW Department of Primary Industries, Wollongbar, NSW 2480 Australia

Abstract

Background

Two pressing issues in broad-acre agriculture are the inefficient use of nitrogen fertiliser and the loss of carbon from the soil. The research reported here tested the hypothesis that granulation of synthetic N fertiliser (urea) with a natural organic C resource (brown coal) would reduce fertiliser N loss from the soil system.

Results

Urea-enriched brown coal granules were simultaneously formed and dried within a pilot-scale superheated steam dryer. After application to the soil, reduced nitrous oxide emission and nitrogen leaching were seen for the urea-brown coal granules when compared to urea alone, with no loss of plant nitrogen availability.

Conclusions

Brown coal-urea blended fertiliser showed potential for more efficient use of nitrogen in the long term and has environmental benefits in retaining more nitrogen in the soil.

Keywords: Superheated steam drying, nitrous oxide, greenhouse gas emissions, soil enhancement, controlled-release fertiliser, brown coal, lignite

1. Background

Two major challenges facing farmers worldwide include improving nitrogen (N) fertiliser use efficiency, and reversing the widespread loss of soil organic matter. Nitrogen fertilisers are routinely applied in many cropping and pasture systems in order to increase yields and grain or fodder protein content. However a significant proportion of applied fertiliser N is often not used by the crop or pasture and the remainder is susceptible to loss through leaching, runoff or denitrification [1]. This lost N represents both an economic inefficiency and an environmental burden, as off-site N movement in water pollutes aquifers and natural water courses, whilst nitrous oxide contributes to greenhouse gas accumulation in the atmosphere [2].

The loss of soil organic matter has also impacted on crop productivity. Soil organic matter provides numerous beneficial functions to crop production, including a high water holding capacity; the capability to provide, retain and recycle nutrients; and the capacity to buffer changes in pH, salinity and other chemical stressors [3]. Soil carbon also contributes to the retention of applied N [4], suggesting that management practices that increase soil C can also reduce fertiliser-N loss. Indeed, Gentile et al. [5] found that incorporating low quality (i.e. low % N) maize residues could immobilize fertilizer-N in field soil and reduce N leaching losses to a greater extent than high quality (high % N) residues, without impacting on crop N uptake over the growing season. A number of studies have also shown that biochars can reduce nitrate and ammonium leaching from applied N fertilisers, but the effectiveness depends on the chemical characteristics of the biochars and their rate of application [6–8].

There is therefore a strong reason to hypothesize that blending common mineral N fertilisers with organic materials as organo-mineral fertilisers could reduce off-site fertiliser N loss. To date, most controlled release N fertilisers (CRFs) rely on polymer coatings that delay fertiliser release; higher-stability chemical fertilisers that take more time to solubilise; or granules coated or mixed with specific compounds that inhibit N transformation pathways, such as urease or nitrification-inhibitors [9, 10]. Of the few studies investigating controlled release organo-mineral N fertilisers, Richards et al. [11] showed that blending of commercial ammonium nitrate fertilizer with sphagnum peat reduced fertilizer nitrate leaching whilst still providing sufficient N for the growth of maize. More recently, Gonzalez et al. [12] found that

urea formulated together with biochar slowed down the release of urea, but none of the biochar CRFs performed as well as a commercial CRF that did not contain biochar.

Brown coal, also known as lignite, is an alternative material with properties that make it appealing for use as a N-fertiliser carrier. Previous work found that brown coal incorporation into soil slightly reduced ammonium availability in one soil, but the study did not look at mineral N leaching or nitrous oxide emissions [13]. One reason that brown coals may differ in their N-retention behaviour compared with biochars that unlike most biochars, brown coals are generally acidic rather than alkaline. Furthermore, whereas most biochars are of limited availability and relatively high cost of $500 – 3000 per tonne [14, 15], brown coal is readily available in many countries at lower cost, for example, approximately $50 per tonne in Australia.

A major drawback to the use of brown coal as a carrier material, however, is its high moisture content (typically 60-70 % for brown coals mined in Victoria, Australia). This makes transportation of brown coal prohibitively expensive and thus makes drying of the coal an essential process. Dried brown coal is prone to crumble into a fine dust when handled, increasing its propensity to undergo spontaneous combustion. This introduces further difficulties for handling and storage. Dried brown coal granules of suitable strength and resistance to attrition may be a viable solution to these issues. The granulation process provides a method for the addition of N-fertiliser in either liquid or solid form.

Granulation is a size enlargement process, where fine particles are agglomerated into larger granules [16]. Methods of granulating coal dust have been investigated as a means to reduce losses and optimise the use of this resource and more recently, the potential of improving the handling properties of brown coal has been investigated [17]. During the granulation process a binder is often required to enable the particles to adhere and form larger particles. In the case of brown coal, it has been found that the water contained within the pores of the coal structure provides most of the binder requirements for the granulation process to occur. As the brown coal particles are subjected to mechanical forces within the granulator drum, the inherent water is forced to the surface of the particle and is available as binder. Additional binder may be required, depending on the brown coal used and the desired properties, such as particle strength, of the final granules. After granulation the brown coal granules still contain water that must be removed to reduce transportation cost, although the location of some of

the inherent water has moved from the interior of the coal particle to the surface of the coal granules.

A suitable drying method is required that both decreases the risk of spontaneous combustion occurring during the drying process and is economically viable. Many dewatering methods have been studied; both evaporative techniques that require the latent heat of vaporisation of water, and non-evaporative techniques that remove the water under pressure or using mechanical manipulation of the coal structure have been identified [18]. In the 1980s superheated steam drying of brown coal was suggested as an alternative [19], providing an oxygen deficient atmosphere for drying that removes the risk of spontaneous combustion and a means of recapturing much of the latent heat required for drying by utilising the steam after the drying process.

The aim of this work was to evaluate the use of urea blended with brown coal as a fertiliser. We first sought to optimise the granulation and superheated steam drying of the urea-brown coal blend, before undertaking a series of soil-based experiments to compare the leaching, nitrous oxide emissions and plant uptake of N from urea-brown coal granules versus conventional urea fertiliser. Our results show that urea enriched brown coal granules can successfully be granulated and dried simultaneously within a pilot scale superheated steam drum drier. Granulation of urea with brown coal reduced the amount of N lost through leaching and the emission of nitrous oxide gas from the soil, without reducing plant N availability. This research provides proof of concept for further optimisation of organo-mineral fertiliser manufacture using readily available lignite resources.

2. Materials and methods

Run-of-mine brown coal (BC) from Loy Yang, Australia, was used for these experiments. The coal had a moisture content of 50% (wet basis) and was milled to <3 mm particle size. For lab trials powdered urea was used (Sigma). For steam drying trials granular urea was purchased from a local hardware store (Richgro, Australia) and used in granular form (granules were ~ 2 mm- 4 mm in diameter).

2.1 Lab granulation

Drum granulation of 3 different formulations for pot trials were carried out. Urea was ground into a powder and hand-mixed in weight ratios urea to wet coal of 1:3 (i.e. high N urea-brown coal blend, hereafter referred to as UBC-H) and 1:10 (low N urea-brown coal blend, UBC-L).

A third formulation contained no urea. Some additional water was used as a binder in the granulation process. For batches made with urea, 500 g of wet coal was used with the appropriate addition of urea. The coal only batch used 1500 g of wet coal and additional water. The granulation was carried out in a stainless steel drum granulator with an internal diameter of 37 cm. The drum speed was set at 34 rpm. Granulation of coal with urea occurred very quickly, in less than 10 minutes; the product granules appeared very wet on the surface. Granulation of coal alone typically took 45-60 minutes. Granules were air dried for at least 72 hours at ambient conditions. Product granules with a typical size of 4 mm were used for further pot trials.

2.2 Combined granulation and superheated steam (SHS) drying pilot-scale trials

Wet Loy Yang run-of-mine BC milled to 3 mm and granular urea were pre-mixed 2.5 days in advance of granulation at a mass ratio urea to wet coal of 1:6 (medium urea-brown coal blend, UBC-M). After this time the urea granules were no-longer visible and assumed to have dissolved into the inherent water contained within the brown coal particles. Additional water (180 ml to 1 kg pre-mixed coal and urea) was mixed with the coal/ urea blend as the feed stock for the granulation and drying trial. This additional water was required to assist the granulation process that occurs at the start of the drum and to prevent excessive dust production, which could negatively impact on the granulation process.

The feed formulation was added into the feed hopper at the start of the drum and then fed into the drum via a screw feeder (Figure 1). In the first section of the drum (approximately ¼ of the drum length), the internal flights had been reduced in height to increase the residence time in this section during which the granule growth could occur. Once the coal progressed further down the drum the increased height of the flights assisted the coal granules to move more quickly along the drum, reducing the residence time in which granule breakage could occur. At the end of the drum another screw feeder removed the granules from the drum and out to the product exit chute. Product samples were collected and the particle size distribution and moisture content were measured.
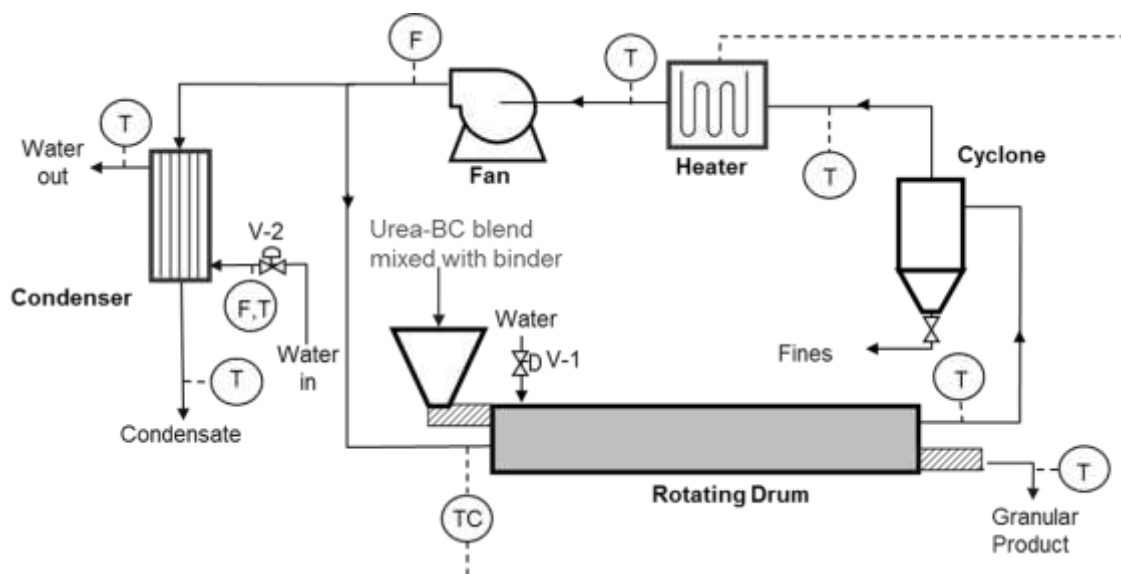
Condition No.	Temperature (°C)	Fan speed (m/s)	Drum Speed (rpm)	Comments
0	150	1.25	Max	Start-up, previous coal only conditions used
1	150	1.75	Max	
2	170	1.75	Max	
3	170	1.25	Max	

Figure 1. Schematic and operating conditions of the pilot-scale superheated steam drum drier

Drum operating parameters of drum speed, fan speed (steam velocity) and steam temperature were adjusted to optimise the particle size distribution and final moisture content of the product. After the initial start-up period, the conditions were changed as shown in Figure 1. Each condition was maintained for one hour.

2.3   Granule Characterisation

Granules were characterised in terms of their particle size, moisture content, crush strength, carbon, hydrogen, nitrogen (CHN) composition and surface morphology.

The mass median particle size, d50, was measured by sieving the sample and determining the particle diameter for which 50 % of the distribution is below that particle size. Similarly the d10 and d90 represent the particle diameter for which 10% and 90% of the distribution have a particle diameter below this value.

The moisture content of the product was calculated on a wet basis using the product mass before and after oven drying at 105°C for 4 hours.

Single particle compressive crush strength tests were carried out on product granules using a bench top scale Instron testing machine. The maximum force applied to break the particle was measured. A minimum of 10 particles from each condition were tested and the average and standard deviation of the crush strength were determined.

The carbon, hydrogen and nitrogen content of the samples were determined by combustion using a PerkinElmer 2400 series II CHNS/O analyser, operated in CHN mode. Oxygen contents of the samples were determined by difference. Samples were analysed in triplicate and a sample mass of approximately 2 mg was used.

The granule surface morphology and cross-sectional area morphology were examined by optical microscopy (Motic SMZ-168 microscope with universal stand). Individual granules from both lab and pilot scale trials were examined. The cross-sectional area of the granules was exposed by fracturing the granules with a scalpel.

2.4   Comparison of steam drying versus air-drying

Although steam drying was considered the technically favourable technique for drying the urea-BC granules in terms of large scale process safety and energy efficiency, the effect of the steam drying on the retention of the urea within the formulation was unclear. Laboratory based drying trials were conducted on a lab granulated batch of 1:6 ratio urea-BC granules, granulation method used as described earlier. Samples (50 g) of granules from this batch were dried under the conditions outlined in Table 1. The CHN analyses of granules from these dried samples and those of batches used in the pot trials were then carried out using the method described above.

Table 1. Conditions used for steam drying versus air drying comparison

Drying Method	Granulation Method	Urea-BC nitrogen content
Air, ambient temperature	Lab granulation	UBC-L
Air, ambient temperature	Lab granulation	UBC-H
Air, ambient temperature	Lab granulation	UBC-M
Air 105°C 1 hr	Lab granulation	UBC-M
Air 130°C 1 hr	Lab granulation	UBC-M

Steam 105°C 60%RH 1 hr   Lab granulation   UBC-M

Steam 130°C 60%RH 1 hr   Lab granulation   UBC-M

Steam 105°C 100%RH 1 hr   Lab granulation   UBC-M

Steam 130°C 100%RH 1 hr   Lab granulation   UBC-M

SHS drum pilot trial   SHS drum pilot trial   UBC-M

2.5   Leaching experiment

A 6-week column experiment was conducted to determine the leaching and denitrification potential of urea-brown coal (urea-BC) blended fertilisers versus conventional urea fertiliser. Twenty polycarbonate columns (18 mm diameter, 250 mm height) were covered at one end with nylon mesh and then packed with 1 cm of washed sand and 88 g of soil (loamy sand). The soil occupied a volume of 60 cm^3, giving a bulk density of 1.4 g cm^{-3}. Soil columns were saturated with 50 mL of water in order to determine field capacity and bed volume. Columns were subsequently allowed to equilibrate for 10 days under free-draining conditions. After this, soils were amended with either conventional urea, UBC-H or UBC-L at a depth of 20 mm, to give a final nominal delivery of 18.4 mg of urea-N per column. This was equivalent to 230 mg N kg^{-1} soil if evenly distributed throughout the entire profile. Two controls were also included: one contained raw brown coal at a rate equivalent to the UBC-L, and an unfertilized control. All treatments were replicated four times.

After treatment applications, soils were wet to field capacity and incubated at 24°C for 42 days. During this time three leaching events were conducted: at days 7, 21, and 35 after treatment application. At each leaching event, soils were adjusted to field capacity moisture and then eluted with half a bed volume (approximately 11 mL) of distilled water. Leachate was collected in 20 mL scintillation vials for 2 hr post-leaching and then frozen for future analysis of mineral N. Greenhouse gas sampling occurred on 1, 3, 8, 10, 13, 17, 22, 24, 27, 31, 36, 38, and 41 days after treatment application, by placing a rubber septum over the top of the columns and sampling gas (20 mL) with a gas–tight syringe immediately after capping and 1 hr later. Gas samples were injected into pre-evacuated 12 mL Exetainer ® vials (Labco, England) for future analysis. Headspace volumes for each column were measured independently.

At the end of the experiment (day 42) columns were dissected into three 8 cm sections. Soil was removed from each section and frozen until analysis for KCl-extractable mineral N (nitrate+nitrite, ammonium) and total N.

2.6   Plant growth experiment

A 6-week glasshouse experiment was conducted to determine the potential of urea-BC blended fertilisers versus conventional urea fertiliser to supply N to wheat. Wheat was grown in 1.5 kg of soil in pots of 10 cm diameter and 20 cm height in the glasshouse for duration of 42 d. Fertiliser was applied at sowing by placing fertiliser granules at a depth of 4 cm below the soil surface (2 cm below the seed). Fertiliser treatments were the same as in the column experiment described above, i.e. urea, UBC-H, UBC-L, brown coal granule control and no fertiliser control, such that each treatment received the same amount of N. Plants were watered weekly to 60% field capacity, with a single 'leaching' event at 20 days after sowing. At this time, soil was watered to field capacity and then an additional 50 mL of water was applied to simulate a heavy rainfall event. Leachate was collected from holes in the bottom of the pots and analysed for nitrate and ammonium. Greenhouse gas emissions were measured weekly at 7, 14, 21 and 35 days after sowing, by connecting a 15 cm height PVC cover with a septum and sampling gas (20 mL) with a gas–tight syringe immediately after covering and 1 hr later. Gas samples were injected into pre-evacuated 12 mL Exetainer ® vials for future analysis. Headspace volumes for each pot were measured independently.

After 42 days of growth, all pots were destructively harvested by removing wheat shoot and roots and partitioning the soil profile into three sections: 0-6 cm, 6-12 cm and 12-20 cm. Soil was analysed for nitrate and ammonium. Plant shoots were oven dried at 70°C, ground and analysed for N content by dry combustion.

2.7   Greenhouse gas analysis

Gas samples were analysed for CO_2 and N_2O using an Agilent 7890A greenhouse gas analyser. This system separates gases on HayeSep Q 80/100 columns followed by detection of CO_2 by flame ionization and N_2O by electron capture. Gas flux over the 60 min sampling duration was checked for linearity periodically throughout both column and glasshouse experiments by measuring at 0, 20, 40 and 60 minutes. The flux of N_2O-N was calculated by converting volumetric gas chromatography data (ppm) to molar equivalents using the ideal gas equation, corrected for temperature and pressure, and accounting for the volume of the

sampling headspace and area of surface flux. For the column leaching study, hourly flux data were integrated over time by taking an average of two consecutive measurements and multiplying by the time interval, in order to calculate cumulative emissions. Because only four sampling N_2O sampling events were taken for the plant growth experiments, data are reported as the hourly flux for each event.

2.8   Granule, soil, plant tissue and leachate analysis

Total C and N in fertiliser granules, soils and plant tissues were measured using a high-frequency induction furnace (LECO Pty Ltd). All materials were finely ground using a stainless steel ball mill prior to analysis.

Mineral N was extracted from soils (homogenised and sieved to < 2mm) with 2 M KCl using a 1:4 soil:extractant ratio. Leachates and soil extracts were filtered through 0.2 micrometre cellulose acetate prior to analysis for mineral N species by spectrophotometry in microplate formats. NH_4^+ was quantified after reacting with salicylate and hyphochlorite in a buffered alkaline solution containing sodium nitroprusside as a reductant [20]. NO_3^- was determined by reduction of nitrate using vanadium (III) combined with detection by acidic Griess reagent [21].

2.9   Statistical analysis

Leaching and plant experiments were established as randomized block designs. Mineral N concentrations in soil and leachate; nitrous oxide fluxes and plant growth and N content were analysed using a one-way ANOVA with 5 levels (Urea, UBC-H, UBC-L, BC control, no treatment control). Position in the glasshouse/laboratory was used as a block factor. Post-hoc testing by least significant difference (P<0.05) was used to separate means. All analyses were conducted with SPSS.

3. Results

3.1   Lab Granulation

Lab granulation experiments produced batches of urea-BC and BC granules for pot trials, leaching experiments and the drying method comparison study. Initial observations suggested that granules with a higher urea content showed signs of urea re-crystallisation on the surface of the granules, as indicated by small white crystals on the exterior of the coal granules (Figure 3c).

3.2   Combined granulation and steam drying pilot scale trials

The results of the superheated steam drying trials are shown in Figure 2. The start-up conditions were maintained for 3 hours, with product samples taken every 20 minutes starting at 100 minutes, denoted as time 0 for the experiment. The dry mass output was initially affected by changes in the fan speed, but returned to an equilibrium level of around 80 g/min after 20 minutes. The mean particle size, d50, was also initially affected by both the change in fan speed and change in temperature, but returned to 2.5- 3 mm after 20 minutes. The error bars displayed in Figure 2 show the d10 and d90, thus represent the width of 80% of the particle size distribution. For this trial, the d50 ranged from 1.5 to 3.5 mm. The product moisture content was relatively stable at 15-20% moisture after the initial start-up phase. The calculated product moisture content ranged from 15 to 27% for the conditions used in this trial. The initial feed moisture content was 58%

At around 240 minutes there was an unexpected 8 minute power outage after which the drum was restarted. Very little change was observed in the median particle size or particle size distribution, although a noted decrease in the product moisture content was observed and likely a result of the increased residence time of the product at elevated temperature during the power outage.
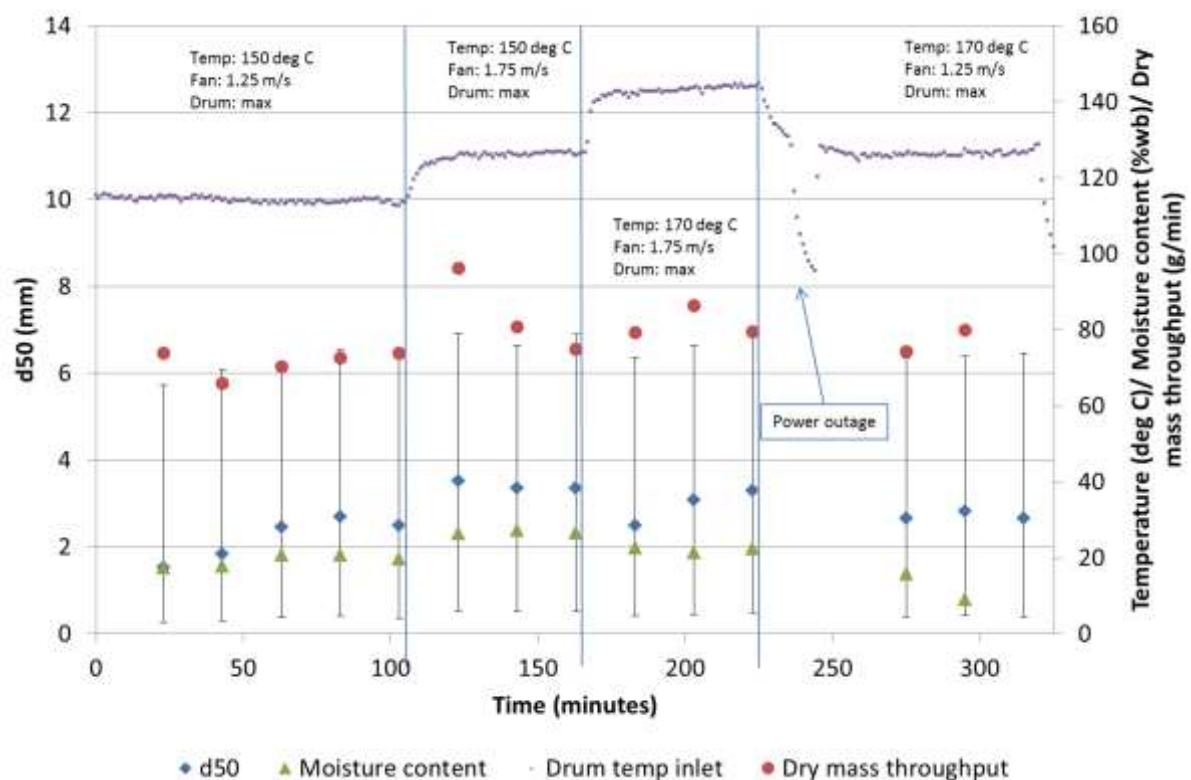
Figure 2. Results of superheated steam drum trials, d50, product moisture content, drum inlet temperature and dry mass throughput. Error bars show the width of 80% of the particle size distribution.

3.3   Granule characterisation

The composite granules at all urea-BC ratios and for both granulation methods significantly increased in nitrogen content compared to the raw coal (Table 2). During granulation of brown coal, the wet brown coal already contains a large reservoir of water within the porous structure of the coal. As the coal is consolidated within the drum, the water is forced out of the pore structure and on to the surface of the coal particles, which allows the water to act as a binder in the granulation process. The surface water on the coal particle forms a binding agent when the particles collide, and the particles coalesce. In the case of urea addition, the urea is thought to dissolve into the inherent water within the coal due to its high solubility and is therefore eluted towards the surface of the particles as the consolidation process occurs.

The granule crush strength was measured for urea-BC granules that were granulated and dried in the pilot scale superheated steam drum drier. Both batches had a urea to wet coal ratio of 1:6 (UBC-M). The average crush strength of 10 granules for each batch is presented (Table 2). The granule crush strength is comparatively low at 2.2 and 2.9 N respectively for the two test batches. For handling purposes the granules crush strength should be at least 13.73 N, a crush strength of 22.56 N or greater being highly desirable (Hignett 1985).

Table 2. CHN and crush strength analysis for raw coal and combined coal and urea granules, percentages on dry basis. ND = not determined.

Urea : wet coal ratio	C %	H%	N%	Crush strength (N)
Typical Victorian BC	65-67	4.5-5	0.5	ND
UBC-H (lab granulation)	46.5	5.7	17.1	ND
UBC-M (pilot granulation)	45.2	5.6	10.7	2.9±1.0
				2.2±0.5

UBC-L (lab granulation)   51.5   5.4   8.7   ND

3.4   Surface morphology

At lower N content, UBC-M and UBC-L, no significant urea crystals are observed on the granule surface or within the cross-sectional area (Figure 3a and 3b). This was true for all drying methods. With the highest N content UBC-H, urea crystals were observed on the surface of the granule, but not throughout the interior as seen in the image of the cross-sectional area (Figure 3c).
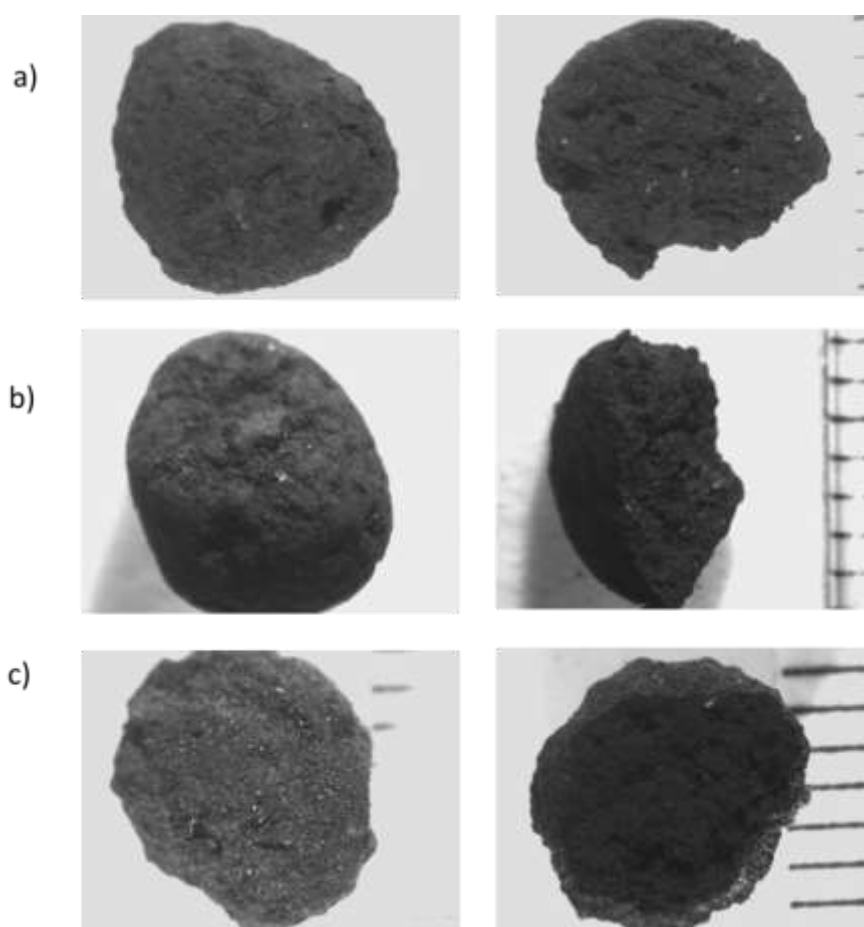

Figure 3. Optical microscopy images of brown coal and urea whole granules and cross-section for a) UBC-L, b) UBC-M and c) UBC-H

3.5   Comparison of drying methods on nitrogen content of formulation

To compare the effects of steam and air drying on the N content of the dried granules, a single batch of UBC-M granules was made in the laboratory drum granulator and dried by different methods (Table 3). The low carbon percentages observed for steam dried samples at 105 $^{\circ}$C for 60 % and 100% RH were likely because the samples were not as dry as the

other samples, and this is also inferred by the higher hydrogen and oxygen content. The carbon to nitrogen ratio (C:N) was calculated to compare the samples without the effect of moisture. The theoretical C:N ratio was calculated from a mass balance that assumed no loss of material during the granulation and drying process. The measured values were in close agreement with the theoretical values for all drying methods and for the different formulations (Figure 4).

Table 3. CHN analysis for coal-urea (UBC-M) granules dried under different conditions

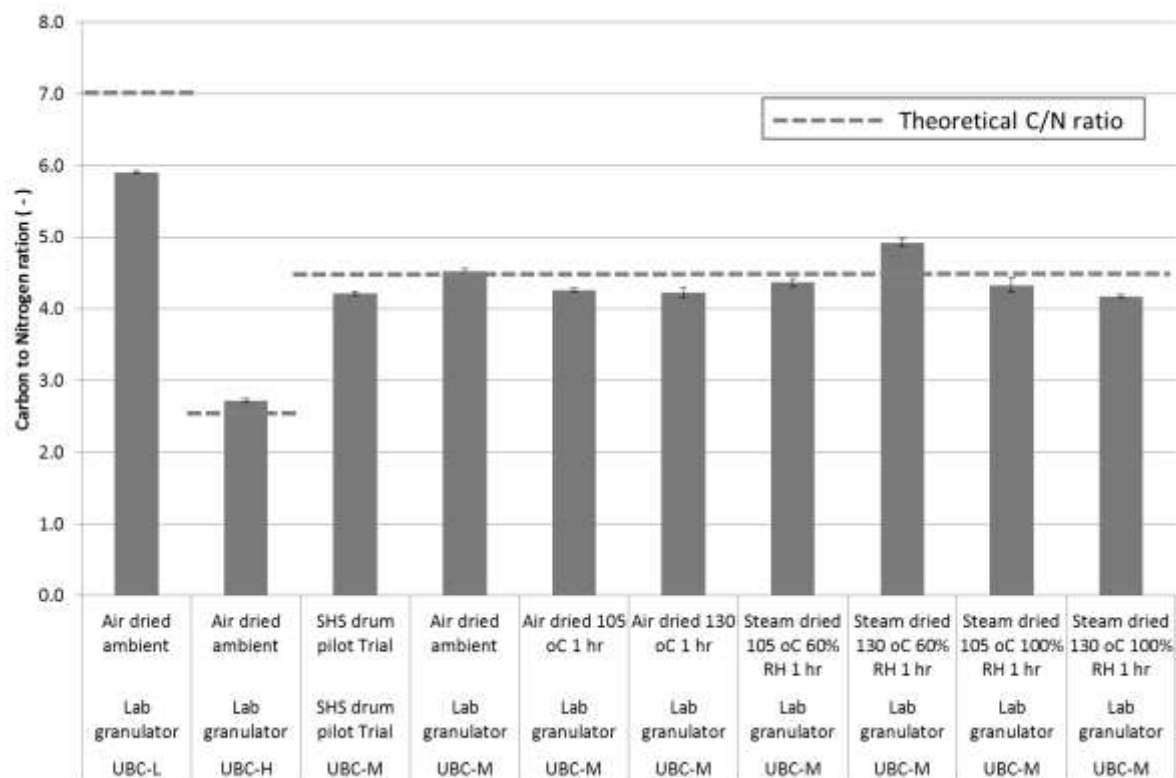| Drying conditions	C %	H %	N%	O% (by difference)
Air dried, ambient, 5 days	50.0	5.4	11.0	31.2
Air dried, oven 105 ^{o}C, 1 hour	42.7	5.6	10.0	39.2
Air dried, oven 130 ^{o}C, 1 hour	45.4	5.6	10.6	35.7
Steam dried, oven 105 ^{o}C, 60% RH, 1 hour	33.6	6.4	7.7	49.8
Steam dried, oven 130 ^{o}C, 60% RH, 1 hour	48.0	5.3	9.8	34.7
Steam dried, oven 105 ^{o}C, 100% RH, 1 hour	34.7	6.1	8.0	48.6
Steam dried, oven 130 ^{o}C, 100% RH, 1 hour	43.6	5.2	10.5	38.5

Figure 4. C:N for urea-BC granules of different blends and dried by different methods.

3.6   Leaching experiment

The addition of urea fertilisers, as either straight urea or granulated urea-BC, significantly increased the concentration of both mineral N species in water leaching from the soil column compared with columns not receiving N fertiliser (Figure 5). Granulation of urea with brown coal significantly reduced the amount of both nitrate and ammonium leached out of the soil profile. Increasing the ratio of BC to N (i.e. the UBC-L granule) reduced the amount of ammonium lost through leaching by over 40%, whilst the amount of nitrate lost via leaching was reduced by almost 20%.
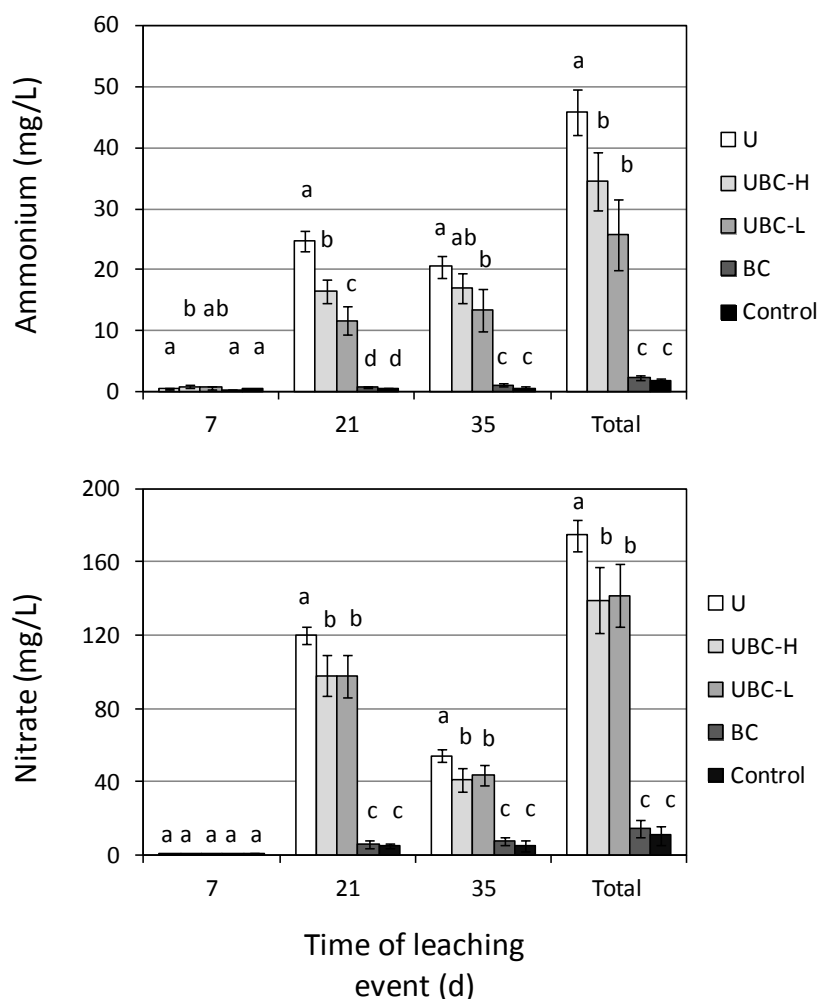
Figure 5: Ammonium and nitrate concentration in leachates at each leaching event. The column to the far right shows the total N leached. Treatment abbreviations are: U – urea, UBC-H – urea brown coal granule (17% N), UBC-L – urea brown coal granule (8.7% N), BC – brown coal granule, control – no N or C addition. Within a specified time, letters above column are different if the value is significantly different (P<0.05).

As expected, the addition of urea fertilisers, as either straight urea or granulated urea-BC, significantly increased the concentration of both mineral N species in the soil column compared with columns not receiving N fertiliser (Figure 6). Granulation of urea with brown coal significantly increased the amount of ammonium residing in the top soil (0-8 cm), and reduced the amount of ammonium in middle layer (6-12 cm). The top soil of urea-BC granules contained almost double the amount of ammonium than that of the soil treated with straight urea. Granulating urea with BC did not significantly alter the amount of nitrate in topsoil compared with straight urea, but soil treated with the low N urea-BC granules had significantly less nitrate in the lower layers than the other two N treatments.
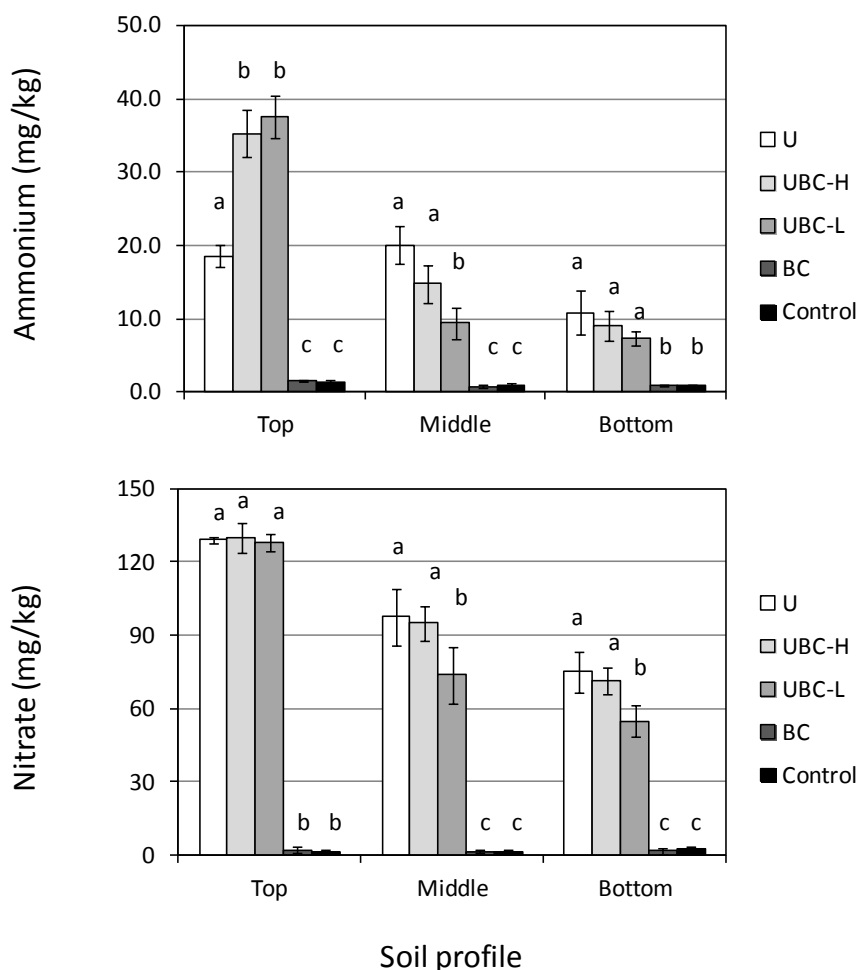
Figure 6. Ammonium and nitrate remaining in soil at 42 days, after 3 leaching events. The depth of the different soil profile layers are top (0-8 cm), middle (8-16 cm) and bottom (18-25 cm). Treatment abbreviations are: U – urea, UBC-H – urea brown coal granule (17% N), UBC-L – urea brown coal granule (8.7% N), BC – brown coal granule, control – no N or C addition. Within a profile depth, letters above column are different if the value is significantly different (P<0.05).

Granulation of urea with BC, in particular the low N urea-BC granulation, also maintained a higher level of total N in the topsoil as compared with straight urea (Table 4).

Table 4. Total N and C in the topsoil at the end of the 42 days incubation. Errors are 95% confidence levels. Letters adjacent to values are different if the values within a column are significantly different (P<0.05).

Treatment	Topsoil (0-8 cm) N content (%)	Topsoil (0-8 cm) C content (%)

U	0.43 ± 0.01 a	1.28 ± 0.05 a
UBC-H	0.46 ± 0.01 b	1.51 ± 0.35 ab
UBC-L	0.50 ± 0.03 c	2.21 ± 0.69 b
BC	0.03 ± 0.01 d	1.17 ± 0.14 a
Control	0.02 ± 0.01 d	1.17 ± 0.2 a

Application of N fertilisers (either straight urea or urea-BC granules) significantly increased the emissions of N_2O from soil (Table 5). The high N urea-BC granules did not reduce the loss of N_2O compared with straight urea. However, the low N urea-BC granules reduced N_2O emissions by approximately 35% over the duration of the experiment, compared with both other N fertilisers.

Table 5. Cumulative emissions of N_2O-N (µg per column) from the surface of the soil columns over the duration of the experiment. Errors are 95% confidence levels. Letters adjacent to values are different if the values within a column are significantly different (P<0.05).

Treatment	Cumulative N_2O-N (µg) emissions at 21 d	Cumulative N_2O-N (µg) emissions at 42 d
U	28 ± 13 a	129 ± 20 a
UBC-H	33 ± 8 a	145 ± 36 a
UBC-L	11 ± 4 b	76 ± 9 b
BC	0.4 ± 0.1 c	1.9 ± 0.3 c
Control	1.4 ± 2.2 c	1.6 ± 2.2 c

3.7   Plant-growth experiment

No significant differences in plant growth were observed between any of the treatments, but some minor differences were observed in terms of N-content (Figure 7). Wheat growing in pots treated with brown coal control alone (no urea) had significantly lower N-content than pots receiving urea or the low urea-BC blend.

Dry weight (g)
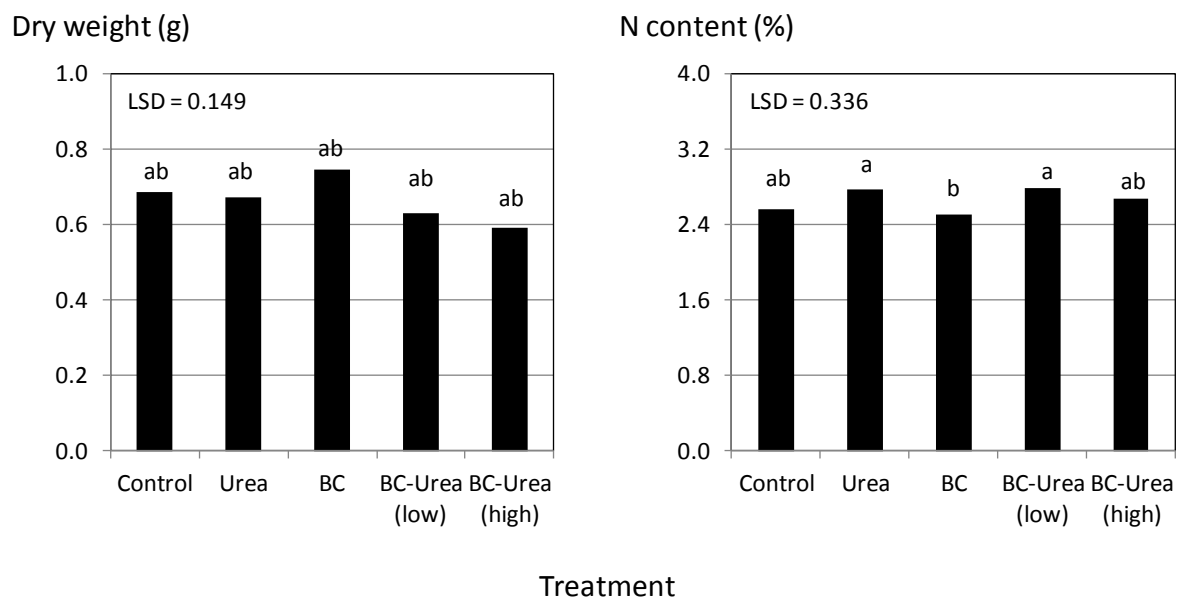

N content (%)

Treatment

Figure 7. Effect of different N-fertilisers on early wheat growth and leaf tissue-N accumulation.

Greenhouse gas measurements over the growth duration of the experiment showed higher emissions of N_2O from pots fertilised with straight urea as compared with urea-BC blends and non-fertilised pots (Figure 8). This was particularly evident after the saturation event on day 21, where N_2O emissions from urea-fertilised plots were more than double that of non-fertilised pots and the high urea-BC blend.
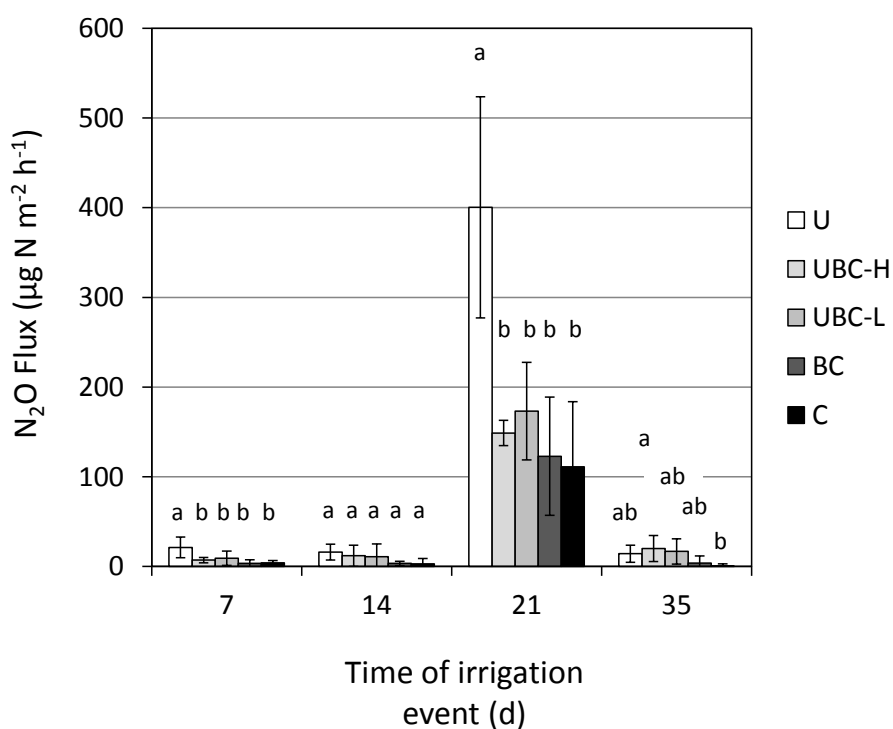

Time of irrigation event (d)

Figure 8. Effect of different N-fertilisers on N_2O emissions ($\mu g\ m^{-2}\ h^{-1}$) at different irrigation events. Note that day 7, 14 and 35 irrigations were to 60% soil water holding capacity; whereas the day 21 irrigation represented a leaching event in which soil was saturated. Within a specified time, letters above column are different if the value is significantly different ($P<0.05$).

At the end of the experiment, significant differences in the concentration of nitrate were observed in the different treatments (Figure 9). Unfertilised pots (control and BC control) contained very low concentrations of nitrate throughout the soil profile, whereas all soils receiving N-containing fertilisers contained significantly ($P<0.05$) higher levels. The high N urea-BC treatment contained significantly ($P<0.05$) higher levels of nitrate in topsoil than the low N urea-BC blend, but both were not significantly different from the straight urea treatment.
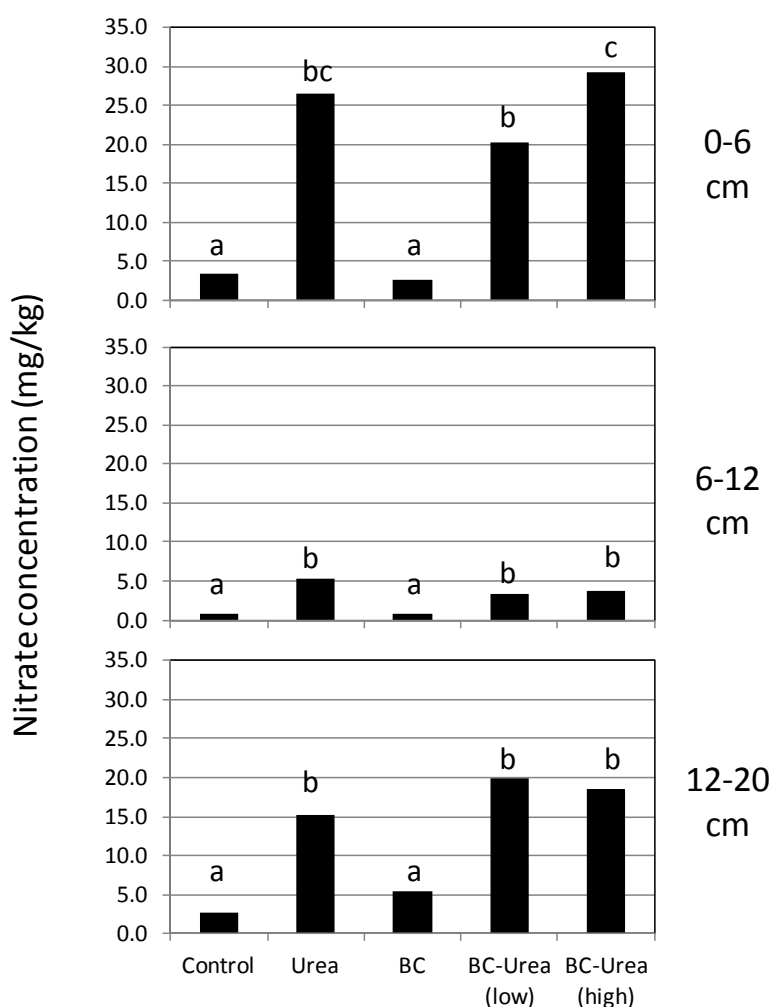
Figure 9. Effect of different N-fertilisers on nitrate concentrations through the soil profile at harvest (42 DAS).

4. Discussion

4.5 Granulation

Urea enriched BC granules were successfully made at both laboratory and pilot scale. The pilot scale granulation was achieved within the drum of a superheated steam drier, thus enabling the simultaneous granulation and drying of the granular product. Superheated steam drying provides an intrinsically safe method for drying BC which has a propensity to undergo spontaneous combustion. The atmospheric pressure of the superheated steam reduces the cost and energy requirement for the drying process and provides the option to recapture the latent heat required to dry the coal [22]. The N content of the dried products at all C:N ratios was close to the theoretical N content determined from the initial amount of urea addition to the wet coal. This was true for all of the drying methods tested here and despite the observation of crystalline urea on the surface of the high N formulation, which may have resulted in lost urea.

The role of the urea within the granulation process should also be considered. This highly soluble fertiliser dissolves into the inherent water within the raw BC, which is partially drawn to the surface of the coal particles, reducing the consolidation time required within the granulation process. This was observed in the significantly reduced granulation time for the laboratory batches of urea-BC compared to the granulation of BC alone. This partial extraction of the inherent water also reduced the requirement for additional water to act as a binder within the granulation process. The tumbling motion and impact forces on the coal particle during the consolidation process drive the inherent water to the surface of the coal particle where it acts as a binder between coal particles to begin the granulation process. As the granules continue to form, the impact forces on the granules drives more water to the surface allowing the granule to grow further. This may also effect the final distribution of the N within the wet granules.

The difference in the drying mechanism between air dried granules (surface drying) and steam dried granules (internal removal of water vapour), may also have an impact on the final distribution of the N within the dried granules. Further investigation would determine if this effect is significant with respect to the final use of the urea-BC granules.

The final strength of the dried granules is significantly less than that of other fertiliser granules currently used in agriculture. To enable the urea-BC granules to be a feasible alternative, further work on the formulation is required to increase the granule strength. An additive to either the binder or the urea-BC solid blend may provide the required strength for the dried granules.

4.6   N-dynamics in unplanted soil treated with urea fertilisers

Granulation of urea with BC had a strong effect on the behaviour of the fertiliser N in the soil system. Both high- and low-N urea-BC granules maintained higher total N and ammonium concentrations in unplanted topsoil, suggesting a mechanism by which the BC either slows the rate of urea hydrolysis or binds to ammonium, making it less mobile. This is supported by the leachate data from unplanted soil, which showed that by granulating the urea with BC, less mineral N (both ammonium and nitrate) was leached from the soil profile as compared with straight urea.

It is important to note that the high N granules did not retain as much N in the top soil. This is similar to the findings of Gentile et al. [5], who demonstrated that fertiliser N retention was higher in soil amended with low quality (i.e. low N) residue than high N residues, due to net N immobilization. However, in their case, it was postulated that immobilization was primarily a consequence of increased microbial demand to match the higher availability of carbon-rich growth substrate. In our case, we believe that microbial immobilization due to a higher C availability is unlikely, since previous studies have shown brown coal to be a poor C source over short time periods [13]. Instead, it is likely adsorption of urea and/or mineralized ammonium to the lignite matrix is the main mechanism responsible for immobilization, as has been observed for high C:N biochars [8, 23]. The lower retention of N in topsoil by the high N granules appears to be a consequence of oversaturation of sorption sites within the brown coal matrix, as shown by the presence of urea crystals throughout the granules (Figure 3). This effectively increases the surface area of the crystalline urea and would promote faster dissolution and associated leaching.

The low N urea-BC granules were also superior to the high N granules in terms of N_2O losses: emissions were significantly reduced by incorporating more BC in the N-fertiliser granules. The fact that there was no significant difference in N_2O emissions between urea and high N brown coal granules suggests that the availability of nitrate for denitrification over the duration of the experiment was similar in these two treatments. In contrast, the reduction in

N_2O emissions from the low N urea-BC granules treatment suggests a lower nitrate availability over the duration of the incubation, or, alternatively, that the nitrate was retained in a zone where the activity of denitrifying organisms was inhibited. There is also speculation that low N (high C:N) biochars can reduce N_2O emissions by catalysing the further reduction of N_2O to N_2 [24, 25], which could represent an additional mechanism by which brown coal blends can reduce N_2O emissions. Further research is needed to elucidate the primary mechanisms responsible for altering N_2O dynamics.

4.7 N-dynamics in planted soil treated with urea fertilisers

In contrast to unplanted soil columns subject to leaching, granulation of urea with brown coal did not drastically alter the movement of N compared with straight urea in the planted soil columns. Part of the reason for this is likely due to the less severe irrigation regime, since planted soil columns were watered to 60% field capacity three times with only one complete saturation event (representing a heavy rainfall) at day 25. Nevertheless, there was still evidence that incorporation of brown coal reduced nitrous oxide emissions, compared with conventional urea, especially under saturated conditions (Figure 8).

Importantly, the granulation of urea with brown coal did not reduce plant growth or the acquisition of N by plants in this limited six-week growth study (Figure 7). In a similar study evaluating organo-mineral N fertilisers, Richards et al. [11] found that blending urea or ammonium nitrate fertiliser with peat reduced total N uptake by 9.1% in three successive, 6 – week corn crops grown under glasshouse conditions. However, under field conditions they found no significant differences in yield or N uptake by corn grown with conventional ammonium nitrate fertiliser or peat-blended ammonium nitrate. In our study, the short-time frame of the trial probably masked any potential effects, as evidenced by the minor differences between N-fertilised treatments and controls not receiving N fertiliser. More work is therefore needed to extend the duration and scale of the plant growth experiments.

Overall our results suggest that granulation of urea with BC can strongly reduce N losses from topsoil, by decreasing N-leaching and gaseous emissions. In doing so, it is anticipated that a greater amount of fertiliser N will be available to crops over a longer time period, increasing the efficiency of fertiliser N use, but this remains to be validated. Furthermore, our results show that varying the C:N ratio of the blended fertilisers has a significant impact on the N dynamics, suggesting that there is further opportunity to optimise the ratio of C:N to minimise N loss from soil whilst maximising crop uptake.

5. Conclusions

Urea and BC was successfully blended, granulated and dried on a pilot scale. The granules formed were of an appropriate size for agricultural use, although the current formulation produces granules that are not strong enough for the handling requirements of a fertiliser. The N retention in the granules is close to that calculated theoretically for the formulation and is consistent for all the air drying and steam drying methods tested. The urea-BC granules significantly reduced the amount of nitrate and ammonium lost though leaching and also reduced the emission of nitrous oxides from the soil, whilst not reducing the plant available N. N losses were lower for the low N urea-BC formulation than for the high N formulation, emphasising the significant role of the brown coal in the N retention. This work provides a proof of concept for the pilot scale production and use of BC blended organo-mineral fertiliser granules.

Competing Interests

Authors' contributions

MTR and EP conceived experiments, conducted experiments, analysed data and drafted the manuscript. BKS and ECWT conducted experiments and assisted in drafting the manuscript. TRC, WRJ and KPH assisted in interpretation of data and writing of the manuscript. AFAH and AFP helped design and conduct experiments, interpret data and write the manuscript.

Acknowledgements

References

1.   Cameron KC, Di HJ, Moir JL: **Nitrogen losses from the soil/plant system: a review**. *Ann. Appl. Biol.* 2013, **162**:145–73.

2.   Vitousek PM, Aber JD, Howarth RW, Likens GE, Matson PA, Schindler DW, et al. **Human alteration of the global nitrogen cycle: sources and consequences**. *Ecol. Appl.* 1997, **7**:737–50.

3.   Allison FE: *Soil organic matter and its role in crop production.* Elsevier Scientific Publishing Company; 1973.

4.   Accoe F, Boeckx P, Busschaert J, Hofman G, Van Cleemput O: **Gross N transformation rates and net N mineralisation rates related to the C and N contents of soil organic matter fractions in grassland soils of different age**. *Soil Biol. Biochem.* 2004, **36**:2075–87.

5.   Gentile R, Vanlauwe B, Van Kessel C, Six J: **Managing N availability and losses by combining fertilizer-N with different quality residues in Kenya**. *Agric. Ecosyst. Environ.* 2009, **131**:308–14.

6.   Ding Y, Liu Y-X, Wu W-X, Shi D-Z, Yang M, Zhong Z-K: **Evaluation of biochar effects on nitrogen retention and leaching in multi-layered soil columns**. *Water, Air, Soil Pollut.* 2010, **213**:47–55.

7.   Zheng H, Wang Z, Deng X, Herbert S, Xing B. **Impacts of adding biochar on nitrogen retention and bioavailability in agricultural soil**. *Geoderma.* 2013, **206**:32–9.

8.   Yao Y, Gao B, Zhang M, Inyang M, Zimmerman AR. **Effect of biochar amendment on sorption and leaching of nitrate, ammonium, and phosphate in a sandy soil**. *Chemosphere.* 2012, **89**:1467–71.

9.   Davidson D, Gu FX: **Materials for sustained and controlled release of nutrients and molecules to support plant growth**. *J. Agric. Food Chem.* 2012, **60**:870–6.

10.   Chen D, Suter H, Islam A, Edis R, Freney JR, Walker CN: **Prospects of improving efficiency of fertiliser nitrogen in Australian agriculture: a review of enhanced efficiency fertilisers**. *Soil Res.* 2008, **46**:289–301.

11.   Richards JE, Daigle J-Y, LeBlanc P, Paulin R, Ghanem I: **Nitrogen availability and nitrate leaching from organo-mineral fertilizers**. *Can. J. Soil Sci.* 1993, **73**:197–208.

12.   González ME, Cea M, Medina J, González A, Diez MC, Cartes P, et al.: **Evaluation of biodegradable polymers as encapsulating agents for the development of a urea controlled-release fertilizer using biochar as support material**. *Sci. Total Environ.* 2015, **505**:446–53.

13.   Tran CKT, Rose MT, Cavagnaro TR, Patti AF. **Lignite amendment has limited impacts on soil microbial communities and mineral nitrogen availability**. *Appl. Soil Ecol.* 2015, **95**:140–50.

14.   Singh B, Macdonald LM, Kookana RS, van Zwieten L, Butler G, Joseph S, et al.:
        **Opportunities and constraints for biochar technology in Australian agriculture:
        looking beyond carbon sequestration**. *Soil Res.* 2014, **52**:739–50.

15.   Jirka S, Tomlinson T: **State of the Biochar Industry—A survey of commercial
        activity in the biochar field.** [www.biochar-
        international.org/sites/default/files/State_of_the_Biochar_Industry_2013.pdf]

16.   Ennis BJ, Lister JD: **Particle Size Enlargement**. *In Perry's Chemical Engineers'
        Handbook.* Edited by Perry R, Green D, Maloney J. McGraw-Hill: New York;
        1997:20.

17.   Tang ECW, Perkins E, Hoadley AFA, Hapgood KP: **Development of lignite
        granulation regime map**. *In Chemeca 2012: Quality of life through chemical
        engineering:* Engineers Australia; 2012:665.

18.   Bergins C: **Kinetics and mechanism during mechanical/thermal dewatering of
        lignite**. *Fuel* 2003, **82**:355–64.

19.   Potter OE, Beeby CJ, Fernando WJN, Ho P: **Drying brown coal in steam-heated,
        steam-fluidized beds**. *Dry. Technol.* 1983, **2**:219–34.

20.   Forster JC: **3-Soil sampling, handling, storage and analysis**. In, editors. *In Methods
        in Applied Soil Microbiology and Biochemistry* Edited by Kassem A, Nannipieri P.
        Academic Press: London; 1995:49–121.

21.   Miranda KM, Espey MG, Wink DA: **A rapid, simple spectrophotometric method
        for simultaneous detection of nitrate and nitrite**. *Nitric oxide.* 2001, **5**:62–71.

22.   Mujumdar AS: **Superheated steam drying**. *Handb. Ind. Dry.* 1995, **2**:1071–86.

23.   DeLuca TH, Gundale MJ, MacKenzie MD, Jones DL: **Biochar effects on soil
        nutrient transformations**. *In Biochar for Environmental Management: Science and
        Technology.* Edited by Lehmann J, Joseph S. Earthscan Publications Ltd: London;
        2015.

24.   Cayuela ML, Van Zwieten L, Singh BP, Jeffery S, Roig A, Sánchez-Monedero MA:
        **Biochar's role in mitigating soil nitrous oxide emissions: A review and meta-
        analysis**. *Agric. Ecosyst. Environ.* 2014, **191**:5–16.

25.   Van Zwieten L, Singh BP, Kimber SWL, Murphy D V, Macdonald LM, Rust J, et al.
        **An incubation study investigating the mechanisms that impact N 2 O flux from
        soil following biochar application**. *Agric. Ecosyst. Environ.* 2014, **191**:53–62.